

VOLUME 84 NO. HY1

UNIVERSITY OF HAWAII

FEBRUARY 1958

PART 1

182 MAY
Mar 6 '58

JOURNAL of the

Hydraulics *Division*

PROCEEDINGS OF THE



AMERICAN SOCIETY
OF CIVIL ENGINEERS

TC1

Journal of the
HYDRAULICS DIVISION

5856-23

Proceedings of the American Society of Civil Engineers

HYDRAULICS DIVISION
EXECUTIVE COMMITTEE

Harold M. Martin, Chairman; Carl E. Kindsvater, Vice-Chairman;
Arthur T. Ippen; Wallace M. Lansford; Joseph B. Tiffany, Jr., Secretary

COMMITTEE ON PUBLICATIONS

James W. Ball, Chairman; Harold M. Martin; Joseph B. Tiffany

CONTENTS

February, 1958

Papers

	Number
Turbulence Characteristics of the Hydraulic Jump by Hunter Rouse, T. T. Siao, and S. Nagaratnam.	1528
The Total Sediment Load of Streams by Emmett M. Laursen	1530
Sediment Transport in Money Creek by J. B. Stall, N. L. Rupani, and P. K. Kandaswamy	1531
Field Investigations of Spillways and Outlet Works by Benson Guyton	1532
Discussion	1558

Journal of the
HYDRAULICS DIVISION
Proceedings of the American Society of Civil Engineers

TC1
A39
V.84

TURBULENCE CHARACTERISTICS OF THE HYDRAULIC JUMP

Hunter Rouse,¹ M. ASCE, T. T. Siao,² and S. Nagaratnam³
(Proc. Paper 1528)

ABSTRACT

Hot-wire measurements of the turbulence in an air-flow model of the hydraulic jump are described for Froude numbers of 2, 4, and 6. Results are analyzed and interpreted in the light of the momentum and energy integrals.

SYNOPSIS

Because the fluid discontinuities produced by entrapped air interfere with the measurement of turbulence in the hydraulic jump itself, the flow pattern of the jump has been simulated in an air duct and the hot-wire anemometer used to determine the corresponding pattern of turbulence for Froude numbers of 2, 4, and 6. In an initial analytical section of this paper the modeling method is justified and the differential and integral forms of the momentum and energy equations pertinent to the investigation are explained. The experimental apparatus and techniques are next described and the basic data presented in diagram form. The measured characteristics of the mean flow and of the turbulence are then correlated in accordance with the foregoing equations, and the process of energy conversion from the mean flow through turbulence to heat is followed in detail. Various aspects of the hydraulic jump long subject to conjecture or misunderstanding are thereby clarified.

Note: Discussion open until July 1, 1958. A postponement of this closing date can be obtained by writing to the ASCE Manager of Technical Publications. Paper 1528 is part of the copyrighted Journal of the Hydraulics Division, Proceedings of the American Society of Civil Engineers, Vol. 84, No. HY 1, February, 1958.

1. Director, Iowa Inst. of Hydr. Research, State Univ. of Iowa, Iowa City, Iowa.
2. Hydr. Engr., Inst. of Hydr. Research, Academia Sinica, Peking, China.
3. Engr., Harza Eng. Co., Chicago, Ill.

INTRODUCTION

Scattered through the twelve discussions of the Bakhmeteff-Matzke paper, "The Hydraulic Jump in Terms of Dynamic Similarity,"⁽¹⁾ are three sorts of information pertinent to the present investigation: first, a well-annotated account of the gradual development of knowledge on this subject; second, a somewhat contradictory mixture of factual matter, hypothesis, and error; third, and by inference only, a guide to further research. At the time the paper and discussions were published (1935), the tools for such research had only recently come into use in other fields, and it is hardly to be expected that they would already have been applied in hydraulics. In fact, the investigation herein described had the purpose of demonstrating the efficacy of the new approach as well as providing greater insight into the phenomenon under consideration.

As was evident from the aforementioned paper and discussions, past advancements had been concerned with the vertical elements - i.e., depths and heads - of the mean flow pattern as correlated by the one-dimensional forms of the continuity, momentum, and energy relationships. Some attention had been given to the empirical evaluation of the longitudinal elements as well, and to the expression of the functional relationships in terms of what is now called the Froude number. Concern with the accompanying pattern of turbulence, however, was almost entirely speculative. For lack of even an approximate evaluation of the turbulence characteristics, their importance to the phenomenon was both over- and underestimated. The first of the present writers, for example, claimed that the computed loss in head at the jump represented merely a transfer of energy from the mean motion to the turbulence, and that the total head would hence be found to remain practically constant through the jump if the kinetic energy of the turbulence could be measured and included as velocity head. Others, on the contrary, underestimated the importance of eddy generation along the surface of discontinuity between the secondary flow of the roller and the primary flow beneath - some even going so far as to claim that the roller played no essential part in the phenomenon.

The difficulty lay, as is now apparent, in the general lack of clarity which then prevailed in nearly all matters involving fluid turbulence. Not only did existing turbulence theories seem to have little connection with hydraulic reality, but the only practicable means of measuring turbulence - the hot-wire anemometer - was restricted to use in air. During the intervening years, progress has been made in the interpretation - if not the quantitative prediction - of the transformation from energy of the mean motion through energy of turbulence to that of heat, and the hot-wire technique itself has been extended to use in water. Means would therefore seem to be at hand for the measurement of the primary and secondary patterns of flow in the hydraulic jump, and at least the evaluation of the various forms at representative sections. Unfortunately, the jump will probably be one of the last hydraulic phenomena to prove susceptible to exploration with the hot-wire instrument, because of the presence of countless fluid discontinuities - bubbles of entrained air - in the region of greatest interest.

To overcome this rather formidable obstacle (yet without taking recourse to the extremely tedious process of statistically analyzing motion pictures of suspended particles), it was resolved at the Iowa Institute of Hydraulic Research to simulate the flow pattern of the hydraulic jump in an air duct, and

then use the hot-wire anemometer for turbulence surveys just as in previous institute studies of other diffusion phenomena. The analog will seem at first glance a rather artificial one, to say the least. However, it must be realized that few model flows portray perfect dynamic similarity with their prototypes, and that for all practical purposes only the pertinent part of the phenomenon need be closely approximated. In the present instance it is not the gravitational action that is to be evaluated but the viscous. If the mean flow patterns are geometrically similar, and if the changes in energy are comparable, then it would seem safe to assume that the patterns of turbulence are also similar - and it is specifically these with which the present investigation is concerned.

Analytical Bases of Experimentation

Air-Water Correlation

With reference to the schematic representation of Fig. 1 and the list of symbols at the end of the paper, application of the simplified continuity, momentum, and energy relationships for one-dimensional flow leads to the following well-known equations for the hydraulic jump in homogeneous liquid flowing through a horizontal, resistance-free channel of rectangular cross section:

$$\frac{d_2}{d_1} = \frac{1}{2} \left(\sqrt{1 + 8 \frac{U_1^2}{gd_1}} - 1 \right) \quad (1)$$

$$\frac{H_L}{d_1} = \frac{1}{2} \frac{U_1^2}{gd_1} \left(1 - \frac{d_1^2}{d_2^2} \right) - \frac{d_2}{d_1} + 1 \quad (2)$$

Both the depth ratio d_2/d_1 and the relative loss of total head H_L/d_1 are seen to be explicit functions of the Froude number of the approaching flow $F_1 = U_1/\sqrt{gd_1}$, as are also such longitudinal characteristics as the relative length of the jump L_j/d_1 and the shape of the flow profile.

Now it is not too difficult to visualize the application to the flow of an upper boundary having the same profile as the mean free surface. Like the spillway profile that is shaped according to the lower surface of the corresponding weir nappe, the presence of the solid boundary may be expected to have some effect upon the flow. In the case of the spillway, the predominant effect is the addition of shear. In the case of the jump, it is rather the elimination of both the freedom of the surface to fluctuate and the presence of entrained air. However, measurements of the pressure head along the floor of a flume under a jump yield values which differ from the local depths by no more than the experimental error, indicating at once that the pressure distribution can be assumed to be hydrostatic and that the quantity of air in suspension is actually insufficient to change appreciably either the density or the specific weight. As for the surface fluctuations, measurement of the resulting wave amplitudes just downstream and approximation therefrom of the resulting wave energy has shown this to be less than a percent of the

energy of the flow itself. It would thus seem reasonable to assume that the presence of the upper boundary would have at the most only a secondary effect upon the flow pattern.

If the foregoing premise is accepted, then it must also be granted (in accordance with the general mechanics of confined flow) that the same pattern would obtain between the upper and lower boundaries at other rates of flow, if only the Reynolds numbers did not differ greatly. However, no longer would the mean pressure intensity along the upper boundary be atmospheric at all points, for it must change in accordance with the Bernoulli equation. On the other hand, if the linear quantities in the foregoing equations are considered to be the piezometric heads h (i.e., the sum of pressure head and elevation, which is presumably constant over any vertical section), the following relationships must continue to prevail between the enclosed model and its free-surface prototype.

$$\frac{h_2 - h_1}{U_1^2/2g} = \frac{d_2 - d_1}{U_1^2/2g} \quad (3)$$

$$1 - \frac{h_2 - h_1}{U_1^2/2g} - \frac{d_1^2}{d_2^2} = \frac{H_L}{U_1^2/2g} \quad (4)$$

Again in accordance with the principles of fluid mechanics, it now makes no difference whether the fluid is a liquid or a gas - just as long as the Reynolds numbers are still comparable and the velocities of the gas are not so high (i.e., two or three hundred feet per second) as to cause compressibility effects. Hence the same patterns of mean flow and turbulence should be obtainable through use of air of density ρ as the experimental fluid. Moreover, since the elevation term could then be neglected in the Bernoulli and related equations, the foregoing model-prototype expressions would reduce to the following pressure forms:

$$\frac{p_2 - p_1}{\rho U_1^2/2} = \frac{d_2 - d_1}{U_1^2/2g} \quad (5)$$

$$1 - \frac{p_2 - p_1}{\rho U_1^2/2} - \frac{d_1^2}{d_2^2} = \frac{H_L}{U_1^2/2g} \quad (6)$$

Although the Froude number cannot be expressed by replacing d_1 with either h_1 or p_1/γ (since the pressure load on the system is no longer determined by free-surface conditions), it will be seen that the right-hand sides of Eqs. (3) and (5) are still completely governed by the prototype magnitude of F_1 - and hence the left-hand sides as well. Moreover, for any Froude number the pressure-distribution terms $(p - p_1)/(p_2 - p_1)$ and $(h - h_1)/(h_2 - h_1)$ should be numerically equal to the profile dimension $(d - d_1)/(d_2 - d_1)$ at homologous sections. To the extent that these equalities

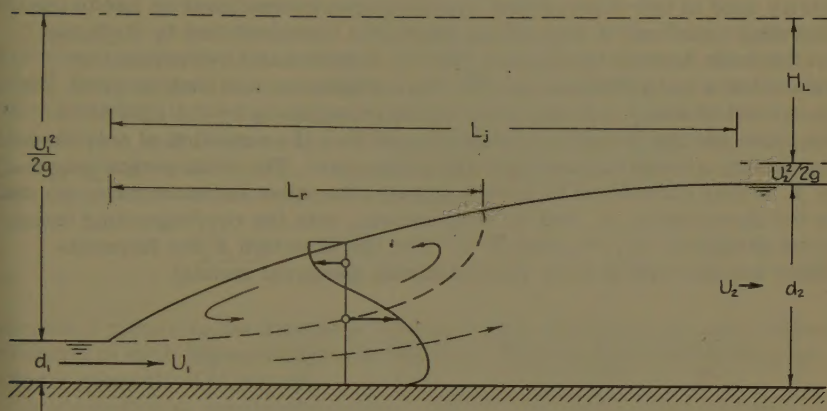


Fig. 1. Definition sketch of hydraulic jump.

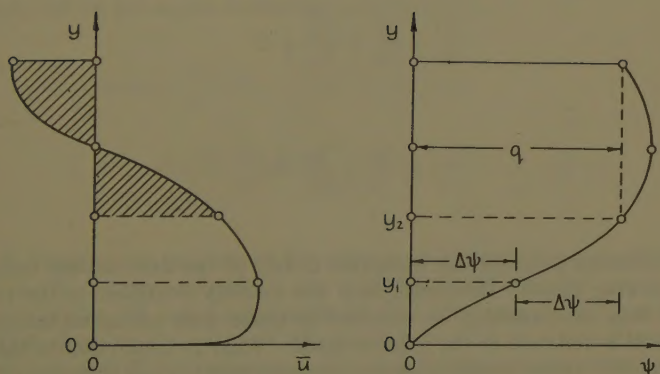


Fig. 3. Location of stream lines from velocity distribution.

are actually realized in prototype and model, the flow patterns themselves may be considered comparable.

Momentum Relationship

To obtain a more precise form of the momentum equation than that customarily used in one-dimensional hydraulics, recourse must be had to the differential equations of motion¹ as adapted to turbulent flow by Reynolds from the form derived for laminar flow by Stokes, and as presented in standard texts on hydrodynamics.⁽²⁾ This adaptation involved, in brief, the replacement of every instantaneous velocity magnitude by the sum of its mean value and its deviation therefrom, and then the retention of only those terms having a temporal average other than zero. The local vector magnitude V is thus considered to have in general the mean components \bar{u} , \bar{v} , and \bar{w} in the directions x , y , and z , respectively, with the corresponding instantaneous deviations u' , v' , and w' . For the direction x the Reynolds equation has the typical form (bars denoting temporal means)

$$\begin{aligned} \bar{u} \frac{\partial \bar{u}}{\partial x} + \bar{v} \frac{\partial \bar{u}}{\partial y} + \bar{w} \frac{\partial \bar{u}}{\partial z} + \overline{u' \frac{\partial u'}{\partial x}} + \overline{v' \frac{\partial u'}{\partial y}} + \overline{w' \frac{\partial u'}{\partial z}} \\ = -\frac{1}{\rho} \frac{\partial \bar{p}}{\partial x} + \bar{X} + \frac{\mu}{\rho} \left(\frac{\partial^2 \bar{u}}{\partial x^2} + \frac{\partial^2 \bar{u}}{\partial y^2} + \frac{\partial^2 \bar{u}}{\partial z^2} \right) \end{aligned} \quad (7)$$

Herein μ is the dynamic viscosity and \bar{X} , the x -component of the body force (such as the attraction of gravity) per unit mass.

This is fundamentally an equation of acceleration, for the terms to the left of the equality sign represent the rates of change of the velocity components of the mean motion and of the turbulence, and the terms to the right represent the pressure, body, and viscous forces per unit mass by which the velocity changes are produced. Through introduction of the two equations of continuity,

$$\frac{\partial \bar{u}}{\partial x} + \frac{\partial \bar{v}}{\partial y} + \frac{\partial \bar{w}}{\partial z} = 0 \quad (8)$$

and

$$\frac{\partial u'}{\partial x} + \frac{\partial v'}{\partial y} + \frac{\partial w'}{\partial z} = 0 \quad (9)$$

1. Space limitations prevent the inclusion in full of the derivations outlined in the following pages. However, they are readily available in the literature, and they can probably be checked by those with advanced training even without reference to the papers cited. What is important to the general reader is the implicit demonstration that (a) the customary jump relationships are one-dimensional approximations, (b) a more refined analysis of the role of turbulence must stem from the basic equations of motion, (c) the derived expressions must in turn be simplified, but only in accordance with experimental evidence, and (d) the final results are broadly significant.

the acceleration terms can be written in the alternative form

$$\frac{\partial(\bar{u}^2)}{\partial x} + \frac{\partial(\bar{u}\bar{v})}{\partial y} + \frac{\partial(\bar{u}\bar{w})}{\partial z} + \frac{\partial\bar{u}^2}{\partial x} + \frac{\partial\bar{u}\bar{v}}{\partial y} + \frac{\partial\bar{u}\bar{w}}{\partial z}$$

which is used in a subsequent derivation.

Since there is an equation of acceleration for each of the three coordinate directions, a considerable saving in space, without sacrifice of clarity, is gained by the use of tensor notation, in which the quantities u , v , and w are represented by u_i or u_j , and x , y , and z by x_i or x_j . In shorthand form, the indices i and j denote in turn each of the three coordinate directions. The foregoing equation and its counterparts for the other two directions are thus represented at one and the same time by

$$\frac{\partial(\bar{u}_i \bar{u}_j)}{\partial x_j} + \frac{\partial \overline{u_i u_j}}{\partial x_j} = -\frac{1}{\rho} \frac{\partial \bar{p}}{\partial x_i} + \bar{X}_i + \frac{\mu}{\rho} \frac{\partial^2 \bar{u}_i}{\partial x_j \partial x_j} \quad (10)$$

wherein i refers to the direction characterizing each equation and j to the direction of each independent term within it. Repetition of indices thus denotes a summation of terms.

Any equation of acceleration may - like the Newtonian equation itself - also be regarded as an equation of momentum, and it will be seen that multiplication of both sides of the foregoing relationship by the mass density will give each term the dimension of rate of change of momentum per unit volume or impulse per unit volume per unit time. The physical significance of this expression becomes the greater as it is integrated over a given space through which the fluid moves. By the Gaussian rule of the calculus relating volume integrals and surface integrals

$$\int_V \frac{\partial(-)}{\partial x_j} dV = \int_S (-) \frac{\partial x_j}{\partial n} dS \quad (11)$$

the result can be put in the following general form:

$$\begin{aligned} \int_S \rho \bar{u}_i \bar{u}_j \frac{\partial x_j}{\partial n} dS + \int_S \rho \overline{u_i u_j} \frac{\partial x_j}{\partial n} dS \\ = - \int_S \bar{p} \frac{\partial x_i}{\partial n} dS + \int_V \rho \bar{X}_i dV + \int_S \mu \frac{\partial \bar{u}_i}{\partial x_j} \frac{\partial x_j}{\partial n} dS \end{aligned} \quad (12)$$

Herein S denotes the surface of the region over which the integration is performed, n the outward normal to the surface, and V the enclosed volume. The terms at the left (each representing nine different quantities) embody the net flux of momentum (three components in each of three directions) of the mean flow and of the turbulence out of the region in question - i.e., the difference between the rates of efflux and influx. The first term at the right denotes the three components of the mean normal force exerted externally on the surface of the region; the second, the three components of the weight of the fluid contained within the region; and the third, the three components of the mean tangential force exerted on the surface.

For the case in which the hydraulic jump is formed on a horizontal bed of great width, the pertinent momentum equation is that for the direction x . If it is assumed that the turbulence is negligible at the initial section, that the pressure distribution is hydrostatic at any arbitrary section, and that both the viscous and the turbulent stresses are negligible over the free surface, the equation reduces to

$$\int_0^d \rho \bar{u}^2 dy - \int_0^{d_1} \rho \bar{u}^2 dy + \int_0^d \rho \overline{u'^2} dy = \frac{\gamma d_1^2}{2} - \frac{\gamma d^2}{2} + \int_0^x \mu \left(\frac{\partial \bar{u}}{\partial y} \right)_{y=0} dy \quad (13)$$

For the limiting case that $x = L_j$ and $d = d_2$, this expression will be seen to differ in the following ways from the simpler version normally used in studying the jump. First, the change in the mean momentum flux, expressed as the difference between the first two integrals, per-force includes the effect of local departure from the average velocity over the vertical section. Second, the change in the momentum flux of the turbulence is represented by the next integral, which embodies the sole effect of turbulence in the force balance. Finally, the effect of variable bed shear $\tau_0 = \mu (\partial \bar{u} / \partial y)_{y=0}$ over the length of the jump is included in the integral at the right. It goes without saying that application of the equation requires the determination of each integral from known distributions of the variables in question - an evident reason for the more customary use of the simplified relationship. Only through the quantitative evaluation of the integral terms, however, can the magnitude of the error arising from the neglect of the distribution details be appraised.

Equations of Energy

An essential characteristic of the Reynolds equations of motion, and hence of the momentum equations derived from them, is the absence of all viscous stresses except those involving the mean velocities. However, although the viscous terms containing the velocity fluctuations are invariably eliminated by the averaging process, there remain certain inertial terms consisting of fluctuation products which can conveniently be considered to have the nature of a stress and hence to take their place. These are the momentum-transport terms of the secondary motion, which may be combined with the terms for mean viscous stress to yield

$$\tau_{ij} = \mu \left(\frac{\partial \bar{u}_i}{\partial x_j} + \frac{\partial \bar{u}_j}{\partial x_i} \right) - \rho \overline{u'_i u'_j} \quad (14)$$

The momentum-transport terms $\rho \overline{u'_i u'_j}$ are known as Reynolds stresses.

If, before averaging, each of the equations of motion is multiplied by the corresponding component of the instantaneous velocity, and the three equations are then added, there will result a differential equation of work and energy⁽³⁾ of the form

$$\begin{aligned} & \bar{u}_j \frac{\partial}{\partial x_j} \left(\frac{\rho \bar{V}^2}{2} + \frac{\rho \bar{V}'^2}{2} \right) + \overline{u_j \frac{\partial(\rho \bar{V}'^2/2)}{\partial x_j}} + \frac{\partial(\bar{u}_i \rho \bar{u}_i \bar{u}_j)}{\partial x_j} \\ &= -\bar{u}_i \frac{\partial \bar{p}}{\partial x_i} - \overline{u'_i \frac{\partial p'}{\partial x_i}} + \rho \bar{u}_i \bar{X}_i + \overline{\mu \bar{u}_i \frac{\partial^2 \bar{u}_i}{\partial x_j \partial x_j}} + \overline{\mu u'_i \frac{\partial^2 u'_i}{\partial x_j \partial x_j}} \end{aligned} \quad (15)$$

Inspection of this equation will reveal not only that many of the fluctuating stresses which disappeared from the momentum equations during the averaging process are now retained, but also that there is a fairly consistent parallel between the terms for the mean flow and those for the turbulence. In fact, it is instructive to segregate the terms of the two categories in the following work-energy relationships for the mean flow and for the turbulence (which are also directly derivable by combining the pertinent equations and velocity components):

$$\bar{u}_j \frac{\partial(\rho \bar{V}^2/2)}{\partial x_j} + \rho \bar{u}_i \frac{\partial \bar{u}_i \bar{u}_j}{\partial x_j} = -\bar{u}_i \frac{\partial \bar{p}}{\partial x_i} + \rho \bar{u}_i \bar{X}_i + \mu \bar{u}_i \frac{\partial^2 \bar{u}_i}{\partial x_j \partial x_j} \quad (16)$$

$$\bar{u}_j \frac{\partial(\rho \bar{V}'^2/2)}{\partial x_j} + \overline{u'_j \frac{\partial(\rho \bar{V}'^2/2)}{\partial x_j}} + \rho \bar{u}_i \bar{u}_j \frac{\partial \bar{u}_i}{\partial x_j} = -\overline{u'_i \frac{\partial p'}{\partial x_i}} + \overline{\mu u'_i \frac{\partial^2 u'_i}{\partial x_j \partial x_j}} \quad (17)$$

As was done with the momentum form of the equations of motion, it is now in order to integrate the differential work-energy equations over a given region of space. After the appropriate volume integrals have been changed by the Gaussian rule to surface integrals, the work-energy equation for the mean flow assumes the form

$$\begin{aligned} & \int_S \frac{\rho \bar{V}^2}{2} u_j \frac{\partial x_j}{\partial n} dS + \int_S \rho \bar{u}_i \bar{u}_j \frac{\partial x_j}{\partial n} dS - \int_V \rho \bar{u}_i \bar{u}_j \frac{\partial \bar{u}_i}{\partial x_j} dV \\ &= -\int_S \bar{p} \bar{u}_i \frac{\partial x_i}{\partial n} dS + \int_V \rho \bar{X}_i \bar{u}_i dV + \int_S \mu \left(\frac{\partial \bar{u}_i}{\partial x_j} + \frac{\partial \bar{u}_j}{\partial x_i} \right) \bar{u}_i \frac{\partial x_j}{\partial n} dS - \int_V \mu \left(\frac{\partial \bar{u}_i}{\partial x_j} + \frac{\partial \bar{u}_j}{\partial x_i} \right) \frac{\partial \bar{u}_i}{\partial x_j} dV \end{aligned} \quad (18)$$

The successive terms have the following significance: That at the extreme left represents the net flux of kinetic energy of the mean motion out of the region in question (i.e., the rate of increase in kinetic energy as the fluid passes through the region). The second and third terms, while also representing energy transport, can best be explained as the rates at which work is done by the Reynolds stresses over the surface and throughout the interior of the region, respectively. The first and second terms at the right of the equality sign are the rates at which work is done by the external pressures and the body forces. The third and fourth are evidently the rates at which work is done by the viscous stresses of the mean flow over the surface and throughout the interior of the region, respectively.

Now the work done externally by the viscous stresses (the third term at the right) is wholly conservative (since, as is evident from the Gaussian transformation, it is derivable from a potential or space derivative), whereas that done internally (the last term) is wholly dissipative. Because of the analogy between the turbulent and viscous stresses, one might seek a further parallel between the types of work done in each instance. In fact, whereas the second term at the left, like the third at the right, is conservative, the

third at the left can be considered dissipative like the last at the right if one assumes that energy transferred from the mean flow to the turbulence can never be recovered. The third term at the left, in other words, represents the rate at which turbulence is produced at the expense of the mean flow. (The integral itself is inherently negative, so that the negative sign before it denotes a positive rate of production.)

The corresponding work-energy equation for the secondary motion is as follows:

$$\begin{aligned} & \int_S \frac{\rho \sqrt{V'^2}}{2} u_j \frac{\partial x_j}{\partial n} dS + \int_S \frac{\rho \sqrt{V'^2}}{2} u_j' \frac{\partial x_j}{\partial n} dS + \int_V \rho \overline{u_i' u_j'} \frac{\partial u_i}{\partial x_j} dV \\ &= - \int_S \overline{p' u_i'} \frac{\partial x_i}{\partial n} dS + \int_S \mu \left(\frac{\partial u_i'}{\partial x_j} + \frac{\partial u_j'}{\partial x_i} \right) u_i' \frac{\partial x_j}{\partial n} dS - \int_V \mu \left(\frac{\partial u_i'}{\partial x_j} + \frac{\partial u_j'}{\partial x_i} \right) \frac{\partial u_i'}{\partial x_j} dV \end{aligned} \quad (19)$$

The first two terms at the left, by analogy to the first in the equation for the primary motion, represent the net flux of kinetic energy of turbulence out of the region by convection and diffusion (i.e., by the mean flow and by the turbulence), respectively. The third is again the rate of production of turbulence, now a negative quantity so far as the work accomplished by the turbulence is concerned. The first term on the right of the equality sign is the rate at which work is done externally on the surface of the region by the fluctuating pressures. The last two terms represent the rates at which work is done by the viscous stresses of the turbulence over the surface of the region and throughout the interior, respectively, the former being conservative and the latter dissipative.

On the previous assumption that the initial section is free from turbulence, that both the mean and turbulent stresses can be neglected over the free surface, and that the pressure distribution is hydrostatic throughout, reduction of the work-energy equation for the mean motion to the case of the hydraulic jump on a level bed of great width yields the following result:

$$\begin{aligned} & \int_0^d \frac{\bar{V}^2}{2g} \bar{u} dy - \int_0^{d_1} \frac{\bar{V}^3}{2g} dy + \int_0^d \frac{\bar{u} \bar{u}^2 + \bar{v} \bar{u} \bar{v}}{g} dy \\ & - \int_0^d \int_0^x \left[\frac{\bar{u}' \bar{v}'}{g} \left(\frac{\partial \bar{u}}{\partial y} + \frac{\partial \bar{v}}{\partial x} \right) + \frac{\bar{u}^2 - \bar{v}^2}{g} \frac{\partial \bar{u}}{\partial x} \right] dy dx = q d_1 - q d \\ & + \int_0^d \frac{\mu}{\gamma} \left[2 \bar{u} \frac{\partial \bar{u}}{\partial x} + \bar{v} \left(\frac{\partial \bar{u}}{\partial y} + \frac{\partial \bar{v}}{\partial x} \right) \right] dy - \int_0^d \int_0^x \frac{\mu}{\gamma} \left[4 \left(\frac{\partial \bar{u}}{\partial x} \right)^2 + \left(\frac{\partial \bar{u}}{\partial y} + \frac{\partial \bar{v}}{\partial x} \right)^2 \right] dy dx \end{aligned} \quad (20)$$

For the limiting case that $x = L_j$ and $d = d_2$, the first two terms on each side of the equation correspond to those of the usual one-dimensional open-channel relationship, with due account taken of the variation in velocity over the cross section. The third terms represent work done on the end section by the turbulent and viscous stresses. The last terms combine to form the quantity H_{Lq} , since they indicate the rate at which turbulence is produced by the mean motion and the rate at which energy is dissipated by the mean

viscous stresses.

Reduction of the energy equation for the turbulent motion to the same conditions yields the following result:

$$\begin{aligned} & \int_0^d \frac{\overline{V'^2}}{2g} \bar{u} \, du + \int_0^d \frac{\overline{V'^2}}{2g} u' \, dy + \int_0^d \int_0^x \left[\frac{\overline{u'v'}}{y} \left(\frac{\partial \bar{u}}{\partial y} + \frac{\partial \bar{v}}{\partial x} \right) + \frac{\overline{u'^2 - v'^2}}{g} \frac{\partial \bar{u}}{\partial x} \right] dy \, dx \\ & = - \int_0^d \frac{\overline{p'}}{\gamma} u' \, dy + \int_0^d \frac{\mu}{\gamma} \left[\frac{\partial}{\partial x} \left(\frac{\overline{V'^2}}{2} + \overline{u'^2} \right) + \frac{\partial \overline{u'v'}}{\partial y} \right] dy - \int_0^d \int_0^x K \frac{\mu}{\gamma} \left(\frac{\partial \bar{u}}{\partial x} \right)^2 dy \, dx \end{aligned} \quad (21)$$

Herein terms appear only for the arbitrary section, since it was assumed that no turbulence existed at the initial section. The proportionality factor K permits what are actually 15 terms to be written as one; its use is further justified by the fact that (a) the dissipation is most intense in the smallest eddies, (b) the smallest eddies tend to be isotropic, and (c) in isotropic turbulence this factor has the constant magnitude of 15.(4) Only if the cumulative production (the third term on the left) and the cumulative dissipation (the third term on the right) are equal will the turbulence at the final section (i.e., for $d = d_2$ at $x = L_j$) be negligible. The extent of the actual inequality of these terms can evidently be ascertained only through detailed measurement and analysis of the mean and fluctuating patterns of flow.

Experimental Equipment and Procedure

To simulate the mean and fluctuating patterns of the hydraulic jump in air, a special duct having a length of 9 feet, a width of 1 foot, and a maximum depth of 1 foot, was built of plywood and plexiglass. Both the front wall and the curved surface were made transparent to simplify the visual setting of instruments, and for added convenience in supporting them the plane surface corresponding to the bed of the channel was placed on top (see Fig. 2). The form of the curved surface was controlled by successive pairs of adjusting screws at 6-inch intervals over the entire length of the duct. Both the plane and the curved surfaces were provided with piezometer holes along the centerline, and a grid with a 0.02-foot mesh was ruled on the rear wall as a guide in controlling the surface profile. At the downstream end the duct underwent a smooth transition to a 12-inch circular section connected to the intake of a 5-horsepower centrifugal blower, which discharged into the surrounding space through a baffled diffuser. The intake end was provided with a rectangular bell having carefully rounded sides. The bottom side of the bell was adjustable in position, and the curved surface of the test section was hinged to it after a 2.5-inch tangent.

Because the velocity of the flow varied greatly in magnitude and direction, even undergoing full reversal in the roller, it was considered desirable to utilize a single instrument that would respond in the same manner to flow in either direction. This precluded the ordinary type of Pitot tube, but either a Pitot cylinder with opposing holes or a simple hot-wire anemometer would have sufficed. The instrument actually used was a double Pitot, symmetrical upstream and down, formed of two L's of 0.04-inch tubing placed back to back



Fig. 2. Photograph of air-flow model.

with stagnation openings 0.6 inch apart. The tube was calibrated in an air stream for both magnitude and inclination of the velocity vector, differential pressures being indicated on a precision manometer reading to 0.001 inch of alcohol. In operation, the tube was inserted through each of a series of centerline openings at 6-inch intervals in the plane top of the duct and a velocity traverse made with the tube in its normal position. On the assumption that the velocity indication corresponded to a zero inclination, the location of the stream lines for equal increments of the stream function Ψ was evaluated from plots of the velocity distribution (see Fig. 3) according to the relationship

$$\psi = \int_0^y \bar{u} dy \quad (22)$$

With the approximate angularity thus indicated by the stream-line pattern, the velocity readings were corrected by means of the angularity calibration, and the determination of stream-line location was repeated. A single correction of this nature usually proved sufficient.

Supplementary measurements for the determination of the local intensity of boundary shear were made with a 0.04-inch stagnation tube in contact with the plane boundary. The tube had been calibrated in connection with other boundary-layer measurements, and Preston's method of shear calculation⁽⁵⁾ was followed in both instances. The various characteristics of turbulence ($\sqrt{u'^2}$, $\sqrt{v'^2}$, $\sqrt{w'^2}$, $\overline{u'v'}$, and $(\partial u'/\partial t)$) were measured with a constant-temperature hot-wire anemometer,⁽⁶⁾ the operation of which is also too specialized for further comment here. It should be remarked, however, that although designed for a precision of $\pm 2\%$ under ideal conditions - the hot wire (like any means of turbulence measurement) must be expected to have a probable error of ± 5 -10% in practice and to range as high as $\pm 20\%$ in zones of abnormally great intensity of fluctuation.

Since the efficacy of the air-model method depends entirely upon the degree of similarity between the model and its water prototype, rather extensive preliminary tests were conducted to determine both the mean-flow characteristics of the jump itself and the accuracy with which they could be simulated in the air duct. The jump was produced at various Froude numbers in the 1-foot glass-walled flume of the Institute at about the same scale as the air duct (i.e., $d_2 = 1$ foot). The form of the free surface was determined by point gage, the pressure distribution on the bottom by water manometer, and the end of the roller by surface float. The several length ratios thus obtained are plotted in Fig. 4. For the Froude number $F = 4$ the velocity distribution was also measured by means of the double Pitot tube (using the technique of flushing before each reading to eliminate errors due to entrapped air). The stream lines are plotted in Fig. 5, at distorted scale to exaggerate the vertical displacement. Superposed on the latter diagram are the corresponding stream lines for flow in the air duct at a comparable depth ratio, surface profile, and Reynolds number, together with the pressure distribution on plane and curved surfaces. The agreement between the model and prototype results is seen to be quite satisfactory.

Inspection of Fig. 4 will show the usual slight deviation of the measured depth ratio from that computed by means of the simplified momentum relationship of Eq. (1). This is attributable primarily to the neglect of boundary shear in the course of the derivation. In fact, it was the measured depth

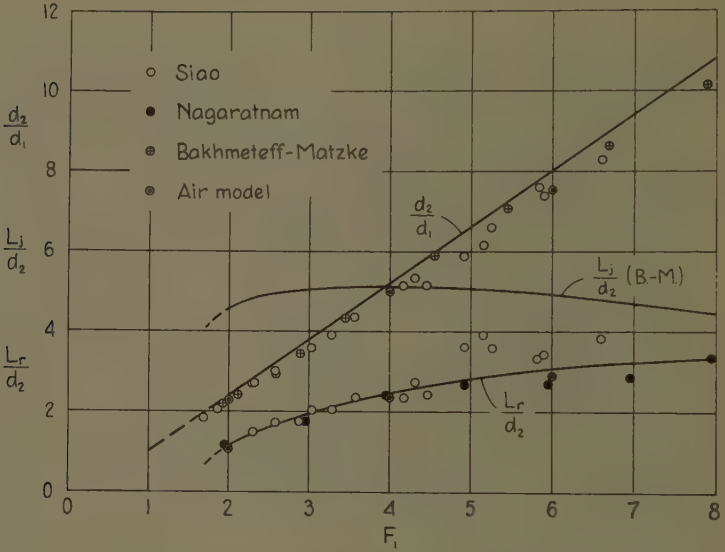


Fig. 4. Linear characteristics of the jump.

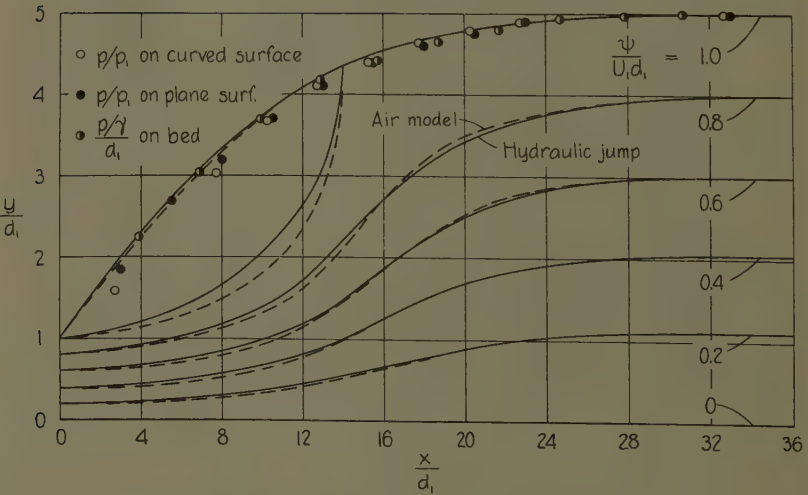


Fig. 5. Comparison of mean patterns of flow in model and prototype for $F = 4$.

ratio rather than the computed that had to be used in setting the duct profile. Moreover, in order to reduce wall shear - and hence its influence upon the flow pattern - to a minimum, after introductory measurements the original duct was rebuilt to a width of 2.5 feet. All further data presented herein were obtained with the wider flow section. Even then, however, wall effects upon the centerline flow were still noticeable, for the unit discharge $q = \int u \, dy$ gradually increased with distance downstream. As a first-order correction for this variation, the local rather than the initial unit discharge was used in computing the reference velocity; in no case did the change exceed 6%. Unfortunately, correction for the volume flux is not the same as that for either the momentum or energy flux, the only means of handling all together being to flare the duct laterally in proportion to the boundary-layer growth.

Following the preliminary tests, systematic measurements were made of the primary and secondary flow patterns for Froude numbers of 2, 4, 6, and 8 - though without attaining a satisfactory degree of approximation at the highest of these. In each instance the downstream dimension was held constant at 1 foot, and the upstream dimension and the surface profile were varied in accordance with the prototype requirements. Reproduction of the necessary conditions was found to become increasingly difficult as the Froude number increased. In no event, of course, was it possible to obtain exact agreement of surface profile, pressure distribution, and flow pattern (as indicated by the length of roller) simultaneously, and hence each case involved slight inaccuracies in all three factors to the end of obtaining the best overall duplication. Barely perceptible inclination of the short tangent section of the bell was of considerable use in this regard. However, no such artifice sufficed to produce a state even roughly approximating similarity at a Froude number of 8, for despite the use of intermediate splitter vanes the rapidly divergent flow could not be stabilized either laterally or longitudinally.

The basic results for the other three Froude numbers are plotted in Figs. 6 and 7, the former diagram embodying the mean-flow data and the latter the turbulence data. (The w' component of turbulence is not shown, for reasons of simplicity; it did not differ greatly from v' , and the measurements, moreover, indicated that $\int_0^d \overline{u'^2} \, dy \approx \int_0^d (\overline{v'^2} + \overline{w'^2}) \, dy$ - i.e., $\int_0^d \overline{v'^2} \, dy \approx \int_0^d \overline{u'^2} \, dy$ Values of the time derivative of u' are introduced later.)

Whereas the initial depth is commonly used as the length parameter in dealing with the jump as such, in comparing the results for various Froude numbers it proved to be more convenient to use the final depth, as this maintains essentially the same longitudinal scale. Purely geometric ratios are hence given in terms of d_2 . The Froude number necessarily involves d_1 , of course, and all other parameters are also expressed in terms of the initial depth and velocity.

Interpretation of Results

Figures 6 and 7, even without further manipulation of the data, display trends of great significance in both the primary and the secondary aspects of the flow. The roller, first of all, is seen to become progressively longer as the Froude number increases. From the curves of velocity distribution three pertinent loci can readily be traced: that of zero velocity, passing

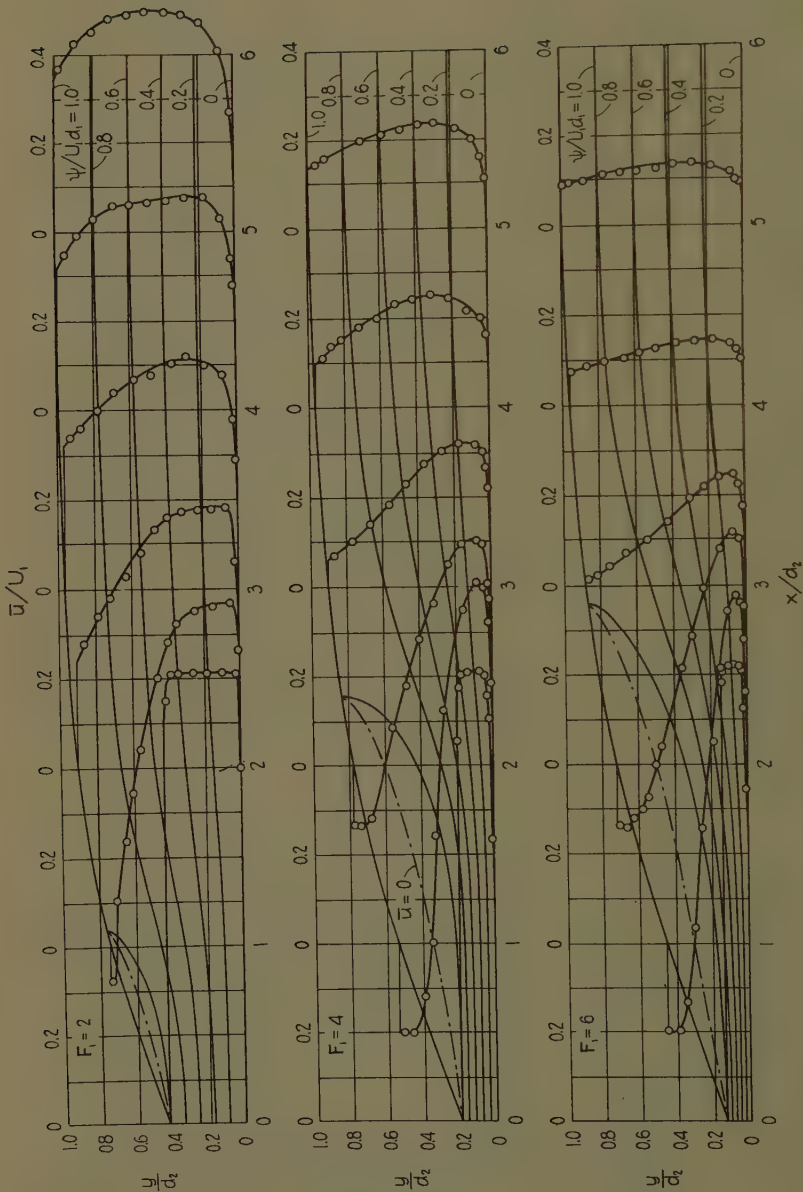


Fig. 6. Distribution of mean longitudinal velocity and corresponding patterns of flow.

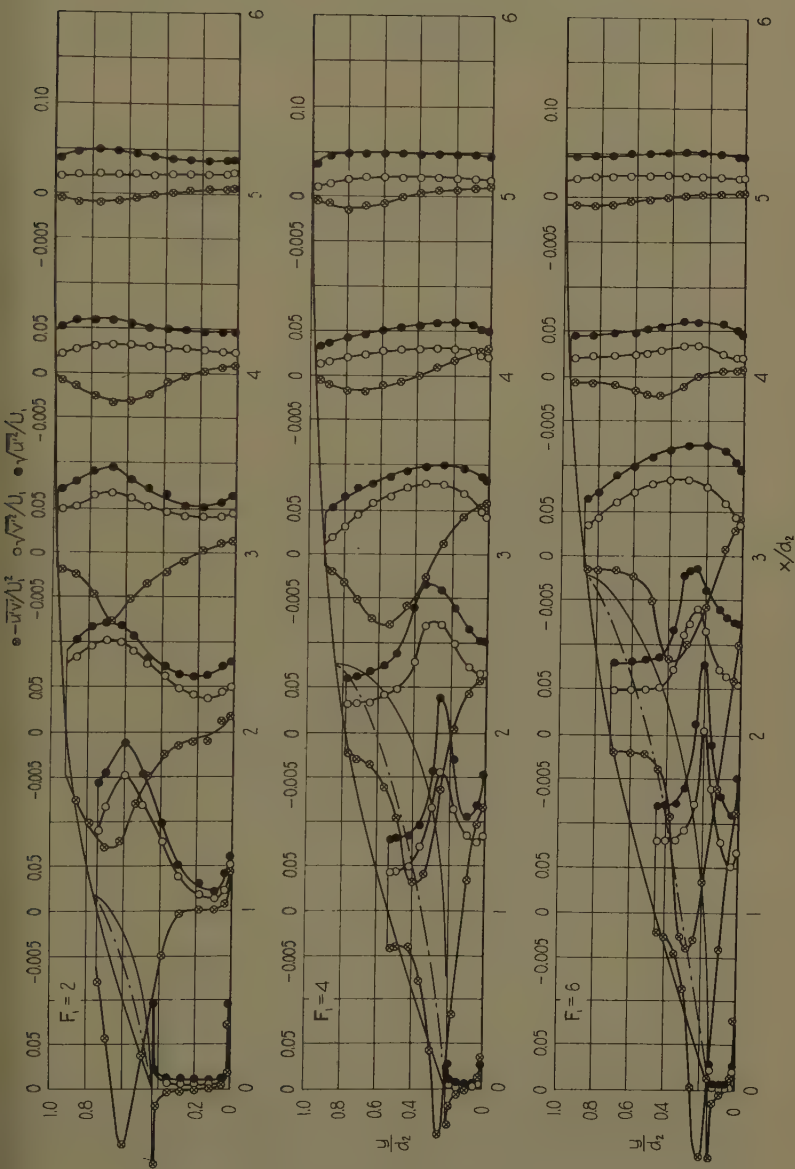


Fig. 7. Distribution of turbulence intensities and mean product of components.

through the middle of the roller; that of maximum velocity gradient near the roller edge; and that of maximum velocity, essentially midway between the roller and the bed. Examination of the curves of turbulence intensity will show that this is a minimum where the velocity gradient is a minimum, and vice versa. The intensity of turbulent shear is likewise highest in zones of maximum velocity gradient, and the distribution curves of $-\overline{u'v'}$ are seen to undergo a change in sign with the velocity gradient much in accordance with the Boussinesq-Prandtl approximation, (7)

$$\tau = -\rho \overline{u'v'} \approx \rho \epsilon \frac{\partial \bar{u}}{\partial y} \approx \rho \epsilon \frac{\partial \bar{u}}{\partial y} \left| \frac{\partial \bar{u}}{\partial y} \right| \quad (23)$$

The data presented in these figures may be utilized directly to evaluate the several terms in the momentum relationship of Eq. (13), reduced to non-dimensional form through division by $\rho U_1^2 d_1 = \rho U_1 q$. The relative magnitudes of the terms can be shown most conveniently by calculating and plotting the sum

$$\frac{1}{U_1^2 d_1} \int_0^d \bar{u}^2 dy + \frac{1}{U_1^2 d_1} \int_0^d \overline{u'^2} dy + \frac{1}{2 F_1^2} \frac{d^2}{d_1^2} + \frac{1}{R_1 U_1} \int_0^x \left(\frac{\partial \bar{u}}{\partial y} \right)_{y=0} dx$$

as a function of longitudinal distance, as shown in Fig. 8. Since the sum should be a constant at all successive sections, departure from its original value is a measure of the experimental (and perhaps computational) error. Of principal significance in connection with these results is the fact that the contribution of the turbulence to the momentum flux, although of considerable importance at intermediate sections, is small at each final section. The contribution of the bed shear, though likewise small, necessarily increases with both distance and Froude number (and, it should be remarked, with the viscous and roughness effects as well).

A comparable analysis of the energy relationship for the mean flow - Eq. (20) - proceeds in much the same fashion. On the assumption (verified experimentally) that the terms involving the mean viscous stresses are of much smaller order than the others, and with $d_1 U_1^3 / 2g = q U_1^2 / 2g$ as common denominator, it is now the non-dimensional sum

$$\begin{aligned} & \frac{1}{U_1^3 d_1} \int_0^d \nabla^2 \bar{u} dy + \frac{2}{F_1^2} \frac{d}{d_1} + \frac{2}{U_1^3 d_1} \int_0^d (\bar{u} \overline{u'^2} + \bar{v} \overline{v'^2}) dy \\ & - \frac{2}{U_1^3 d_1} \int_0^d \int_0^x \left[\overline{u'v'} \left(\frac{\partial \bar{u}}{\partial y} + \frac{\partial \bar{v}}{\partial x} \right) + (\overline{u'^2} - \overline{v'^2}) \frac{\partial \bar{u}}{\partial y} \right] dy dx \end{aligned}$$

that should be constant from section to section. Calculation of the various quantities from the data presented in Figs. 6 and 7 yields the curves shown in Fig. 9. The gradual change that characterized the corresponding sum in the momentum calculations is now even more pronounced - particularly for $F = 4$. No explanation is evident beyond experimental error, including the effect of wall retardation upon the central flow.

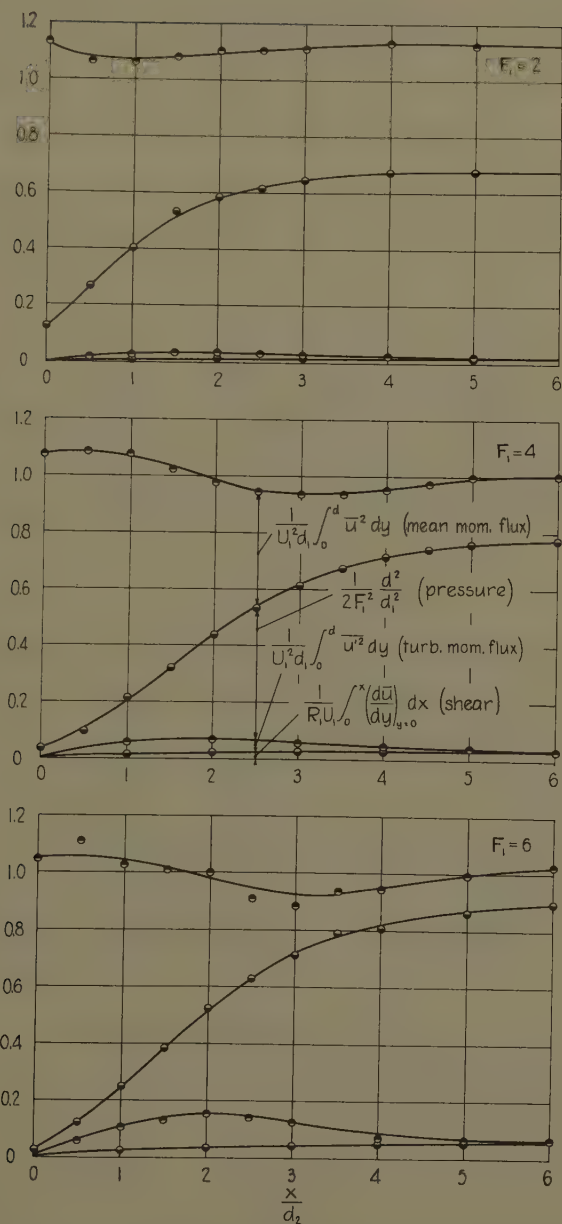


Fig. 8. Dimensionless plots of momentum balance.

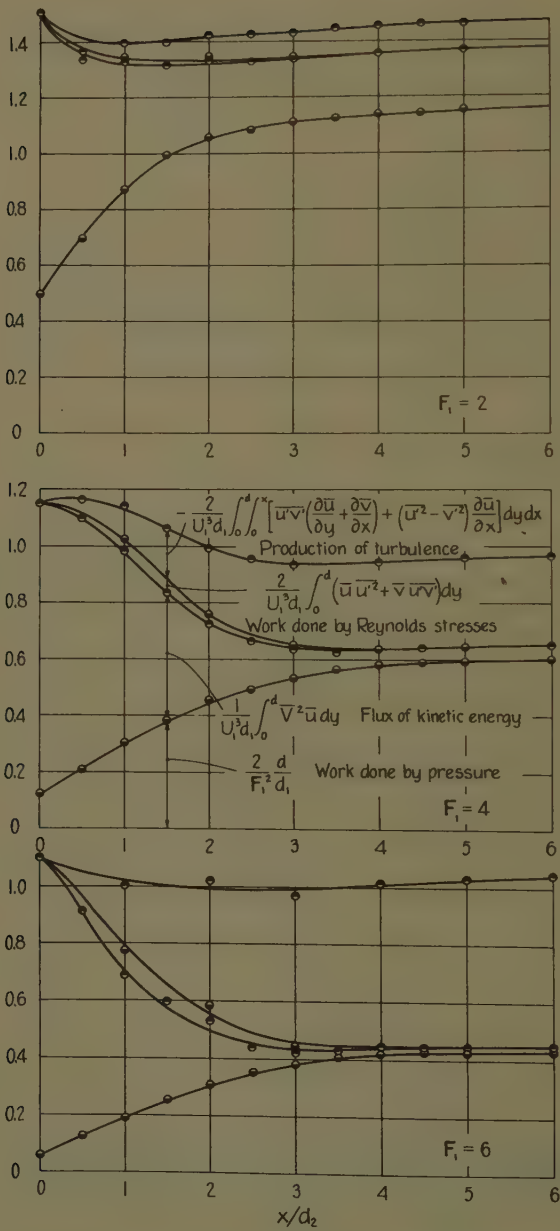


Fig. 9. Dimensionless plots of mean-energy balance.

Since it reappears in the energy equation of the turbulence, it is the turbulence-production term - the last member of the foregoing sum - that remains of primary interest. In fact, its variation in comparison with that of the turbulence-dissipation term is particularly significant - not only from section to section but over each section as well. For this reason the non-dimensional form of the local rate of production

$$- 2 \frac{d_1}{U_1^3} \left[\overline{u'v'} \left(\frac{\partial \bar{u}}{\partial y} + \frac{\partial \bar{v}}{\partial x} \right) + (\overline{u'^2} - \overline{v'^2}) \frac{\partial \bar{u}}{\partial x} \right]$$

(the double integral of which was used in preparing Fig. 9) is shown in detail in Fig. 10. Superposed on the same figure is the corresponding distribution of the local rate of dissipation

$$2 \frac{K}{R_1} \frac{d_1^2}{U_1^2} \overline{\left(\frac{\partial u'}{\partial x} \right)^2}$$

the measured mean-square temporal gradient $\overline{(\partial u' / \partial t)^2}$ having been used to approximate the required mean-square spatial gradient through division by \bar{u}^2 . The integrals of these distribution curves over the vertical sections are plotted against longitudinal distance in Fig. 11, together with the corresponding integral for the rate at which the kinetic energy of the turbulence is convected past each section:

$$\frac{1}{U_1^3 d_1} \int_0^d \overline{v'^2} \bar{u} dy$$

Use of the isotropic value $K = 15$ would have yielded dissipation curves differing only slightly from those plotted. However, estimation of the remaining terms of Eq. (21) for the final section of the jump showed them to be so small that the cumulative production and dissipation of turbulence energy through the jump (the areas under the curves of Fig. 11) could be considered essentially equal. This permitted bulk values of K to be calculated for each of the Froude numbers, the results being 12.2, 13.5, and 15.0 for 2, 4, and 6, respectively. How much significance can be attached to the trend in magnitude is a moot question. In any event, the curves plotted in Figs. 10 and 11 correspond to these values.

In studying the energy transformation of the turbulence, the non-dimensional sum that should be constant (i.e., essentially zero) from section to section is

$$\begin{aligned} & - \frac{2}{U_1^3 d_1} \int_0^d \int_0^x \left[\overline{u'v'} \left(\frac{\partial \bar{u}}{\partial y} + \frac{\partial \bar{v}}{\partial x} \right) + (\overline{u'^2} - \overline{v'^2}) \frac{\partial \bar{u}}{\partial x} \right] dy dx - \frac{1}{U_1^3 d_1} \int_0^d \overline{v'^2} \bar{u} dy \\ & - \frac{1}{\rho U_1^3 d_1} \int_0^d \overline{p'u'} dy - \frac{1}{U_1^3 d_1} \int_0^d \overline{v'^2 u'} dy - \frac{2K}{R_1 U_1^2} \int_0^d \int_0^x \overline{\left(\frac{\partial u'}{\partial x} \right)^2} dy dx \end{aligned}$$

The corresponding diagrams for the three Froude numbers are presented in Fig. 12. Not included in either the foregoing sum or the diagram itself is the

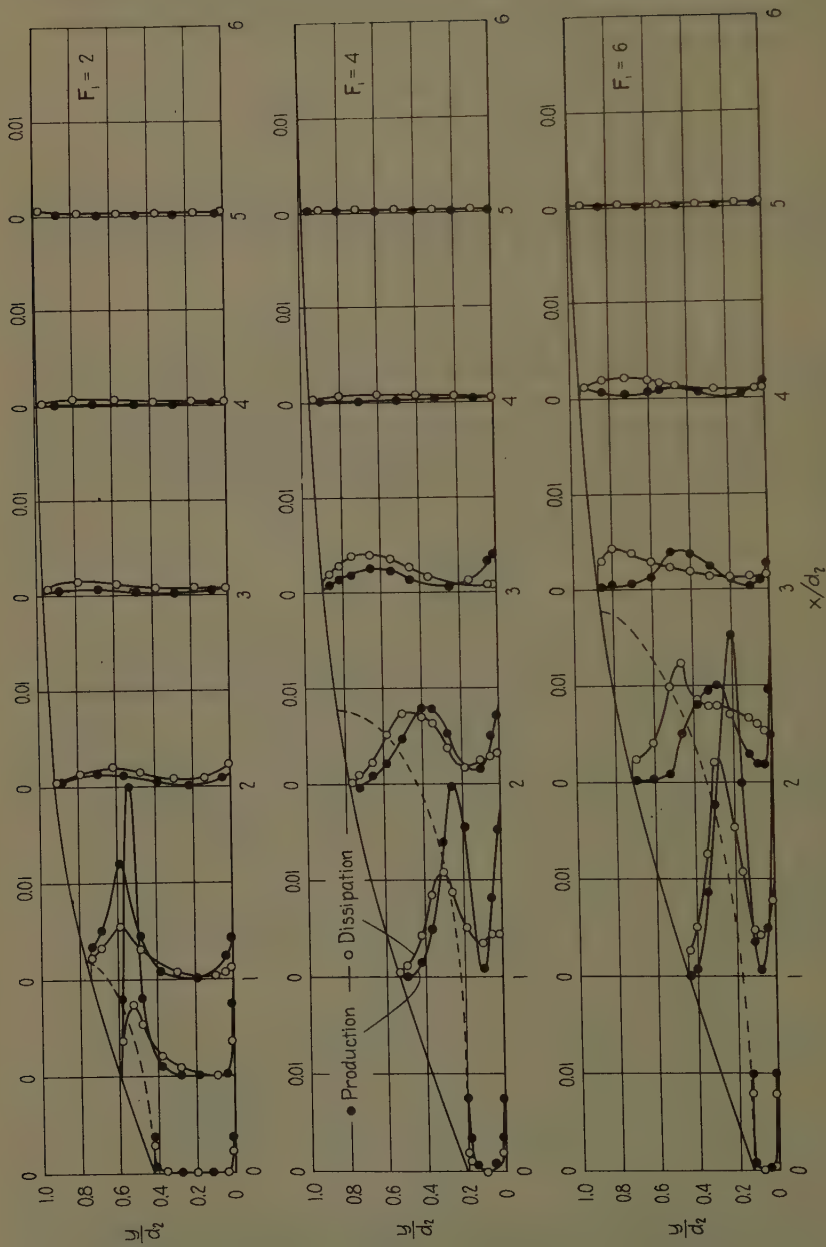


Fig. 10. Distribution of turbulence production and dissipation.

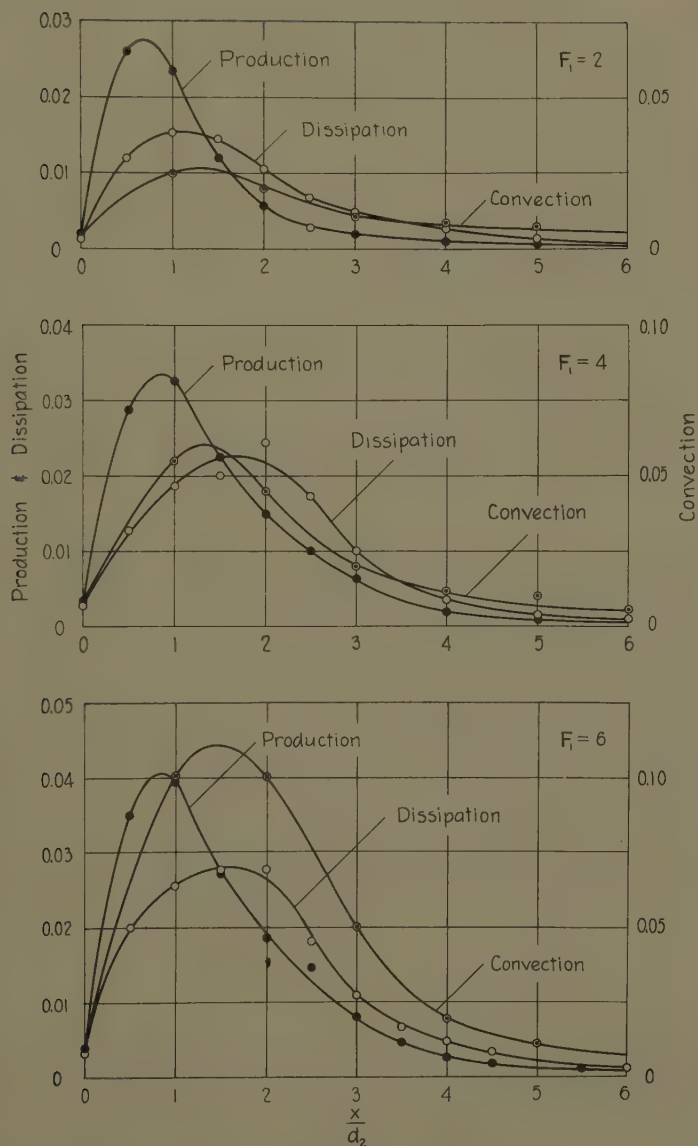


Fig. 11. Longitudinal variation in rates of production, convection, and dissipation of turbulence.

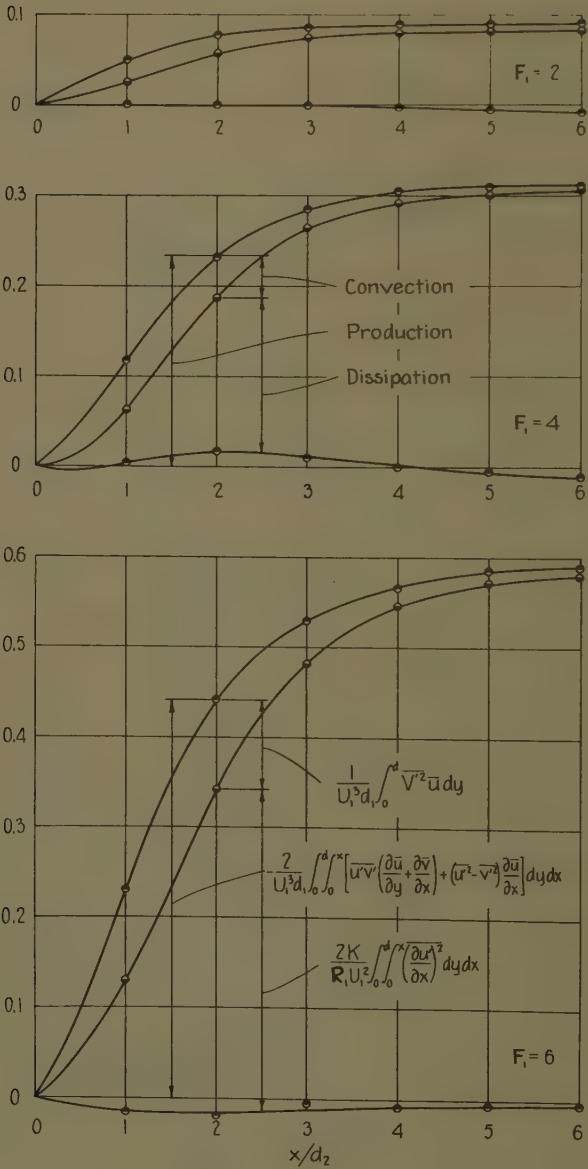


Fig. 12. Dimensionless plots of turbulence-energy balance.

rate at which work is done externally by the viscous stresses, for calculation of this term (the fifth) in Eq. (21) showed it to be of much smaller order than the others. It was impossible, on the other hand, to evaluate either the rate at which work was done by the fluctuating pressures or the rate of diffusion of the turbulent energy, since neither the velocity-pressure correlation involved in the former nor the triple velocity correlation in the latter could be measured with available equipment. The small difference between the computed values of the other terms might hence be assumed to represent - except for experimental error - the sum of these two.

Several related characteristics of the turbulence are to be noted in Figs. 10, 11, and 12. In the first of these, the locus of points of maximum production coincides closely with the border of the roller, whereas that for maximum dissipation lies appreciably higher, and the vertical spread of the dissipation curves is likewise greater. This emphasizes the fact that the turbulence is not wholly dissipated at its point of formation but is convected by the mean motion (including the secondary flow of the eddy) and diffused by its own mixing action. Much the same situation is seen from Fig. 11. Whereas the maximum rate of production per section occurs even ahead of the middle of each roller, the maximum rate of dissipation per section - as well as the maximum cross-sectional energy of the turbulence itself - occurs shortly before its end. As shown graphically by Fig. 12, the difference between the cumulative production and cumulative dissipation rates up to a given section is represented with close approximation by the rate of convection of turbulence past that section.

The most essential of the foregoing results are summarized in the three geometric diagrams of Fig. 13. Whereas these correspond to the usual one-dimensional representations of the jump, not only are they drawn to proper scale longitudinally as well as vertically, but they are quantitatively significant within the non-uniform zone of transition as well as in the uniform zones up- and downstream. They are, to be sure, approximations rather than exact renditions of the phenomenon, for the least important of the variables have been ignored and the discrepancies evident in Figs. 9 and 12 have been distributed among the remaining terms. All in all, however, the inaccuracies are judged to be no greater than the variable effects of bed roughness and slope encountered in the field.

Lowermost among the curves plotted in Fig. 13 are those showing the variation of depth - i.e., the profile of the free surface - for each of the Froude numbers. Next are those representing the addition of the velocity head of the mean flow to the depth, much as in the usual manner. However, whereas the correction factor

$$\alpha = \frac{1}{U^2 q} \int_0^d \nabla^2 \bar{u} dy$$

compensating for use of the mean velocity $U = q/d$ is usually assumed to be unity, its magnitude within the non-uniform zone was found to rise as high as 4; at the end of the transition, on the other hand, it was within 5% of unity in every case. The two sets of curves just discussed, it should be noted, are the only two included in the customary diagrams.

Third in the sequence illustrated are the curves showing the increase in head resulting from the inclusion of the velocity head of the turbulence. For

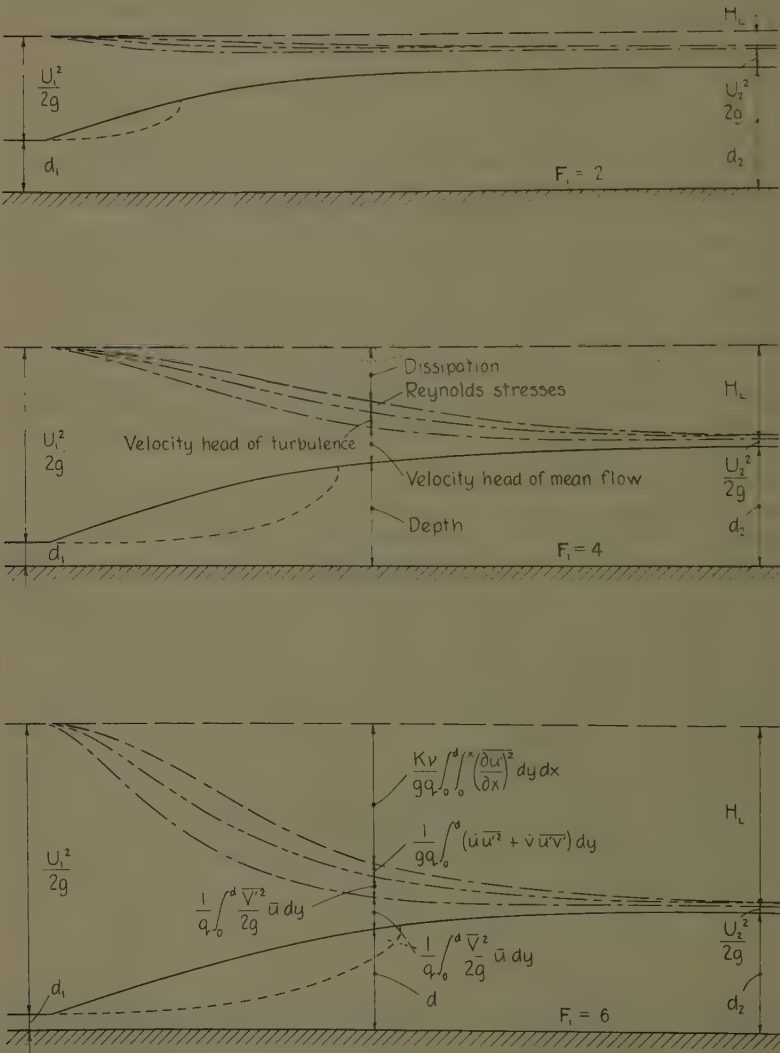


Fig. 13. Generalized diagrams of energy transformation through the jump.

the effect that the turbulence has upon the flow, the relative magnitude of this term is surprisingly small, even at the sections where it is a maximum; at the beginning of the jump, of course, it was purposely made insignificant; at the end it is small compared to the maximum value that it attained, though still an appreciable fraction of the final mean velocity head. Next in order are the curves indicating the addition of the terms for the work done by the Reynolds stresses - quantities that are very small in zones of normal turbulence but too great to be completely ignored in zones of pronounced mixing. The only other quantity with a magnitude comparable to those already plotted is the head lost through viscous dissipation, and this is represented by the drop in the sum of all the other terms from section to section. As has already been emphasized, this drop is essentially complete at the end of the jump.

CONCLUSION

Through the analysis of turbulence measurements conducted in an air-flow model of the hydraulic jump under conditions simulating three representative Froude numbers, significant information has been obtained on the energy transformation associated with the phenomenon. In particular, the part played by the roller in producing the turbulence by which the transformation is effected has taken on new clarity. Although the measurements were necessarily lacking in both precision and completeness, their analysis proceeded in accordance with the basic equations of motion, and conclusions based thereon can be considered to have both qualitative and quantitative worth.

As in any other type of flow past a zone of discontinuity, at the juncture between the oncoming stream and the return flow or roller of the hydraulic jump there is a pronounced velocity gradient, and the resulting shear gives rise to the rapid generation of turbulence. The effect of the turbulence, as usual, is twofold. On the one hand, the mixing process diffuses all characteristics of the flow - momentum, energy, and even the turbulence itself - both laterally and longitudinally. On the other hand, the increased viscous shear produces a rapid conversion of mechanical energy to heat. Were it not for the roller, the formation of the turbulence - and hence the dissipation of energy - would be minimal, as can be demonstrated in a closed duct. Except for Froude numbers well below 2, however, the hydraulic jump without a breaking front is physically impossible. The roller is thus an inseparable part of the phenomenon.

In view of the customary practice of considering the length of the jump to be the distance between the limiting sections of uniform flow, it should be noted that the roller extends about half this distance, and that half the energy of the turbulence is produced within the first half length of the roller. Because of both the convective effect of the mean flow and the diffusive effect of the turbulence itself, this energy is not wholly dissipated at the point that it is produced, but rather some distance away both vertically and longitudinally. In other words, there is a distinct lag between the loss of energy to the mean flow in the form of turbulence and its ultimate dissipation in the form of heat.

Of interest in this connection is the surprisingly small kinetic energy of the turbulence at any section, even in the zones of maximum production and

dissipation between the mid-section and end of the roller. At the final section of the jump, moreover, it is already small in comparison with the maximum value that it attained. Hence the belief that the energy lost to the mean flow persists for a considerable distance in the form of turbulence is definitely in error. In fact, the hydraulic jump is not only an effective means of reducing mean-flow energy but a very efficient mechanism for restoring conditions of uniformity to the flow.

ACKNOWLEDGMENTS

Development of the experimental technique and method of analysis, as well as the complete investigation for the intermediate Froude number in the original duct, formed the dissertation project of the second author⁽⁸⁾ and one of his assignments as Research Associate of the Iowa Institute. Measurement and evaluation of data for all three Froude numbers in the enlarged duct served as the thesis project of the third author⁽⁹⁾ and his sole assignment as Research Assistant. Both were frequently assisted by Dr. Philip G. Hubbard, Assoc. M. A.S.C.E., in the operation of the hot-wire anemometer. The first author conceived and directed the investigation and prepared the final manuscript. Partial support was received from the Office of Naval Research under Contract N8onr-500(03) with the Institute.

REFERENCES

1. Bakhmeteff, B. A., and Matzke, A. E., "The Hydraulic Jump in Terms of Dynamic Similarity," Transactions A.S.C.E., Vol. 101, 1936.
2. Lamb, H., Hydrodynamics, 6th edition, New York, 1946.
3. Townsend, A. A., The Structure of Turbulent Shear Flow, Cambridge, 1956.
4. Goldstein, S., Modern Developments in Fluid Dynamics, Oxford, 1938.
5. Preston, J. H., "The Determination of Turbulent Skin Friction by Means of Pitot Tubes," Journal of the Royal Aeronautical Society, Vol. 58, 1954.
6. Hubbard, P. G., Operating Manual for the IHR Hot-Wire and Hot-Film Anemometers, State University of Iowa Studies in Engineering, Bulletin 37, 1957.
7. Rouse, H., "Modern Conceptions of the Mechanics of Fluid Turbulence," Transactions A.S.C.E., Vol. 102, 1937.
8. Siao, T. T., "Characteristics of Turbulence in an Air-Flow Model of the Hydraulic Jump," Ph.D. Dissertation, State University of Iowa, 1954.
9. Nagaratnam, S., "The Mechanism of Energy Dissipation in the Hydraulic Jump," M.S. Thesis, State University of Iowa, 1957.

List of Symbols

- = depth of flow
- = Froude number
- = acceleration of gravity
- = piezometric head (sum of pressure head and elevation)
- = total head (sum of velocity and piezometric heads)
- = head lost in jump
- = tensor subscript, corresponding to coordinate direction of equation of motion
- = tensor subscript, corresponding to each coordinate direction in succession
- = dissipation coefficient
- = Prandtl mixing length
- = length of jump
- = length of roller
- = pressure intensity
- = rate of flow per unit width
- = Reynolds number
- = surface area
- = time
- = instantaneous longitudinal component of velocity at a point
- = average of u across vertical section
- = instantaneous vertical component of velocity at a point
- = instantaneous magnitude of velocity vector at a point
- = volume
- = instantaneous lateral component of velocity at a point
- = longitudinal coordinate
- = longitudinal component of body force per unit mass
- = vertical coordinate
- = lateral coordinate
- = velocity-head coefficient for energy equation
- = specific weight
- = Boussinesq mixing coefficient
- = dynamic viscosity

ρ = mass density

ψ = stream function

A bar ($\bar{}$) denotes the temporal mean value of the quantity beneath it;

a prime (\prime) denotes an instantaneous deviation from the temporal mean.

Journal of the
HYDRAULICS DIVISION

Proceedings of the American Society of Civil Engineers

THE TOTAL SEDIMENT LOAD OF STREAMS¹

Emmett M. Laursen,² A.M. ASCE
(Proc. Paper 1530)

ABSTRACT

Relationships are proposed which give both the quantity and quality of the total, suspended, and bed loads as functions of the stream and sediment characteristics. In the process of empirically defining the relationships, an encouraging correlation of laboratory and field data (including some original experiments) was obtained.

SYNOPSIS

Although a rigorous analysis of the general problem of sediment transportation is not yet possible, by means of a descriptive analysis the various factors involved have been isolated and the relationships among them qualitatively indicated. Parameters linking the hydraulic characteristics of the flow and the characteristics of the bed material were then formed through the use of appropriate approximations. The relationships between these parameters, however, could only be defined empirically.

The experimental data which were used for this purpose included original experiments conducted at the Iowa Institute of Hydraulic Research and published data from other sources. Empirical curves were drawn for the total, suspended, and bed loads, and a computation procedure devised to consider the non-uniformity of the bed material. The correlation of laboratory data which was finally achieved was good considering the probable errors of the measurements. The proposed relationships were also used to predict the

Discussion open until July 1, 1958. A postponement of this closing date can be obtained by writing to the ASCE Manager of Technical Publications. Paper 1530 is part of the copyrighted Journal of the Hydraulics Division, Proceedings of the American Society of Civil Engineers, Vol. 84, No. HY 1, February, 1958.

A dissertation submitted in partial fulfillment of the requirements for the degree of Doctor of Philosophy in the Department of Mechanics and Hydraulics of the State University of Iowa.

Research Engr., Iowa Inst. of Hydr. Research, Iowa City, Iowa.

sediment-transporting characteristics of three natural streams with encouraging results.

INTRODUCTION

That the flow in a channel will exert a tangential force on the boundary of the channel is well known. If the boundary is composed of discrete particles, it is readily apparent that those particles may thus be set in motion. Not as apparent is the functional relationship which must exist between the flow and the particle movement. The paramount example of the general problem is the transport of sediment in alluvial streams. Despite the fact that rivers and canals have been the concern of man since the dawn of history, even today their behavior cannot be predicted with complete satisfaction or certainty.

Most investigations in the past have been concerned with the particle movement at the bed—i.e., the bed load. As a result, many formulas for the rate of bed-load transportation have been proposed. None, however, has achieved general acceptance. More recently, the phenomenon of sediment suspension has been investigated both experimentally and analytically. Aside from certain secondary, but nevertheless material, considerations that are as yet unresolved, the distribution of suspended sediment has thereby been satisfactorily formulated. The latest studies, several contemporaneous with the one of which this analysis is a part, have now progressed to the most general phase of the sediment transport problem—i.e., the combined bed load and suspended load, or total load. The experimental phase of the investigation of the total sediment load conducted at the Iowa Institute of Hydraulic Research is only included briefly herein. It is reported in detail, including all pertinent experimental data, in a final report to the Office of Naval Research, the sponsors of the study.

Qualitative Analysis

Bed Load

The total sediment load can be divided into two parts: the bed load, in which the particles move essentially in contact with the fixed (or semi-fixed) boundary, and the suspended load, in which the particles move entirely surrounded by and at essentially the velocity of the water. Although under some conditions the bed load may be only a small fraction of the suspended load, the bed load is fundamentally the more important, because it is necessary to the existence of the suspended load.

In order to set any individual particle of bed sediment into motion, the flow will have to exert upon it a finite force of some certain magnitude which depends on the shape, size, and density of the particle and its placement among the particles that surround it. The force exerted on this particular particle will depend on the average tangential force per unit area exerted by the flow, the position of the particle with respect to other particles in the neighborhood, and, if the flow is turbulent, on the particular instant of observation. Unless, however, one subscribes to the notion that turbulent fluctuations can be infinitely large, there is a limiting mean-flow condition below which this particle will not move. More importantly, there is a limit below

which none of the particles making up this semi-fixed boundary will move. Usually this limiting flow condition is characterized by a "critical tractive force," $\tau_c = (\gamma y_0 S)_c$ (see List of Symbols), which, although real, is difficult to define except subjectively.

If the tractive force on the boundary is greater than the critical, some of the particles on the surface will move; the number, the size, and the velocity of the particles in motion will then determine the rate of bed-load transportation. The mode of movement will be rolling and sliding over other stationary particles, although, because the surface is rough, the moving particles could conceivably lose contact with the boundary briefly. The force exerted by the flow on the moving particles must be transmitted to the stationary particles forming the fixed boundary. This notion does not ignore the acceleration and deceleration experienced by the particle, but recognizes that in a statistical steady-state condition of bed-load transport the total tractive force on the flow must eventually be transmitted to the stationary boundary.

Many equations have been suggested for the prediction of the rate of bed-load transportation as a function of the flow conditions and the sediment properties. In several of the equations the total tractive force, $\tau_0 = \gamma y_0 S$, is the only flow characteristic considered; in almost all of the others either the total tractive force or the slope is included, together with either the velocity or the discharge. Although some degree of similarity can be demonstrated among these various equations⁽¹⁾ (see References), the difference in rate of transport as predicted by them is fully as great as one might expect from one's first impression of the dissimilarity of the formulations of the different equations.⁽²⁾ Unfortunately, none of the equations can be shown to be better than the others on grounds of either expediency or principle. All agree with some data, but none fits all data. Little or no basis in theory is claimed for most of the suggested equations. Rather, they are relationships which have been found by cut-and-try curve fitting or more or less arbitrary equation forms together with experimentally determined coefficients.

Two equations for the rate of bed-load transportation, proposed comparatively recently by A. A. Kalinske⁽³⁾ and H. A. Einstein^(4,5) have the distinction of being considered theoretical. To the extent that both could be derived, logically, from explicit, but different, sets of assumptions, they can be so considered. Both, however, can be criticized on a number of counts, especially as to the implications of some of the necessary assumptions. For example, Kalinske at an intermediate step in his presentation equated the number of particles in motion to the number of particles on the bed. This assumption implies that the number of particles in motion is constant no matter what the rate of transport. The principal objections that can be raised in respect to Einstein's development cannot be as simply stated (elsewhere they have been reviewed in detail),⁽⁶⁾ but they are equally damaging to the confidence that can be placed in his equation. Unfortunately, therefore, the "theoretical" equations are no more acceptable than the "empirical" equations. In the subsequent section still another bed-load equation will be presented which is basically empirical, although it has some rationality—its merit being that it is an integral part of the total load relationship.

Suspended Load

A suspension of particles heavier than the fluid (and too large for Brownian movement) is possible because of the mixing action of the turbulent flow.

In a turbulent flow there is a constant exchange of fluid masses, or volumes, across planes everywhere in the field of flow. For reasons of continuity equal volumes of fluid must move up and down past any horizontal plane. It is readily apparent that, since the particles are falling with respect to the fluid surrounding them whether the fluid is moving up or down, the mixing action can offset the action of gravity only if there are more particles in the fluid volume moving up than there are in the fluid volume moving down. That is to say, that there must be a concentration gradient such that the concentration is greater at lower levels if the mixing action is to maintain a statistically steady-state condition.

The equation expressing the equilibrium state of a sediment suspension is

$$w c = -\epsilon_s \frac{dc}{dy} \quad (1)$$

the left-hand side of the equation representing the rate at which sediment is falling per unit area across a horizontal plane under the influence of gravity, and the right-hand side the net rate at which sediment is being lifted by the mixing action of the turbulent flow at the same elevation y . The mixing coefficient ϵ_s is obviously a measure of the rate of fluid exchange, at least as a first approximation.

Similarly, the equation for the apparent shear in turbulent flow can be written as

$$\tau/\rho = \epsilon_m \frac{dv}{dy} \quad (2)$$

If one disregards secondary effects such as viscous stress and virtual mass, it would seem that the two mixing coefficients ϵ_s and ϵ_m should be the same. It is possible, however, that the mixing concept as represented by these two equations is oversimplified and that in moving a finite vertical distance the fluid does not transfer, on the average, the temporal mean conditions of its point of origin. That is to say that a natural-selection process may actually occur in the mixing action.

The usual expression for the distribution of sediment in the vertical is obtained by assuming proportionality of the mixing coefficients ($\epsilon_s = \beta \epsilon_m$), linear variation of the shear, and logarithmic velocity distribution.⁽⁷⁾ The differential equation for the sediment suspension can then be integrated to give

$$\frac{c}{c_a} = \left(\frac{y_0 - y}{y} \frac{a}{y_0 - a} \right)^z \quad (3)$$

where $z = w/\beta K \sqrt{\tau_0 \rho}$. Only a relative distribution is thereby obtained, as the concentration at any level y is expressed in ratio to the concentration c_a at some level a . Obviously, if the concentration c_a could be specified by some other means, the average suspended-load concentration \bar{c}_s could be obtained by integration of the expression

$$\bar{c}_s = 265 \frac{q_{ss}}{q} = \frac{\int_0^{y_0} c v dy}{\int_0^{y_0} c dy} \quad (4)$$

The two factors which will dominate in determining the average concentration of the suspended load are c_a and $\sqrt{\tau_0/\rho}/w$. The range of variation of other

factors such as β and κ is small in comparison to the possible variation in these two.

As can be seen from Eq. (3) the ratio of the shear velocity to the fall velocity is the primary factor determining the degree of uniformity of the concentration. Given a value of c_a at the lower-most level of suspension, the more uniform the dispersion of the sediment (i.e., the larger the value of $\tau_0/\rho/w$) the greater will be the value of the mean concentration \bar{c}_s . Although perhaps not observable, there should be a level, or zone, near the bed where the concentration becomes less dependent on the mixing action of the turbulent flow than on the rate at which particles are cast up, or entrained, from the bed.

The assumptions made by Einstein in expanding his bed-load function to permit the calculation of the total load⁽⁵⁾ were that the reference level could be taken as twice the diameter of the sediment particle and that the concentration in this zone was proportional to the rate of bed-load transport divided by the shear velocity associated with the sediment particle and the distance from the reference level to the bed. Implicitly he also assumed that the mechanism of entrainment was the mixing action of the turbulent flow which is so effective at higher levels, and that the logarithmic velocity distribution (and, therefore, the concentration distribution) was valid as close as this to the bed.

Earlier Lane and Kalinske⁽⁸⁾ had suggested that, for the sediment particles of a size class represented by a mean fall velocity w , the concentration at the "bottom" was proportional to the percentage of the bed of that particular size and a function of the shear-velocity/fall-velocity ratio. Experimental investigations under their direction resulted in modifications of the originally proposed relationship. Pien⁽⁹⁾ simply adopted a distance from the bottom of 0.1 the depth of flow as the reference level. Hsia,⁽¹⁰⁾ because he used a very fine sediment which was almost uniformly dispersed in the flow, considered the bottom concentration equal to the mean concentration, but found that a second parameter, $d\sqrt{\tau_0/\rho/\gamma}$, proportional to the ratio of the particle diameter to the thickness of the laminar sublayer, was needed. The basic concept in both the original and modified relationships was that the vertical turbulent fluctuations "picked up" material from the bottom.

Interchange Between the Bed and the Flow

A sediment particle which is suspended in the turbulent flow will follow an erratic path which will depend on the velocity of the fluid about it from instant to instant. Each of the many particles which pass through any point in the field of flow will, of course, follow a different path. Although the paths of the individual particles cannot be predicted, in the aggregate a pattern of diffusion of the particles passing through the given point will obtain. Even if the particles were of the same density as the fluid, within a nominal distance some of them would reach the bed of the stream because of the turbulent mixing action. In order to maintain a steady state of suspension within the field of flow for every particle that returns to the bed, a particle must, by some means, be removed from the bed and injected into the flow.

Considering the importance of the interchange phenomenon to the understanding of the phenomenon of the suspended load, there has been surprisingly little speculation as to the mechanism whereby the sediment particles are removed from the bed. The two notions that have been advanced are (1) that the

flow around the particle results in a lift force greater than the weight of the particle and that the particle consequently moves up from the bed into the flow, (11,12) and (2) that the mixing action of the turbulent flow is sufficiently strong at the bed level to remove the particle from the bed. (12,13)

It cannot be disputed that there might be lift forces on a particle on the bed, because the particle is not in a uniform or even symmetrical flow field but in a velocity gradient, because the pressure may approach the stagnation magnitude under some particles, or because the velocity possesses locally a component in the upward direction. No matter how this possible lift force may come into being, however, there will also be a drag force on the particle such that the particle will begin to move or, if already moving, will move faster parallel to the bed—i.e., in the direction of the drag force. If the lift became almost equal to the weight of the particle, any small drag force would be sufficient to roll or slide the particle. Since the forces exerted by the flow on the particle are the result of the relative motion of particle and fluid, they could be expected to decrease once the particle is accelerated. How a lift force greater than the weight of the particle could develop on a particle that is free to move is, therefore, difficult to envision, except possibly through the action of vertical components of large scale turbulence.

This possibility is, of course, the same as the notion that the mixing action of the turbulent flow extends to the level of the bed. For a smooth, solid bed it is readily apparent that at least the vertical turbulent fluctuations will decrease with proximity to the boundary to the limit of zero at the boundary. Although a rough, porous boundary such as is formed by the sediment might either result in, or permit, larger turbulent fluctuations than have been found in the vicinity of smooth boundaries, one would still expect the mixing action of the turbulent flow to grow weaker as the boundary is approached. Although the process cannot be categorically ruled out, it would seem that the turbulent exchange which can be quite effective in the interior of the flow would be minimal and rather inadequate at the boundary.

A more plausible explanation of how a sediment particle can leave the bed can be based on Newton's first law of motion—that a body in motion will move uniformly in a straight line until acted upon by some force. Consider now a particle moving up the weather slope of a dune. The forces on the particle are the propelling forces of pressure and shear due to the flow around the particle, the force of gravity, and the reaction force of the bed that can be resolved into a normal, support force and a tangential, resistance force. Just before the crest of the dune all of these forces will be acting on the particle; just after the crest of the dune the bed forces supporting the particle and resisting the motion will be lost, but the fluid forces and the gravitational force will continue to act on the particle (although the fluid forces may change because the flow around the particle changes). The motion of the particle will then depend on the velocity (both direction and magnitude) of the particle as it leaves the crest of the dune and the forces which thereafter act upon it.

If the velocity of the particle and the propelling forces are small and the weight of the particle under water is large, the particle will merely roll over the crest and down the lee slope of the dune. This, of course, is a description of bed-load movement. If the gravitational force is small in comparison to the momentum (mass times velocity) of the particle, the particle will only gradually deviate from its initial direction of motion and will tend to move in the parabolic path of a projectile. This ideal path, of course, will be modified by the effect of the fluid forces on the particle.

Although the prediction of the path of the particle may not be possible, it should be clear that, if the velocity of the particle moving as bed load is great enough, the particle can leave the immediate vicinity of the bed in what might be described as a self-launching action. Moreover, the factors which will govern the motion of the particle, other than the properties of the fluid and the particle itself, are the form of the bed, the flow pattern (including the velocity magnitude), the gravitational force, and the velocity of the particle at the crest of the dune. The amount of material involved in this action will be related to the number of particles in motion and the size of the particles. Since the product of the number, size, and velocity of the particles is the volume rate of bed-load transportation, it is immediately apparent that the bed load will play a primary role in the determination of the suspended load.

If the bed is covered with dunes, this self-launching action is easy to visualize. Even more to the point, it can be observed. If there are no dunes—i.e., if the bed is plane—the same action is still possible, because the bed-load particles must move over roughness elements of their own size. As a result, the direction of motion of the particle can be away from the bed and, if its velocity is great enough, the particle can escape from the immediate neighborhood of the boundary. If the moving particle in the case of the duned bed can be likened to a ski-jumper, in the case of the plane bed it can be likened to a hot grounder in a sand-lot baseball game.

The secondary motion, or large-scale vortices, of the turbulent flow can also result in a movement of the particles in contact with the bed whereby they can be self-launched into the flow. This can be demonstrated simply in a glass jar filled with water with a bed of fine sand on the bottom. By moving a pencil in a small orbit an almost irrotational vortex can be induced. Because of the secondary motion, the sand particles move inward in spiral paths and a small, sharp-pointed, cusped dune is formed. If the velocity of flow near the bed, and consequently, the velocity of the particles, is sufficiently great, the same self-launching action from the peak of the dune is observable. The importance of macroturbulence such as this in the movement of sediment has been noted by Matthes⁽¹⁴⁾ although the mechanism whereby the particles are removed from the bed is not described. A similar phenomenon has also been noted by Lane.⁽¹⁵⁾ In a stream or a laboratory flume this action is quite impossible of observation. It can be readily observed every autumn, however, with dust and fallen leaves as the sediment particles. On a large scale, of course, it is the tornado of the western plains.

Observations

Equipment and Technique

Since most previous investigations of sediment transportation have been concerned with bed-load movement, very few data on the rate of transport of total load, or even suspended load, were available at the time this study was initiated. An experimental phase of the investigation, therefore, was essential to the determination of quantitative information relative to this most general phase of sediment movement. Because the data which was gathered were so important in the development of the relationships for the sediment load, a brief description of the experimental phase is included herein.

The principal item of experimental equipment was a recirculating, tilting

flume with an overall length of 105 feet, shown in Fig. 1. The test section was 90 feet long and had a cross section 36 inches wide and 18 inches deep. In order to permit visual observation of the flow, the sides of the test section were made of 1/4-inch plate glass.

Because the resistance to flow will depend in large measure on the roughness of the self-formed alluvial bed, the discharge and the depth of flow (and hence the velocity) are usually fixed in experiments such as these, and the slope is allowed to develop as required. In order to speed up the deposition-erosion process whereby the slope is established, it is expedient to be able to tilt the entire flume during operation. The mechanism which was used to accomplish this was a system of interconnected cams.

The rate of flow was controlled by the speed of the pumps and measured by calibrated, segmental orifices in each line in conjunction with an air-water manometer. The depth of flow was determined by the volume of water in the system and the water-surface elevation was measured at 10-foot intervals along the test section by piezometers connected to an open manometer board. The water-surface and sand-bed elevations relative to the flume could be determined by means of point gages mounted on carriages which in turn slid on stainless-steel rails which were parallel to the flume bottom. The slope of the flume itself was obtained by measuring the travel of the lower end with a vernier and scale made from a standard point gage.

Values of velocity and concentration at a point were obtained by means of the combination instrument shown in Fig. 2. Two Pitot tubes, modified to produce a larger differential reading, were mounted on each side of a rectangular sampler nozzle. The differential-head indication was obtained with an air-water manometer. A small variable-speed pump was used to establish any desired rate of flow into the sampler-intake nozzle. The rate of flow was measured by a calibrated Venturi meter and air-water manometer. The pumped sample was collected at first in quart milk bottles; later large glass tubes were obtained to simplify the handling of the sample. The amount of sediment in the samples was determined by weighing in calibrated pycnometers. For small concentrations a standard 10-ml pycnometer with a fitted stopper having a capillary hole was used and for large concentrations a 500-ml flask with a narrow, graduated neck.

In order to measure the total load, a low submerged weir was installed at the downstream end of the test section. The weir was formed of a quarter cylinder cut from a nominal 4-inch brass pipe, and placed so that the convex side was upstream and a tangent to the top edge, or crest, of the weir was parallel to the flume bottom. The crest of the weir was approximately an inch above the mean elevation of the sand bed and slightly above the crest of the dunes.

In a study such as this the operation and the measuring techniques must be designed first to establish normal equilibrium transport conditions and then to obtain a reliable and complete description of those conditions. Although equilibrium here refers specifically to a state of flow in which there is neither aggradation nor degradation of the bed, it also implies that there is no change in state with time. Because the rate of change from a non-equilibrium to an equilibrium state will depend primarily upon the degree of non-equilibrium, the desired steady state will tend to be approached asymptotically.

Arbitrary, but judicious, operation of a sediment-transport flume can materially reduce the time required to attain a normal equilibrium condition.



Fig. 1. Flume.

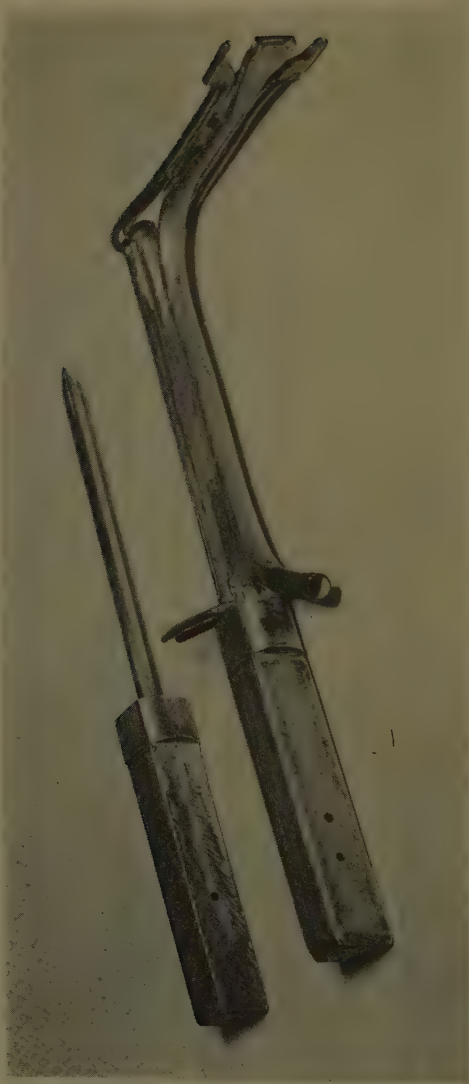


Fig. 2. Combination Pitot tube and sampler.

To confirm the establishment of equilibrium, however, repeated measurements over considerable periods of time are necessary. To verify the uniformity of a reach, measurements at successive sections are required.

Given a width of section (which is fixed by the construction of the test section) and a bed material (which can be chosen arbitrarily) only two of the three primary flow characteristics (discharge, depth, and slope) can be considered to be independent variables. In a natural stream the slope and the discharge are the imposed conditions and the depth is conditional upon these and upon the configuration of the stream. Operation of a recirculating, tilting flume is simpler if the discharge and depth are chosen as the imposed conditions and the other characteristics of the flow are allowed, or helped, to attain their natural value or form.

In the first runs measurements were taken of all pertinent characteristics of the flow as the condition of equilibrium was approached. The slope proved to be the most sensitive index, as it was affected by both the non-uniformity of the flow and the roughness of the bed. As deposition and scour occurred, remolding the overall bed so that the rate of sediment transport at every section was the same, there was a concomitant change in the water-surface slope. As the natural ripple or dune pattern developed, the roughness of the bed changed. Therefore, the resistance to flow changed, and, consequently, the slope of the water surface. The velocity distribution and concentration distribution were affected by the position of the dunes relative to the measuring section—especially, of course, near the bed. As a result, the spatial variation of these measurements was of the same order as the temporal variation, unless the flow was adjusting itself quite rapidly toward the normal equilibrium condition.

For the coarser of the two sands used, the slope proved to be a sufficient indicator of the attainment of the normal equilibrium condition. When the bed had been remolded and its configuration established, the slope of the water surface no longer varied with time. (Tilting the flume, in effect, simply reduced the time necessary for remolding the bed.) A reach of approximately 50 feet, from about 35 feet to about 85 feet from the entrance, would then exhibit uniformity—as defined by a constant slope and constant depth of flow.

For the finer sand the water-surface slope alone was not found to be an adequate measure of the state of flow. This was because the length of the reach displaying uniformity was only about 30 feet, and, therefore, the measurement of the slope could not be as precise. Measurements of the sand-bed slope and elevation were found to be necessary also. In order to measure the sand bed the flow had to be stopped and the run interrupted. Therefore, the sand-bed measurements were only used as a final check after the water-surface slope indicated stability.

Fortunately, because the total time required for a single complete run made continuous operation impractical, interruption of a run did not affect materially either the attainment or the state of equilibrium. If care was taken in stopping and then resuming a run, the state of flow at the time of interruption was reestablished within an hour at the most. As has been mentioned before, the criterion for normal equilibrium flow is that the characteristics of flow do not change with time. Since this state is approached asymptotically, it is obvious that the final determination of whether the desired state has been reached must rest on the judgment of the operator. When normal equilibrium had been attained—in the operator's judgment—measurements were made of water-surface elevations, velocity distribution, concentration distribution, and sand-bed elevations.

For the coarser sand, only centerline distributions of velocity and concentration were determined. For the finer sand, complete traverses during several runs were made across the flow section in the uniform zone and over the low quarter-circle weir. Measurements of the dune size could be obtained in the case of the coarser sand. However, for the very fine sand the material settling out of suspension almost obliterated the dune forms.

Water-surface and sand-bed elevations could be read to 0.001 foot. Although errors in any single determination could be greater, the error which might be expected in the average of repeated measurements should not exceed this value. The depth of flow ranged from about 0.25 to about 1.00 foot. At the smallest depths the percentage error, therefore, could be of the order of 1%. The slope ranged from about 0.0004 to about 0.0018 over the 50-foot reach of the coarser sand and from about 0.0008 to about 0.0012 over the 30-foot reach of the finer sand. Errors as large as 10%, therefore, are possible.

Few of the individual velocity determinations in the interior of the flow should be in error by more than 2 or 3%. Near the sand bed, however, the possible error in the measurements became larger as the boundary was approached, because the velocity became smaller. Moreover, the position of the dune relative to the measuring section was unknown, so that the meaning of the measurements near the sand bed was somewhat indefinite.

The samples which were taken for the determinations of point concentrations were large enough to give a good time average. Fig. 3 shows the long-period fluctuations of the concentration at a point as a function of time. The short-period fluctuations have been averaged out because each successive determination of concentration was made from a 1-quart sample, each quart being equivalent to a stream tube almost the length of the test section. In the first runs 5-quart samples were taken to reduce this source of error in the concentration measurements. The slightly larger 5000-cc tubes, later substituted for the milk bottles, were equivalent in volume, and the procedure of transferring the sediment sample to the pycnometer was simpler.

Experimental Results

The size-frequency distribution of the two sands which were used is shown in Fig. 4. Despite the fact that the finer sand is within what is generally considered the silt range, it is a true sand. Both sands were fractions of the Ottawa deposit (the coarsest fraction of which is the standard concrete testing sand) and are almost pure silica.

The experimental results for the coarser sand are summarized in Table I. A more detailed summary is included in the report to the sponsor.⁽¹⁶⁾ In regard to the basic problem being investigated—the correlation between the sediment load and the flow and sediment characteristics—little can be learned from comparing the pertinent values for different runs, even with the aid of simple plots. An empirical relationship describing this correlation was found only after a qualitative analysis of the problem had indicated parameters which could be taken as expressing the factors governing the phenomena involved. This qualitative analysis and the relationships finally obtained are the subject of the following section. Several general characteristics of interest, however, are immediately apparent from the tabulated summary.

The recorded dune heights h and l show that within the range of conditions represented here, the size of the dunes did not vary greatly—except that in one run a plane bed was formed. (A number of other attempts to obtain a

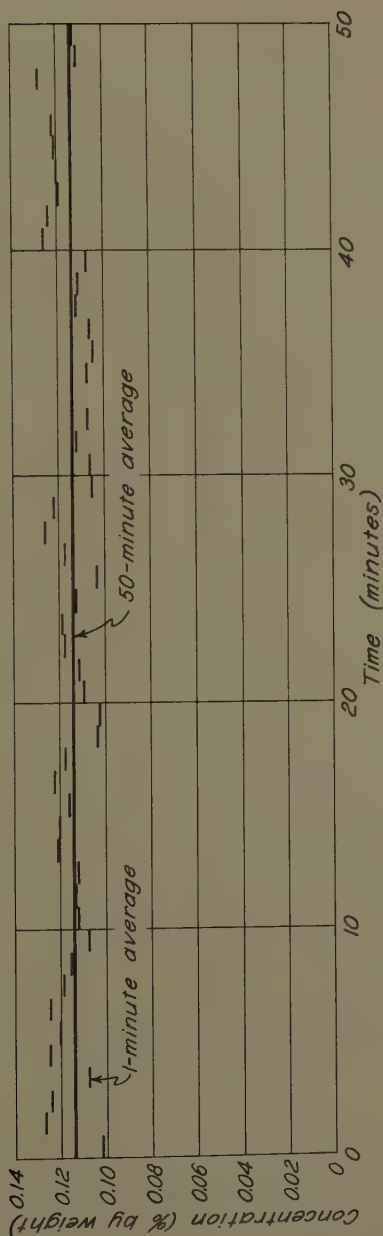


Fig. 3. Variation of concentration with time.

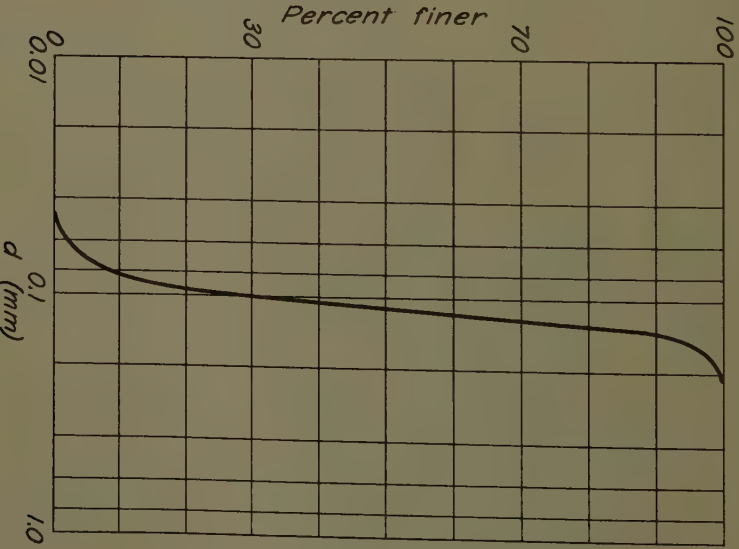
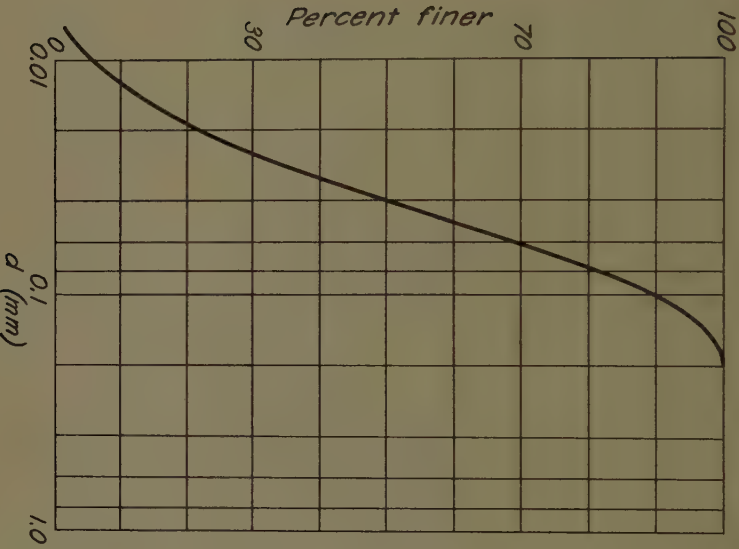


Fig. 4. Size-frequency distribution of sands.

Table I. Summary of results for 0.1-mm sand

Run	\bar{c}	V	y_0	S	T	h	l	$2y_0/h$	f	l/m	κ	z	z_1	β
1	0.225	1.69	0.561	0.00122	20.6	0.085	0.48	13.6	0.062	3.85	0.32	0.40	0.58	1.40
2	0.029	1.36	0.751	0.00055	21.8	0.077	0.48	19.6	0.058	4.35	0.33	0.32	0.72	2.25
3	0.014	1.33	0.928	0.00043	22.8	0.074	---	25.0	0.058	4.75	0.41	0.45	0.72	1.60
4	0.270	2.31	0.927	0.00101	24.0	0.084	0.51	22.0	0.045	4.15	0.38	0.63	0.47	0.75
5	0.424	1.92	0.514	0.00152	21.3	0.094	---	11.0	0.055	3.85	0.30	0.41	0.54	1.32
6	0.313	1.70	0.518	0.00144	21.6	0.100	0.48	10.4	0.066	3.45	0.29	0.40	0.53	1.32
7	0.066	1.32	0.533	0.00106	23.3	0.108	---	9.8	0.084	3.45	0.31	0.42	0.61	1.45
8	0.156	1.73	0.756	0.00092	21.6	0.100	0.56	15.2	0.060	3.45	0.31	0.42	0.55	1.31
9	0.061	1.59	0.995	0.00058	26.5	0.110	0.38	18.0	0.058	3.35	0.29	0.44	0.61	1.59
10	0.272	1.55	0.381	0.00186	24.9	0.101	0.44	7.6	0.076	3.15	0.28	0.42	0.55	1.31
11	0.055	1.07	0.311	0.00160	26.4	0.109	0.44	5.8	0.112	3.35	0.36	0.49	0.65	1.33
12	0.103	1.28	0.382	0.00150	21.5	0.080	0.45	9.6	0.090	3.45	0.29	0.40	0.61	1.52
13	0.131	1.69	0.725	0.00080	23.7	0.075	0.45	19.4	0.052	4.00	0.32	0.40	0.61	1.52
14	0.143	1.15	0.250	0.00210	19.8	0.063	0.45	8.0	0.102	3.25	0.31	0.34	0.63	1.85
15	0.515	3.36	0.472	0.00120	22.8	Plane	(2640)		0.013	4.75	0.17	0.97	0.61	0.63
16	0.305	2.20	0.709	0.00107	23.2	0.072	---	19.8	0.040	3.25	0.25	0.68	0.53	0.78

plane bed were unsuccessful. The combinations of velocity and depth giving Froude numbers of about 0.8 resulted in very unstable flow conditions in the flume.) As can be seen in the respective tabulations, the relative roughness $2y_0/h$ of the duned bed exhibited a greater variation than did the absolute roughness h .

In Fig. 5 the Weisbach resistance coefficient is plotted as a function of the relative roughness together with the relationship for fully rough-pipe flow based on the Nikuradse experiments with sand-roughened pipes. Despite the scatter of the experimental points a very good agreement is evident between the two kinds of roughness in the two flow systems. In fact, one should probably interpret the superposition of the points on the curve as due to a fortuitous choice of a typical roughness length until further evidence is available as to the effect of roughness shape and spacing on the resistance coefficient. One can conclude, however, that the bed configuration is of major importance in the resistance to flow of alluvial streams.

Similarly the roughness has an effect on the velocity distribution, which—except for the plane bed—is in accord with the Nikuradse experiments. Fig. 6 shows the power-law exponent as a function of the relative roughness together with the Nikuradse relationship. The values of the exponent m were obtained from log-log plots of the velocity distribution. Semi-logarithmic plots of the velocity distribution were also made and the values of κ obtained therefrom are listed in the table. No systematic correlation for the variation of κ was found with either the concentration or the roughness.

Similarly, no pattern of variation was found for the values of β listed in the table. The value of β was taken as the ratio of the theoretical exponent of the concentration distribution z_1 to the measured exponent z as obtained from log-log plots of the concentration distribution. In the theoretical evaluation of z_1 the fall velocity obtained in a bottom-withdrawal-tube determination of the size-frequency distribution and the nominal value of 0.4 for κ were used. The effect of the concentration would be to decrease the fall velocity and, therefore, z_1 by less than 10%. Use of the experimental values of κ would increase z_1 and, therefore, β . For most of the runs this increase would be of the order of 30%.

Table II summarizes the results for the finer sand. From the tabulated β values in this table it can be seen that the resistance to the flow for these runs with the finer sand is about the same as for those with the coarser sand. Although meaningful measurements of the roughness could not be obtained because of the deposition of the suspended load, it could be observed that the size of the dunes was approximately the same as for the previous series of runs. The velocity distribution characterized by the exponent m as obtained from log-log plots is also indicative of a rough boundary similar to the runs with the coarser sand. The values of κ from semi-logarithmic plots listed in Table II are slightly smaller for this series. A comparison of theoretical and measured concentration distribution by taking a ratio of the appropriate z values results again in β values greater than unity, and about the same as those found for the coarser sand. Correction of the fall velocity for the concentration effect would decrease β by as much as 40%, but use of the experimentally determined values of κ would almost double the value of β .

Of perhaps greater significance is the fact that the total load measured over the weir was almost the same as the suspended load measured in the normal sections. In fact, the errors in measurement of the suspended load were larger than the bed load. It is estimated that the bed load for these runs was probably not more than 1% of the total load.

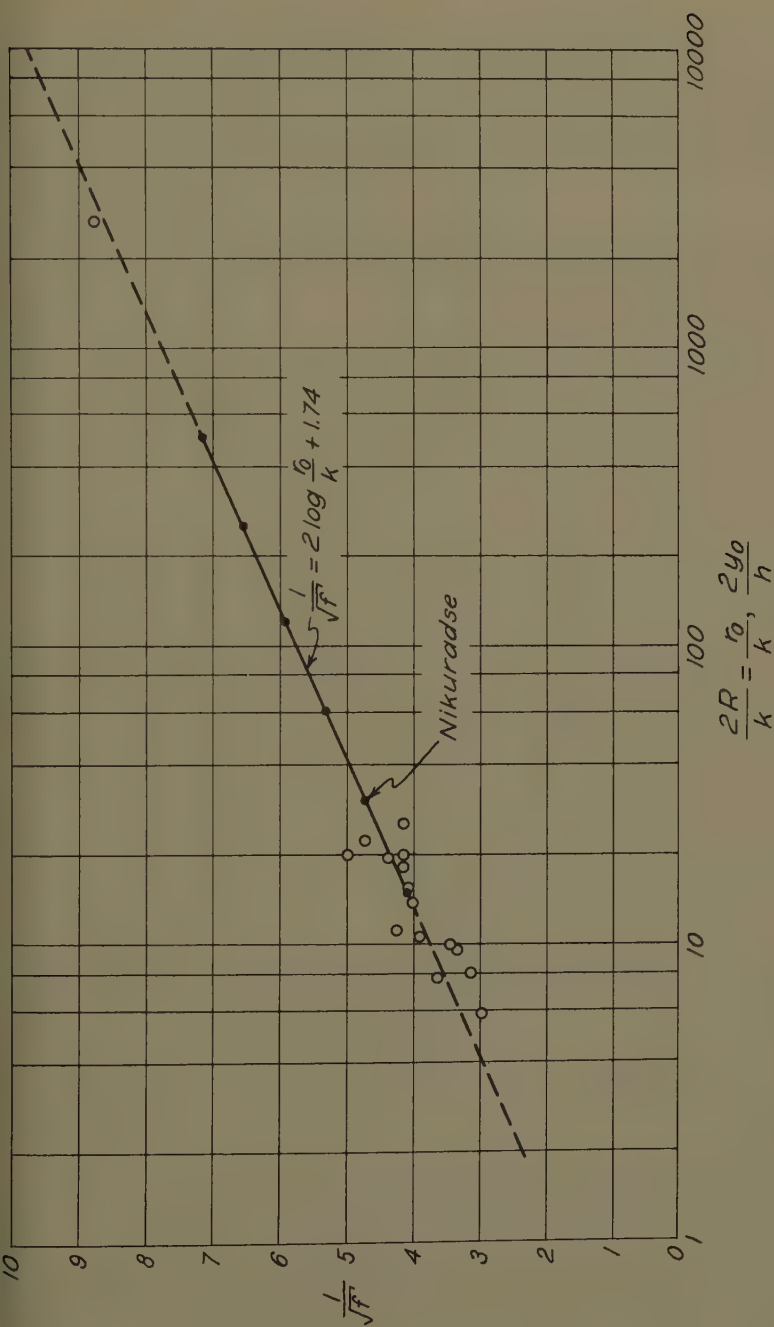


Fig. 5. Effect of roughness on resistance to flow.

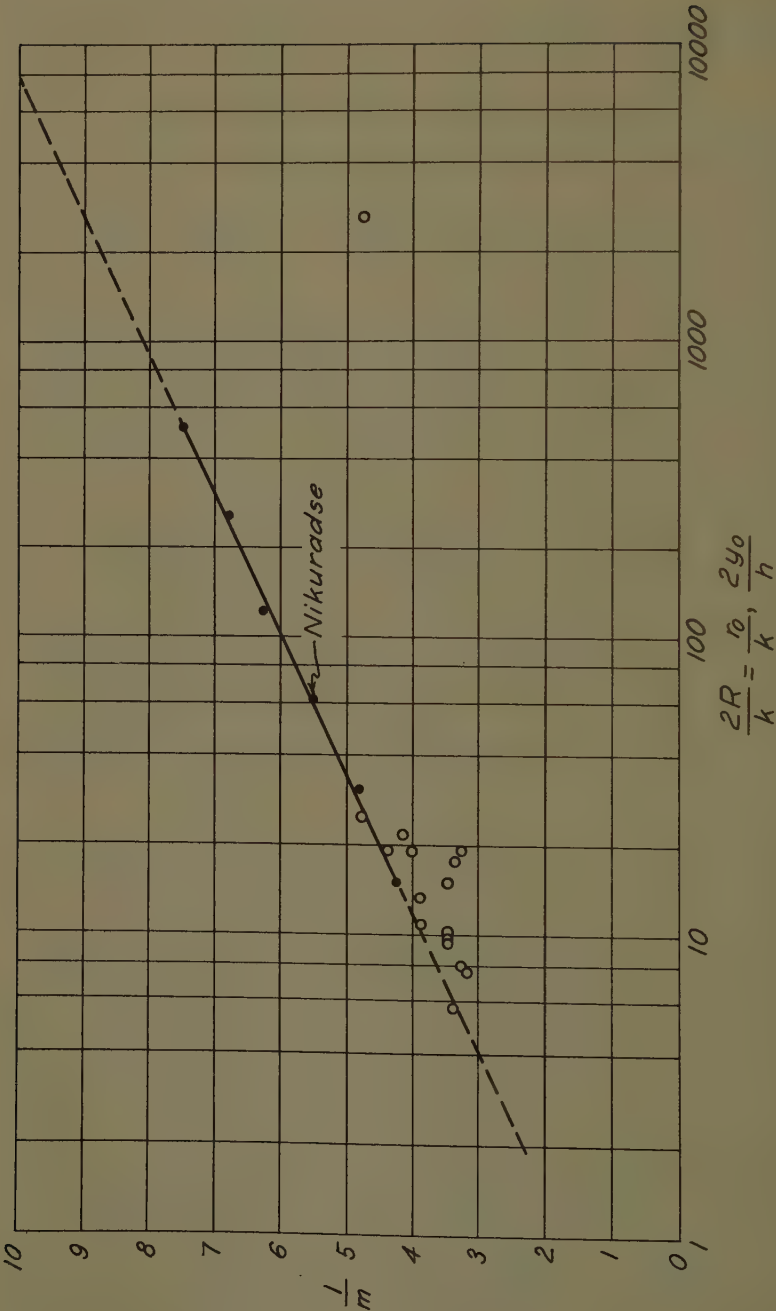


Fig. 6. Effect of roughness on power-law exponent.

Table II. Summary of results for 0.04-mm sand

Run	\bar{c}_t	\bar{c}_s	V	y_0	S	f	1/m	κ	z	z_1	β
101	8.34	6.90	1.87	0.566	0.00101	0.042	2.94	0.19	0.076	0.088	1.16
102	8.20	6.72	1.74	0.462	0.00117	0.046	3.44	0.27	0.065	0.091	1.40
103	5.84	5.76	1.91	0.674	0.00086	0.057	3.22	0.24	0.062	0.088	1.42
104	9.70	9.48	2.13	0.478	0.00107	0.029	2.63	0.18	0.092	0.095	1.03
105	8.34	8.76	2.61	0.565	0.00114	0.024	5.00	0.11	0.102	0.097	0.95
106	3.03	3.07	1.23	0.542	0.00081	0.075	3.12	0.25	0.050	0.098	1.96
107	0.73	0.75	0.85	0.380	0.00078	0.107	5.00	0.25	0.030	0.124	4.10
108	9.81	9.99	2.42	0.663	0.00100	0.029	4.75	0.25	0.083	0.095	1.14

Relationships for the Sediment Load

Development of the Relationships

Given a flow condition (mean velocity, depth, and slope), and a sediment (mean size, frequency distribution, specific gravity, and shape), there will be a corresponding rate of sediment transport, partly as bed load, partly as suspended load. The qualitative discussion of the mechanism of sediment movement in the preceding sections was for the purpose of selecting the factors which determine the rate of transport. If the hydraulic and sediment characteristics can be linked in parameters descriptive of these factors, then at least empirical relationships for the sediment load may be obtained. (At the present time any attempt at a rigorous analysis is defeated at the outset because the fluid forces on the individual particles cannot be specified in sufficient detail.) One of the desired parameters is readily apparent—the shear-velocity/fall-velocity ratio, $\sqrt{\tau_0/\rho}/w$. This ratio expresses in large measure the effectiveness of the mixing action of the turbulence and, of a certainty, should be included in the relationship for the suspended-sediment load.

The other desired parameters cannot be as confidently stated. Especially needed is a clear understanding of the forces acting on the particles in motion as bed load. For the present it is practically necessary to relate the forces causing motion to the tractive force, and the forces resisting motion to the critical tractive force for the beginning of movement. Only in the case of the plane bed, however, can the total tractive force be considered significant. If there are dunes on the bed (the more common condition) the part of the total tractive force which is resisted by the tangential component of the integrated pressure distribution along the duned boundary cannot be considered effective in causing the sediment particles to move. An approximate measure of the remainder of the tractive force can be obtained by the use of the Manning formula and Strickler's expression for n as a function of the sediment diameter: (17)

$$\tau_0' = \frac{v^2 d^{1/3}}{30 y_0^{1/3}} \quad (5)$$

Although this expression may be only a crude approximation for the shear in the rather complex flow along the weather slope of the dune, it has the advantage of being computationally simple.

An expression for the critical tractive force can be written as

$$\tau_c = C d \quad (6)$$

where C is a coefficient dependent on the sediment characteristics and the flow conditions near the boundary. Both τ_0' and τ_c are representative of the average shear per unit area of the bed, rather than the force on the particle which is moving or about to move. Although neither is a true measure, even in approximate form, of the desired forces, one might conjecture that each is related to these forces in much the same manner. Thus, the ratio τ_0'/τ_c can be assumed to be a significant parameter descriptive of bed-load transportation. Moreover, if the rate of bed-load transport is a primary factor in the interchange phenomenon, as seems likely, this ratio would also be important to the suspended-load movement.

A third parameter, which is also suggested by the discussion of the preceding sections, is the ratio of the velocity of the sediment particles moving as bed load to their fall velocity. This ratio would be a measure of the tendency for self-launching and would be important for suspended-load rather than bed-load movement. Similarly, the form of the bed might be descriptive of the opportunity for self-launching. In the final analysis of the data, the influence of such a self-launching parameter could not be assessed—partly because of the scatter due to experimental errors, and partly because it would necessarily resemble the other parameters.

To test the significance of the ratio τ_0'/τ_c , the data obtained in this study were plotted as $\bar{c} = 265 q_s/q$ against $(\tau_0'/\tau_c)-1$, and an almost linear variation was found for each sand. For reasons more intuitive than rational, the factor

$$\frac{\sqrt{\tau_0'/\rho'} d}{v y_0} \propto \left(\frac{d}{y_0}\right)^{7/6} \quad (7)$$

was included in the relationship and a plot made of

$$\frac{\bar{c}}{\left(\frac{d}{y_0}\right)^{7/6} \left(\frac{\tau_0'}{\tau_c} - 1\right)} = f\left(\frac{\sqrt{\tau_0'/\rho'}}{w}\right) \quad (8)$$

using the data of this study and other published data. The resulting relationship is shown in Fig. 7. The solid curve drawn through the points represents the total load and the dashed curve the bed load. Table III summarizes the source and the pertinent information for the various data plotted in Fig. 7. Only those runs for which the particle shear approached or was less than the critical shear were rejected. A simple ratio like τ_0'/τ_c , of course, cannot be expected to describe conditions at this limit.

For the data of Toch and Hsia, C values for the critical tractive force of 8 and 16, respectively, were used; otherwise a value of 4 was employed. These values are plotted together with Shields' curve in Fig. 8. The values used are approximately in agreement with the recommendations of White,⁽¹⁸⁾ and for values of d/δ' above 0.2 with Shields⁽¹⁹⁾ as well. For smaller values, where the laminar sub-layer completely envelops the particles, the variation of the critical tractive force with the diameter of the particle is not clear. It should be noted that Shields' data did not include values of d/δ' much less than 0.2.

It was noted, especially on the larger work sheet from which Fig. 7 was prepared, that there was a systematic scatter to the points for any series as identified by the different symbols. It was surmised that this tendency for the sets of points to cross the mean curve might be due to the non-uniformity of the sediments, and a computational procedure was devised to consider the composition of the bed material. This computational procedure is represented by the equation

$$\bar{c} = \sum p \left(\frac{d}{y_0}\right)^{7/6} \left(\frac{\tau_0'}{\tau_c} - 1\right) f\left(\frac{\sqrt{\tau_0'/\rho'}}{w}\right) \quad (9)$$

wherein the contributions of each fraction p of size d are summed to obtain the mean contribution. Values of τ_c and w were determined for the mean diameter d of the fraction, but the same values of τ_0' and $\sqrt{\tau_0'/\rho'}$ were used for all fractions, τ_0' being determined from the mean diameter of the total sediment sample.

Table III. Summary of data in Figs. 7 and 8

Investigator	Symbol	d_m (mm)	\bar{c}	$\sqrt{\tau_0/\rho/w}$	τ_0'/τ_c	Remarks
Lin, Rand (Table I) [16]	●	0.11	0.014 - 0.52	3.6 - 5.4	2.77 - 23.8	Susp
Toch (Table II) [16]	●	0.04	0.73 - 9.99	20.2 - 28.4	1.96 - 11.3	Total
Hsia [10]	●	0.011	0.64 - 11.1	168 - 451	1.89 - 18.0	Total
Pien [9]	●	0.18	0.013 - 0.24	2.0 - 4.3	4.0 - 10.9	Susp
MacDougall [22]	●	1.44	0.012 - 0.13	0.15 - 0.22	1.11 - 2.43	Bed
	●	0.66	0.018 - 0.12	0.23 - 0.43	1.17 - 2.99	Bed
O'Brien [22]	○	0.37	0.001 - 0.13	0.43 - 1.21	1.11 - 8.85	Bed
Brooks [23]	●	0.088	0.019 - 0.53	5.0 - 6.9	2.01 - 14.0	Total
	●	0.145	0.020 - 0.24	2.5 - 3.1	1.86 - 9.5	Total
Lin, Barton [24]	●	0.18	0.003 - 0.37	1.8 - 3.1	1.45 - 19.3	Total
WES [25]	●	0.20	0.004 - 0.08	1.4 - 2.2	1.26 - 8.2	Total
	●	0.50	0.006 - 0.05	0.46 - 0.57	1.30 - 2.91	Bed
	●	4.08	0.002 - 0.03	0.12 - 0.15	1.02 - 1.20	Bed

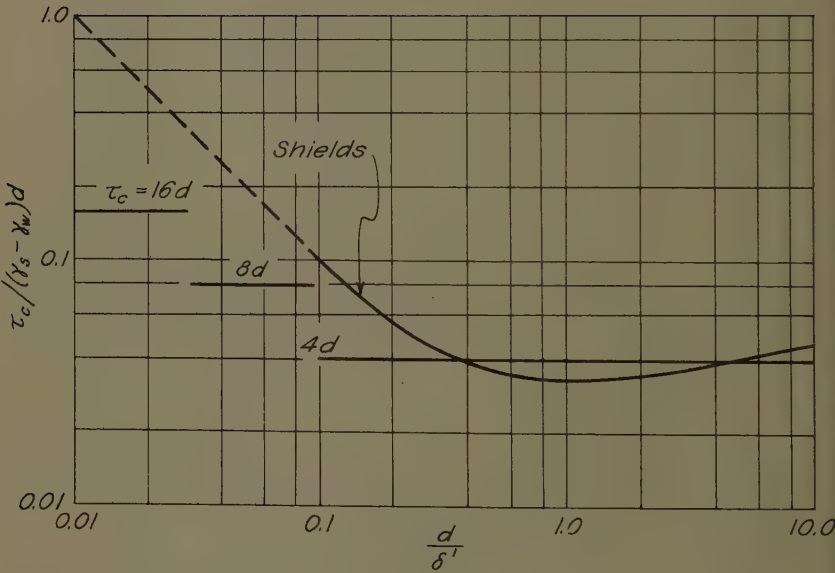


Fig. 8. Critical tractive force.

Fig. 9 shows a comparison between the measured mean concentration and the concentration as computed in this manner. A tendency for the plane beds to have a measured concentration less than computed could be noted, as well as a hint that there might be a systematic scatter with the ratio τ_0'/τ_0 . It is readily apparent that this ratio could be taken as a measure of the roughness of the bed; together with the other parameters which have been introduced it might also be taken as descriptive of the ratio of the velocity of the bed-load particles to their fall velocity. The unsystematic scatter due probably to errors in measurement, was too great to assess the possible influence of these two factors. Actually a rather good correlation is indicated over the ten-thousand-fold range in concentration represented in this plot.

Equation (9) also allows the prediction of the composition of the sediment load (bed load, suspended load, or total load depending on the function of the shear-velocity/fall-velocity ratio employed). Fig. 10 shows a comparison with measurement of such a prediction for several runs.

Although the data used in Figs. 7 and 9 represent a large variation in sediment size and concentration, the measurements were all made in laboratory flumes under controlled conditions. Therefore, an attempt was made to predict the sediment load under field conditions using the data published by H. A. Einstein for Mountain Creek in South Carolina and West Goose Creek in Mississippi,⁽²⁰⁾ and by the USGS for the Niobrara River near Cody, Nebraska.⁽²¹⁾ The results are shown in Figs. 11, 12, and 13, respectively.

In the upper part of the figures the velocity and slope data are plotted together with the mean curves which were used in conjunction with Eq. (9) to obtain a predicted sediment load. On the left a curve, or curves, for the predicted load and the data of the measured load are plotted as a function of the discharge. On the right are plotted the predicted composition of the sediment load and the measured composition of the bed material.

In the case of Mountain Creek the predicted load was in general less than measured. It may be noted, however, that artificial flash floods were used to obtain much of these data (Fig. 11), with a difference in conditions between rising and falling stage as indicated in the figure. The measured points of the largest flood are connected in the figure by light lines indicating the temporal continuity. The measured difference between the rising and falling stages is roughly comparable to the predicted difference. Of perhaps greater significance is the discrepancy between the predicted and measured composition of the bed load. The predicted mean size of the bed load was 0.6 mm as compared to a measured value the same as the bed material, or 0.9 mm. If a smaller value for τ_c had been used, the predicted load would, of course, have been greater and the composition of the bed load would have more closely approached that of the bed material.

The predicted bed load for West Goose Creek (Fig. 12) agrees very well with that measured for lower discharges, but it is considerably too large for higher discharges. It is noteworthy that the discrepancy is pronounced only at velocities of flow above 2.5 fps. Based on the experience of the writer, it seems doubtful that a slot 2 feet in width such as was used would capture much more than half the load at this high a velocity with so fine a sand (0.3 mm). The predicted size of the bed load for West Goose Creek is only slightly smaller than the size of the bed material, and is well within the scatter of the measured composition of the bed load.

The excellent prediction of the sediment load for the gaging-station section of the Niobrara River (Fig. 13) does not include some fifty-nine measurements

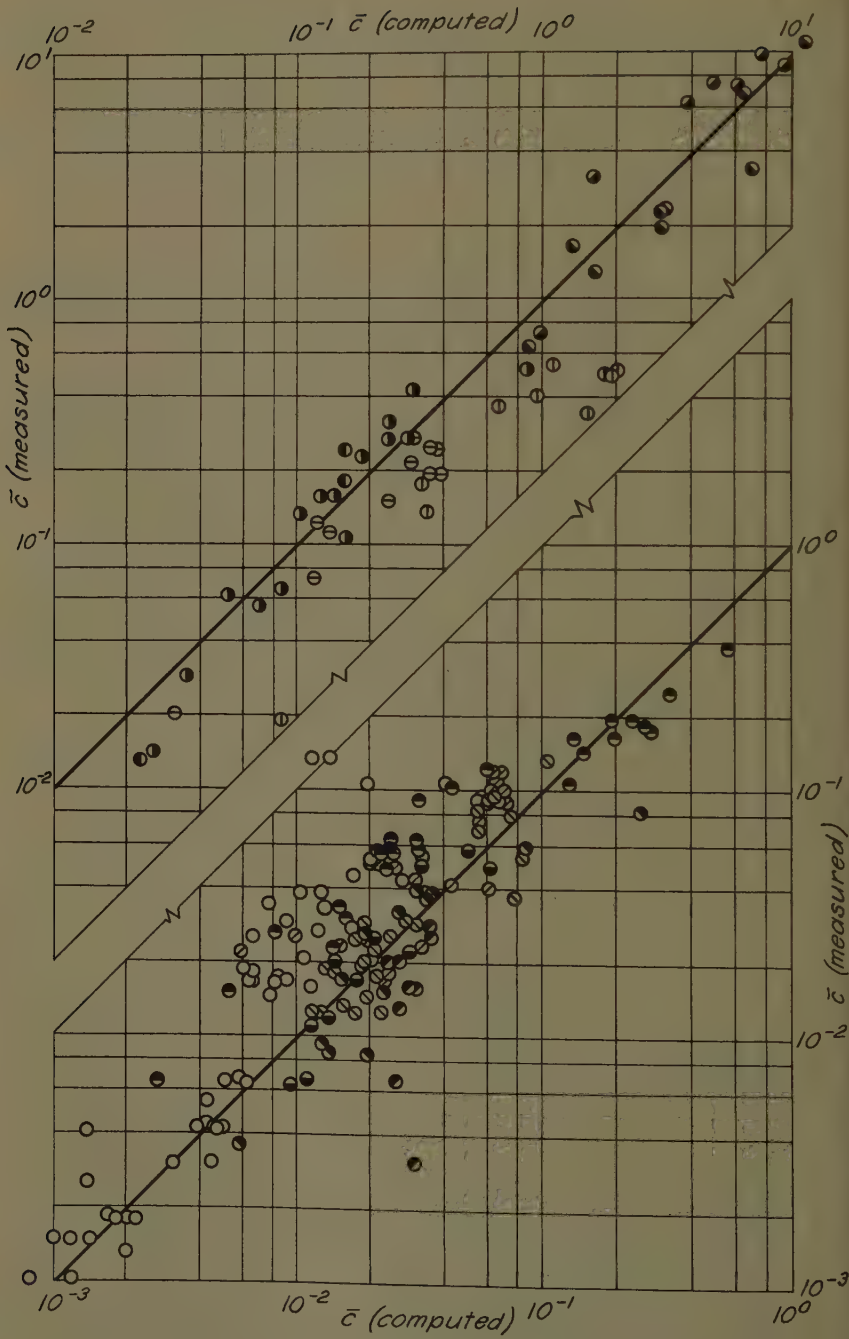


Fig. 9. Comparison of computed and measured concentrations.

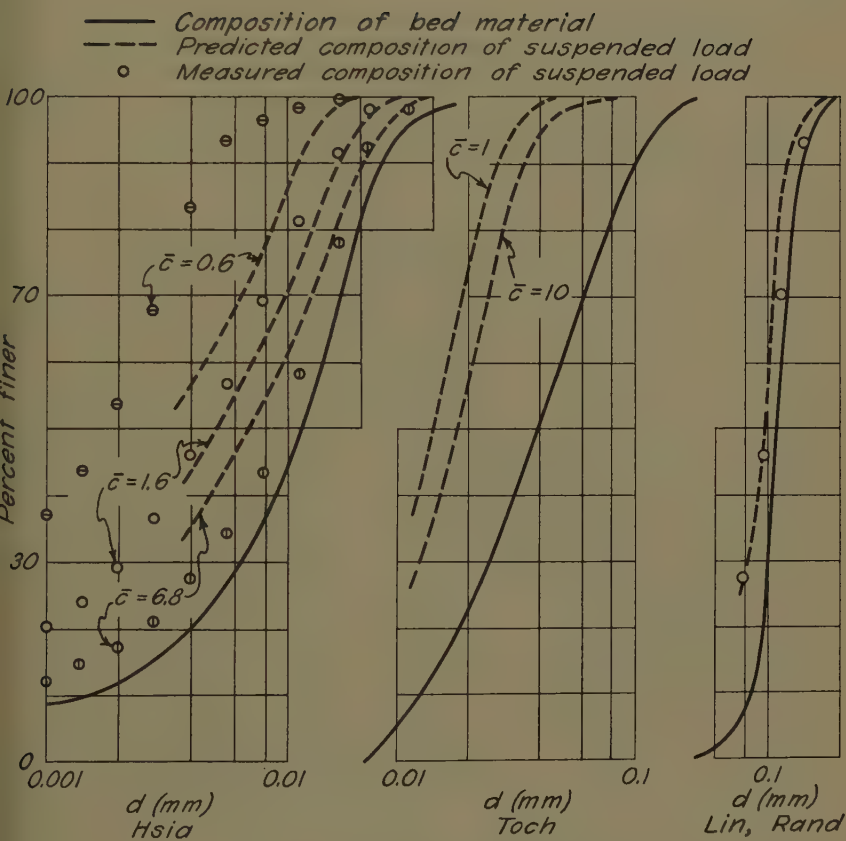


Fig. 10. Predicted composition of suspended load.

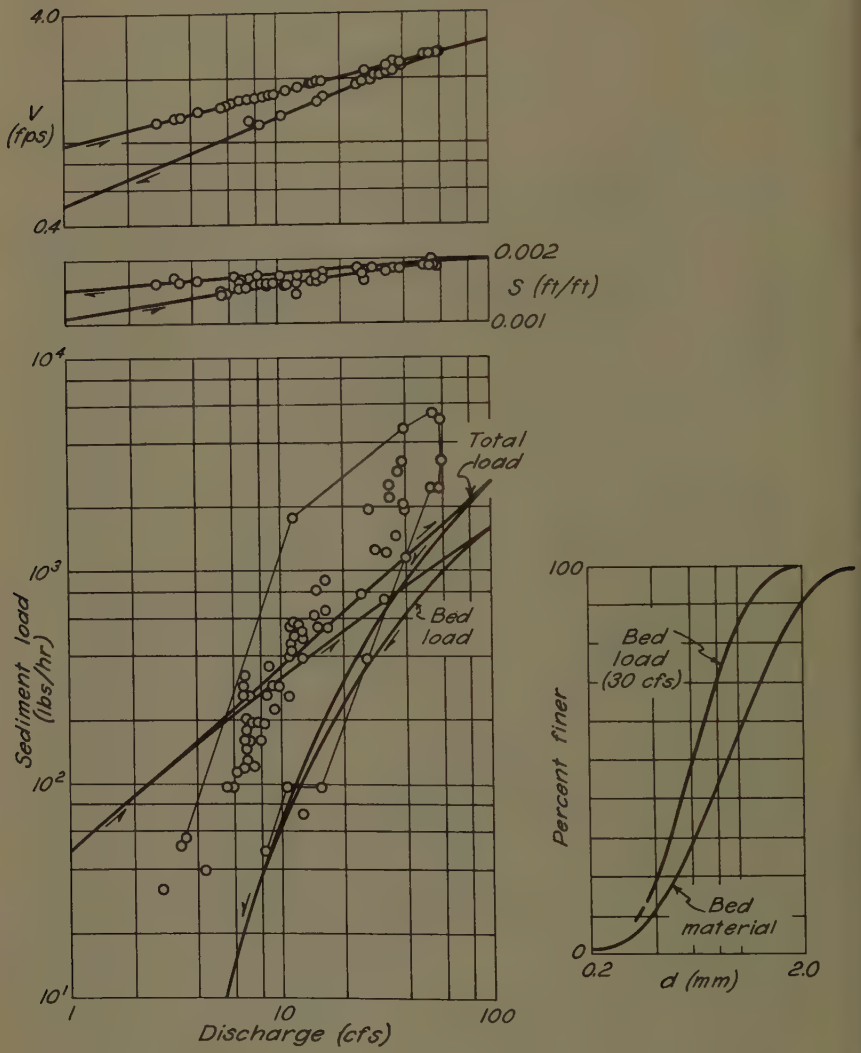


Fig. 11. Prediction of sediment load of Mountain Creek.

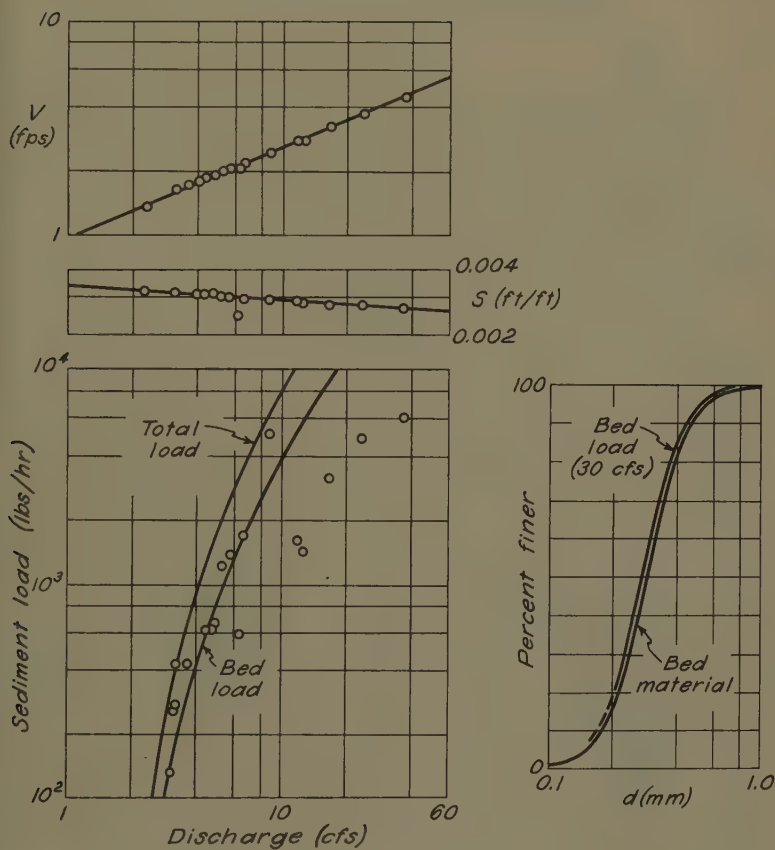


Fig. 12. Prediction of sediment load of West Goose Creek.

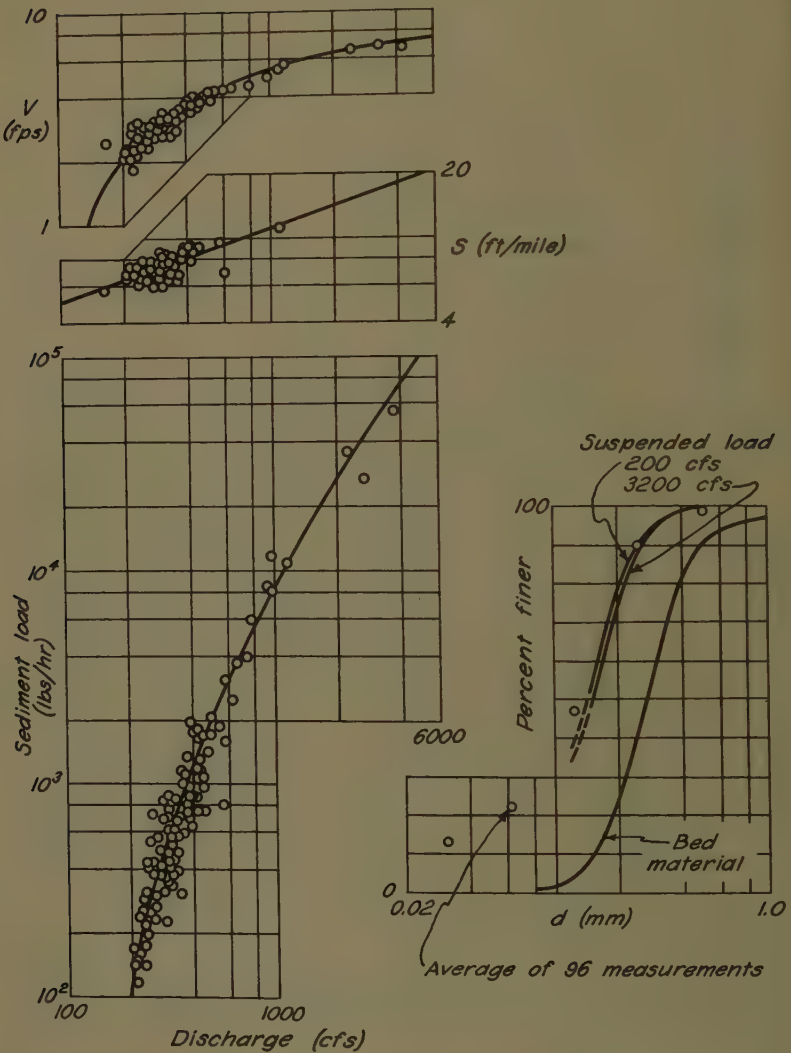


Fig. 13. Prediction of sediment load of Niobrara River.

the range of 200 to 2000 tons per day which would fall on the computed curve or on points next to the curve. In order to compare the predicted and measured composition of the suspended load, seventeen measurements which included a large amount of fine material (the result of surface erosion) were rejected. It should be noted, however, that the measured values of concentration have not been corrected for the inherent sampling error due to the fact that the sampler does not traverse the entire depth.

Applicability of the Proposed Relationships

The proposed rate-of-transport relationships, Eq. (9) and Fig. 14, give both the quantity and the quality of the total, suspended, and bed loads as functions of the basic hydraulic characteristics of the stream and the characteristics of the bed sediment. Thus, they can be applied directly and simply to the prediction of the sediment-transporting characteristics of a stream from other measurable or computable characteristics. However, it should be kept in mind that the relationships are basically empirical and hence can be used with confidence only within the range of conditions for which they have been tested against actual measurements.

In order to increase the reliance that can be placed on their applicability, the proposed relationships must be tested against reliable measurements over an ever wider range of conditions. Special field studies would be particularly valuable—not only to extend the scale to include large rivers, but also to assess the effect of such stream characteristics as channel shape and alignment. Such continued testing could result in the addition of secondary parameters as well as some modification of the present relationships between the basic parameters.

Because approximations had to be made in the formulation of those parameters, continued study of the factors entering into the sediment-transport relationships is also indicated. For example, from Fig. 8 it is quite evident that the critical tractive force relationship for fine materials is not adequately understood. An investigation of the magnitude and distribution of the forces at a boundary of composite roughness such as a duned bed is also needed. It is readily apparent that studies such as these would permit better formulations of the parameters governing the sediment load. Other investigations that would be desirable concern the mutual interference of particles of various sizes and the formation of dunes and ripples.

Unfortunately, the need for a means of predicting the sediment-transporting characteristics of a stream cannot wait on the completion of all desirable research. Since considerable rationality can be ascribed to the parameters of the proposed relationships, and since their ability to correlate measured laboratory and field data has been demonstrated, it would seem reasonable and proper to attempt to apply the relationships to field problems—so long as there is full realization that they are new and comparatively untried.

For any stream which has been gaged for a period of years the hydraulic factors needed for the prediction of the sediment load should be available. Information as to the characteristics of the normal bed material should then permit the construction of load-discharge relations such as those in Figs. 11, 12, and 13. Sheet erosion during heavy rains will contribute a temporary fine fraction to the normal bed material. The "wash" load which results therefrom cannot be predicted from the proposed relationships unless the temporary fine fraction can be estimated. For streams of which the gaging

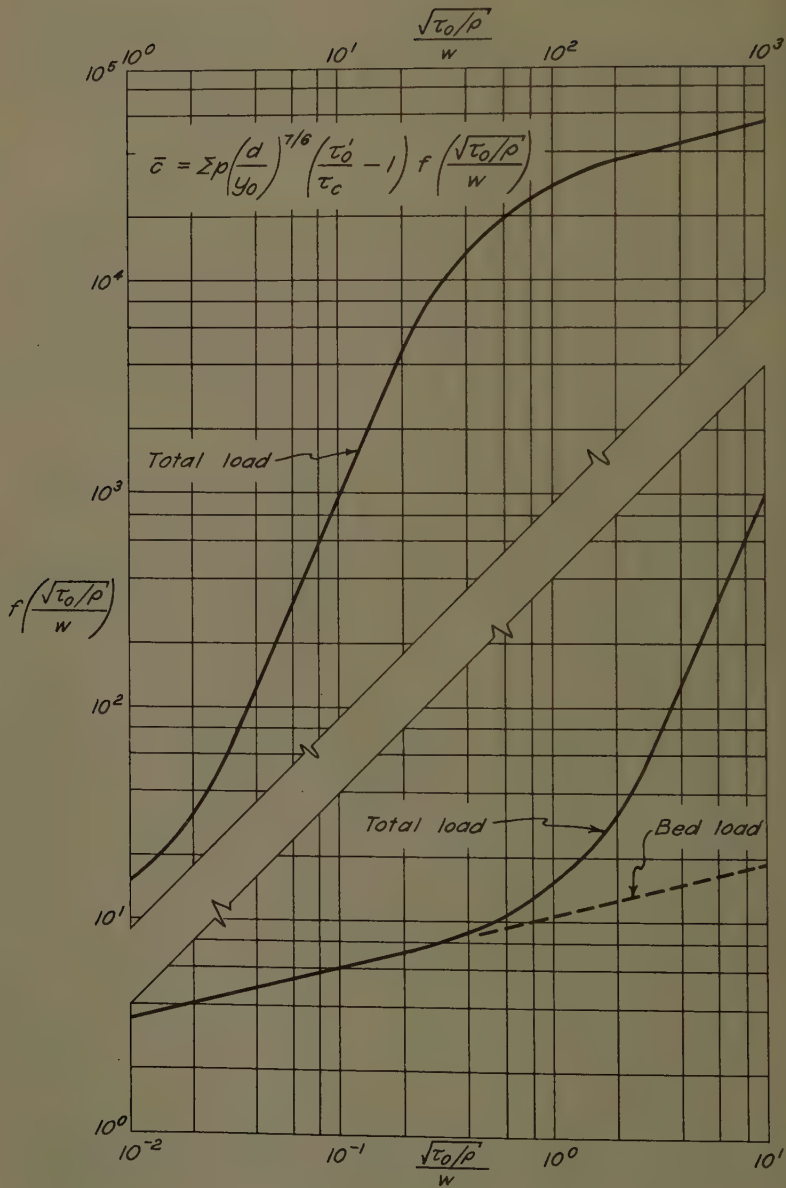


Fig. 14. Relationships for sediment load.

program has included suspended-sediment measurements it may be possible with the aid of the proposed relationships to correlate the wash load with the watershed and rainfall characteristics such as soil type, cultivation, basin slopes, season, intensity of rain, antecedent rain, etc. The utility of such a correlation of unmeasured streams is obvious.

In the case of degradation studies, the influence of the wash load should be small; since the bed material can be considered known, the rate and location of the degradation should be predictable. The case of aggradation studies is more difficult, because the source of the excess sediment load will determine its composition. In this respect the aggradation problem is similar to the problem of wash load on poised streams.

CONCLUSIONS

Through the use of (1) a qualitative analysis, (2) original experiments of a specialized nature, and (3) supplementary data from other sources, empirical relationships for the primary aspects of the sediment load have been obtained. These relationships permit the composition and the rate of transport of the total load, the suspended load, and the bed load to be evaluated from the hydraulic characteristics of the stream (mean velocity and depth of flow and energy gradient) and the characteristics of the bed sediment (frequency distribution of size and fall velocity).

In the process of defining the relationships between the parameters which were found to govern the sediment loads, a correlation of laboratory data representing a ten-thousand-fold range in rate of transport was obtained with scatter probably not much greater than the error in the experimental observations. The extent to which the proposed relationships could predict field conditions was demonstrated for three natural streams. The degree of approximation was especially encouraging, since the ultimate goal of the search for a general sediment-transport function is its application to practical engineering problems.

ACKNOWLEDGEMENTS

The experiments reported herein were performed by Messrs. Pin-Nam Lin, Walter Rand, and Arthur Toch, Research Associates of the Iowa Institute of Hydraulic Research, with the aid of various Research Assistants. Their work was conducted under the immediate supervision of the writer and the general supervision of Dr. Hunter Rouse, Director of the Institute. The investigation was partially supported by the Office of Naval Research under contract N5onr-500(02).

REFERENCES

Laursen, E. M., "The Application of Sediment-Transport Mechanics to Stable-Channel Design," Jour. Hyd. Div. ASCE, Vol. 82, No. HY 4, Aug. 1956.

Lara, J. M., discussion of "The Present Status of Research on Sediment Transport" by Ning Chien, Trans. ASCE, Vol. 121, 1956, pp. 871-6.

3. Kalinske, A. A., "The Movement of Sediment as Bed Load in Rivers," Trans. AGU, Vol. 28, 1947, pp. 615-20.
4. Einstein, H. A., "Formulas for the Transportation of Bed Load," Trans. ASCE, Vol. 107, 1942, pp. 561-77.
5. Einstein, H. A., "The Bed Load Function for Sediment Transportation in Open Channel Flows," Tech. Bulletin No. 1026, U. S. Dept. of Agriculture Soil Conservation Service, 1950.
6. Laursen, E. M., discussion of "Application of the Modified Einstein Procedure for Computation of Total Sediment Load" by K. B. Schroeder and C. H. Hembree, Trans. AGU, October 1957.
7. Rouse, H., "Modern Conceptions of the Mechanics of Fluid Turbulence," Trans. ASCE, Vol. 102, 1937, pp. 463-543.
8. Lane, E. W. and Kalinske, A. A., "The Relation of Suspended to Bed Material in Rivers," Trans. AGU, Vol. 20, 1939, pp. 637-41.
9. Pien, C-L., "Investigation of Turbulence and Suspended Material Transportation in Open Channels," Ph.D. Dissertation, State University of Iowa, 1941.
10. Hsia, C. H., "A Study of Transportation of Fine Sediments by Flowing Water," Ph.D. Dissertation, State University of Iowa, 1943.
11. Jeffrys, H., "On the Transportation of Sediment by Streams," Proc. Cambridge Phil. Soc., Vol. 25, 1929, pp. 272-6.
12. Rubey, W. W., "The Force Required to Move Particles on a Stream Bed," U. S. Geol. Survey Professional Paper 189-E, 1938.
13. Rouse, H., "An Analysis of Sediment Transportation in the Light of Fluid Turbulence," U. S. Dept. of Agriculture, Soil Conservation Service, SCS-TP-25, 1939.
14. Matthes, G. H., "Macroturbulence in Natural Stream Flow," Trans. AGU, Vol. 28, 1937, pp. 255-61.
15. Lane, E. W., "A New Method of Sediment Transportation," Trans. AGU, Vol. 25, 1944, p. 900.
16. Laursen, E. M., "An Investigation of the Total Sediment Load," Final Report to the Office of Naval Research, Iowa Institute of Hydraulic Research, State University of Iowa, June, 1957.
17. Einstein, H. A. and Barbarossa, N. L., "River Channel Roughness," Trans. ASCE, Vol. 117, 1952, pp. 1121-46.
18. White, C. M., "Equilibrium of Grains on Bed of Stream," Proc. Royal Society (London), Vol. 174A, 1940, pp. 322-34.
19. "Sediment Transportation," Chap. XII, Engineering Hydraulics, ed. Hunter Rouse, John Wiley and Sons, 1950.
20. Einstein, H. A., "Bed-Load Transportation in Mountain Creek," U. S. Dept. of Agriculture, Soil Conservation Service, SCS-TP-55, 1944.
21. Colby, B. R. and Hembree, C. H., "Computations of Total Sediment Discharge, Niobrara River near Cody, Nebraska," U. S. Geol. Survey Water

Supply Paper 1357, 1955.

22. Johnson, J. W., "Laboratory Investigations on Bed-Load Transportation and Bed Roughness," U. S. Dept. of Agriculture, Soil Conservation Service, SCS-TP-50, 1943.
23. Brooks, N. H., "Mechanics of Streams with Movable Beds of Fine Sand," Proc. ASCE, Vol. 81, Separate No. 668, April, 1955.
24. Barton, J. R. and Lin, P-N., "A Study of Sediment Transport in Alluvial Channels," Research Report, Civil Engineering Department, Colorado A and M College, 1955.
25. "Studies of River Bed Materials and Their Movement with Special Reference to the Lower Mississippi River," U. S. Waterways Experiment Station Paper 17, Jan. 1935.

List of Symbols

a	elevation of reference concentration c_a , ft
c	sediment concentration at a point, percent by weight
\bar{c}	mean concentration, $265 q_s/q$ (subscripts s, b, t refer to suspended, bed, and total load, respectively), percent by weight
c_a	concentration at reference level a, percent by weight
C	coefficient relating critical tractive force to sediment size
d	diameter of sediment particle (mean diameter of fraction p of bed material), ft
d_m	mean diameter of bed material, ft
f	Weisbach resistance coefficient
F	Froude number, $V/\sqrt{gy_0}$
h	dune height, ft
l	dune length, ft
m	exponent in power-law velocity distribution
n	Manning roughness coefficient
p	fraction of bed material of diameter d
q	rate of flow per unit width, Vy_0 , cfs/ft
q_s	volume rate of sediment transport per unit width (subscripts s, b, t refer to suspended, bed, and total load, respectively), cfs/ft
R	hydraulic radius, ft
R	Reynolds number, $2Vy_0/\gamma$
S	energy gradient, ft/ft
v	velocity of flow at a point, fps
v_s	surface velocity obtained by extrapolating power-law velocity distribution, fps

V	mean velocity, q/y_0 , fps
w	fall velocity of sediment particle, fps
y	elevation above stream bed, ft
y_0	depth of flow, ft
z	measured exponent for concentration distribution
z_1	theoretical exponent for concentration distribution
β	coefficient of proportionality between ϵ_s and ϵ_m
γ	specific weight of water, lb/ft ³
δ'	thickness of laminar sub-layer, ft
ϵ_m	mixing coefficient for momentum
ϵ_s	mixing coefficient for sediment
κ	coefficient in logarithmic velocity distribution
ν	kinematic viscosity of water, ft ² /sec
ρ	density of water, γ/g , lb sec ² /ft ⁴
τ	intensity of shear, lb/ft ²
τ_c	critical tractive force for beginning of sediment movement
τ_0	boundary shear, or tractive force, at stream bed, $\gamma y_0 S$
τ'_0	boundary shear associated with sediment particles

Journal of the HYDRAULICS DIVISION

Proceedings of the American Society of Civil Engineers

SEDIMENT TRANSPORT IN MONEY CREEK

J. B. Stall,¹ A.M. ASCE, N. L. Rupani,² and P. K. Kandaswamy,³ A.M. ASCE
(Proc. Paper 1531)

SYNOPSIS

Lake Bloomington, an impounding reservoir, has been subjected to detailed surveys in 1948, 1952 and 1955 to determine the deposition of sediment. During each of these surveys samples of the sediment were obtained. Particle size distribution analyses of 30 of these sediment samples were utilized to determine the tons of sediment deposited in the lake during each of these sedimentation periods. Postulating that sediment particles which had a diameter greater than 50 microns had been moved into the lake as bed material load, the total tons of this sized material was calculated based on the sediment samples.

An hydraulic study was made of the 2-1/2 mile reach of Money Creek immediately upstream from Lake Bloomington to determine its sediment-carrying capacity. A series of sediment samples were taken of the bed material of the Money Creek channel. Utilizing these data, curves of water discharge versus sediment discharge were computed utilizing three different methods: the Einstein procedure, the Schoklitsch formula, and the DuBoys formula.

At the lower end of this stream reach, immediately upstream from Lake Bloomington is a stream-gaging station for which flow records were available for each of the three sedimentation periods. Utilizing flow duration information from this stream gage, the total quantity of bed material moved through the Money Creek reach was calculated utilizing each of the three sediment transport relationships developed. The actual bed material-size sediment in Lake Bloomington is compared with the sediment transport as computed by the three methods.

Note: Discussion open until July 1, 1958. A postponement of this closing date can be obtained by writing to the ASCE Manager of Technical Publications. Paper 1531 is part of the copyrighted Journal of the Hydraulics Division, Proceedings of the American Society of Civil Engineers, Vol. 84, No. HY 1, February, 1958.

. Associate Engr., Illinois State Water Survey Div., Urbana, Ill.

. Formerly Asst. Engr., Illinois State Water Survey Div., Urbana, Ill.

. Formerly Asst. Engr., Illinois State Water Survey Div., Urbana, Ill.

INTRODUCTION

Purpose

The purposes of this investigation are: (1) to attempt to compute the sediment moved as bed material load in Money Creek, Illinois, for a reach immediately upstream from a stream-gaging station and from Lake Bloomington, (2) to provide a comparison of three well-known bed-load formulas including the most recent one proposed by H. A. Einstein⁽¹⁾ and (3) to compare the results of these formulas with bed material measured by actual survey in Lake Bloomington.

Most sediment transport formulas are derived from laboratory flume studies. The importance of this study is believed to be the check of three formulas under natural conditions.

General

The city of Bloomington is located in the central part of McLean County, Illinois. A public water supply derived from wells was installed for the town in 1875. The wells were utilized until 1929 when Lake Bloomington was formed by the construction of an earth dam across Money Creek, a tributary to the Mackinaw River about 15 miles northeast of Bloomington. Since that time Lake Bloomington has been used for the public water supply. The lake has a drainage area of 61.0 square miles, a surface area of 487 acres, and had an original storage capacity of 2.17 billion gallons. Fig. 1 shows the location of Lake Bloomington and Money Creek watersheds.

A detailed survey was conducted on Lake Bloomington in August 1948 to determine the volume of sediment deposition. At that time a series of 19 cross sections of water depth and sediment thickness were taken on the lake as shown in Fig. 2. In August 1952 and in July 1955 soundings were repeated along these same cross sections to measure the further sediment deposition during the intervening periods. These cross sections were plotted and the total quantity of sediment (including the bed-load and wash-load) deposited in the lake was calculated by the method devised by the Soil Conservation Service.⁽²⁾

Table 1 is a summary of the results of the three surveys. It will be seen that the capacity of the lake has been depleted every year at an average rate of about 0.46 percent of the original capacity. The 1955 survey showed a total loss in capacity of 791 acre feet or 258 million gallons.

During a period of low inflow and low lake level during 1954 less sediment was carried into the lake and a portion of the deposited sediment bed in the upper portion of the lake was exposed to air drying and consequently compacted. The specific weight of the sediment deposit in each segment of the lake was determined by a series of sediment samples obtained during each of the three surveys. A total of 30 samples were utilized to determine the tons of sediment deposited in the lake during each of the sedimentation periods.

Choice of Reach

Lake Bloomington and its watershed have been the subject of an hydrologic study by the State Water Survey since 1933.⁽³⁾ The principal tributary to Lake Bloomington is Money Creek. Immediately upstream from the headwaters of the lake is located a stream-gaging station. This gage is sponsored

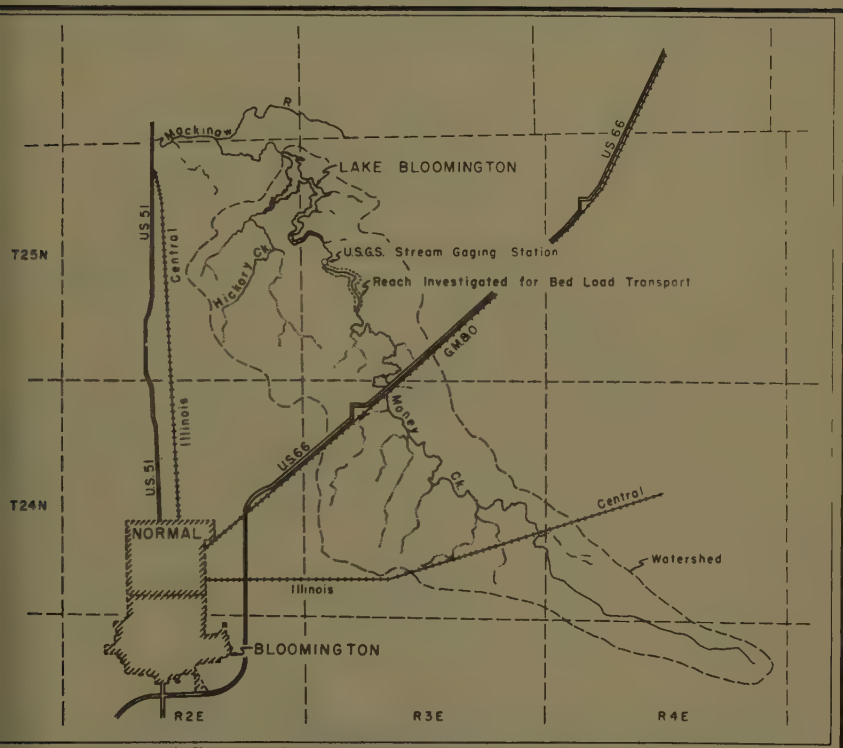


Figure 1 - Location of Money Creek and Lake Bloomington

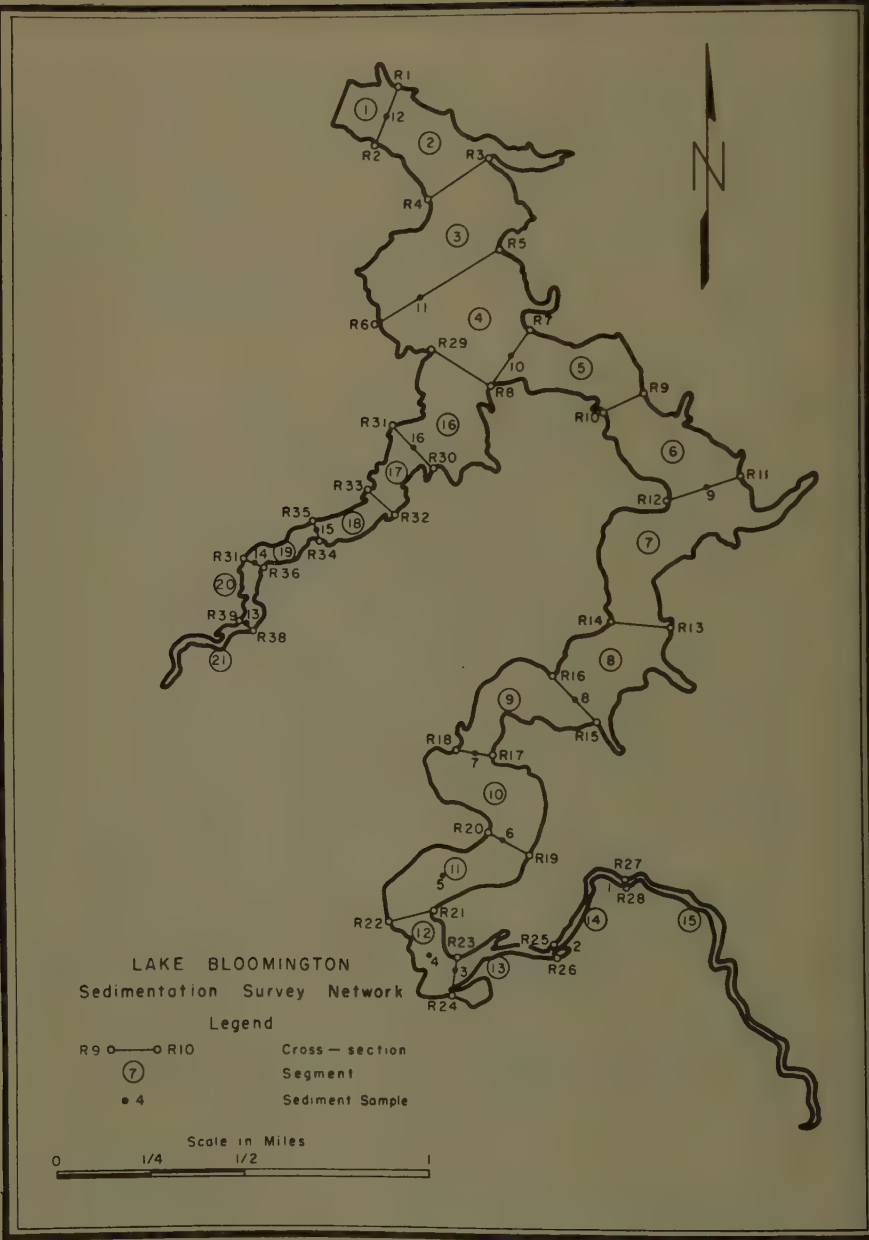


Figure 2 - Sedimentation Survey of Lake Bloomington

Table 1. Summary of Sedimentation Data
Lake Bloomington, Illinois

AGE

Dec. 1929 - Aug. 1943	- 18.7 yrs.
Aug. 1946 - Aug. 1952	- 4.0 yrs.
Aug. 1952 - July 1955	- 2.9 yrs.
Dec. 1929 - July 1955	- 25.6 yrs.

WATERSHED

Total area	- 61.0 sq. miles
	39,040 acres
Land area	- 60.2 sq. miles
	38,553 acres

RESERVOIR

Area at spillway crest - 487.2 acres

	<u>1929</u>	<u>1948</u>	<u>1952</u>	<u>1955</u>	<u>Units</u>
<u>Storage Capacity</u>	6654	6062	5905	5863	Acre-feet
	216 ⁸	1975	1924	1911	Mil. gal.
<u>Capacity per sq.mi.</u> <u>of drainage area</u>	109	99	97	96	Acre-feet

<u>SEDIMENTATION</u>	<u>1929-1948</u>	<u>1948-1952</u>	<u>1952-1955</u>	<u>1929-1955</u>	
Total	592	157	42	791	Acre-feet
<u>Average Annual Accumulation</u>					
From entire watershed ¹	31.7	39.3	14 ²	30.8	Acre-feet
Per sq.mile ¹	0.53	0.65	0.23 ²	0.51	Acre-feet
Per acre ¹	36.1	44.2	15.7 ²	34.7	Cubic-foot
Tons per acre ¹	0.74	0.91	0.34	0.72	Tons

DEPLETION OF STORAGE

Loss of original capacity				
Total period	8.90	2.36	0.63 ²	11.89 Per cent
Per Year	0.48	0.59	0.21 ²	0.46 Per cent

¹Land area only.

²Volume compacted due to drying.

by the State Water Survey and is operated by the United States Geological Survey. It records the drainage from 51.9 square miles of the total lake watershed. Records are available at this station from June 1933 to date. Because of the availability of these discharge records, the stream reach immediately upstream from this gage was given consideration for the present study.

In selecting a river reach for sediment transport calculations, it must be remembered that such a function can be applied only to a river reach of uniform flow. This means that the length of the channel must be sufficient to permit adequate determination of the over-all slope. Also the channel itself must be sufficiently uniform in shape, sediment composition, slope and outside effects such as bank vegetation, that it is possible to treat the reach as a uniform channel characterized by an over-all slope and by an average representative cross section. Practically, it is difficult to realize such an ideally uniform channel. After a field inspection of Money Creek, however, it was decided that this reach was sufficiently uniform to be utilized for bed-load calculations.

Hydraulic and Hydrologic Determinations

Hydraulic Properties of Channel

A field investigation was made of the 2-1/2 mile reach immediately upstream from the gaging station to determine hydraulic properties. A series of 13 cross sections was taken of the stream at approximately 1000-foot intervals. The slope of the water surface was determined to be 0.000905 by utilization of these 13 stations. The slope measurement was taken during a time when the average discharge was 160 cubic feet per second. Flow duration studies showed discharge equalled or exceeded this amount for six percent of the period of record.

To determine the stage-area relationship for the reach, each of the 13 cross sections was plotted in actual position in elevation. The average cross section for the reach was then determined by sliding all cross sections down the channel along the slope 0.000905 into the plane of the section at the lower end of the reach. This downstream cross section was at the stream-gaging station, giving a means of comparison between the mean cross section for the reach and the actual cross section of the gaging station. The stage-area curve for the reach determined in this manner is shown in Fig. 3.

In a similar manner the average stage-wetted perimeter curve was obtained and is shown in Fig. 4. In a wide channel like Money Creek the width of the channel was considered as the wetted perimeter for a known elevation. Consequently, corresponding values of the two curves made it possible to compute the hydraulic radius for the same elevation. These are shown in Fig. 5. The curve of stage versus hydraulic radius with bank friction was computed by means described by Einstein.⁽¹⁾ The stage-discharge relationship with and without bank friction is shown in Fig. 6 as compared to the actual stage-discharge relationship as measured at the gaging station.

In order to determine the width of the stream bed along which transportation takes place, the average widths of the stream at various stages of all of the 13 cross sections were plotted and are shown in Fig. 7. As reported by Chang⁽⁴⁾ and by Einstein⁽⁵⁾ the movement of bed material is reasonably expected to take place only along the bed portion of the channel. From Fig. 7 a

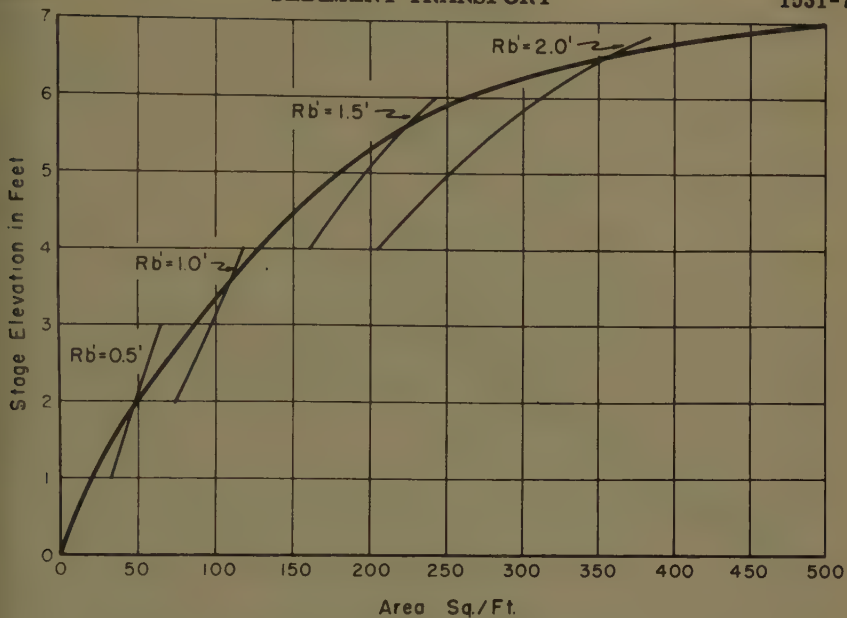


Figure 3 - Stage-Area Relationship for Money Creek

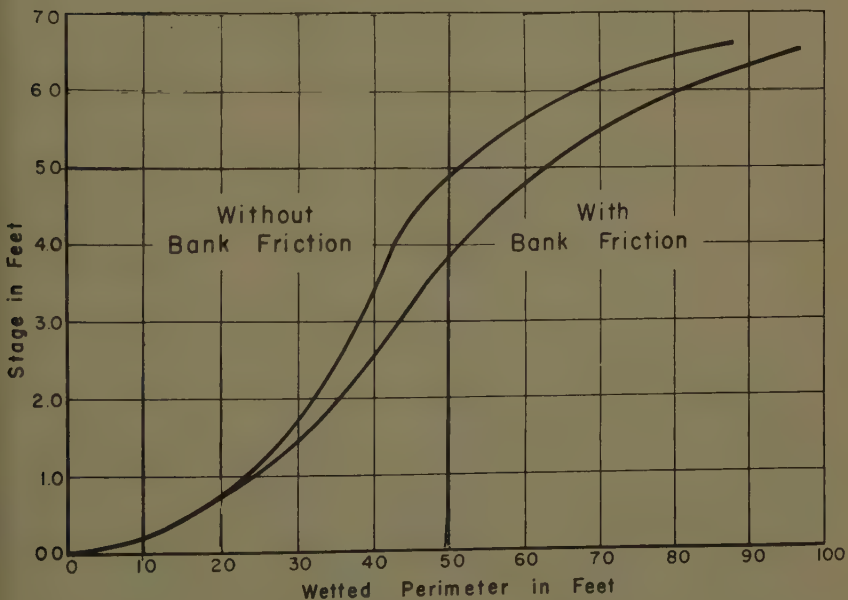


Figure 4 - Stage-Wetted Perimeter Relationship for Money Creek

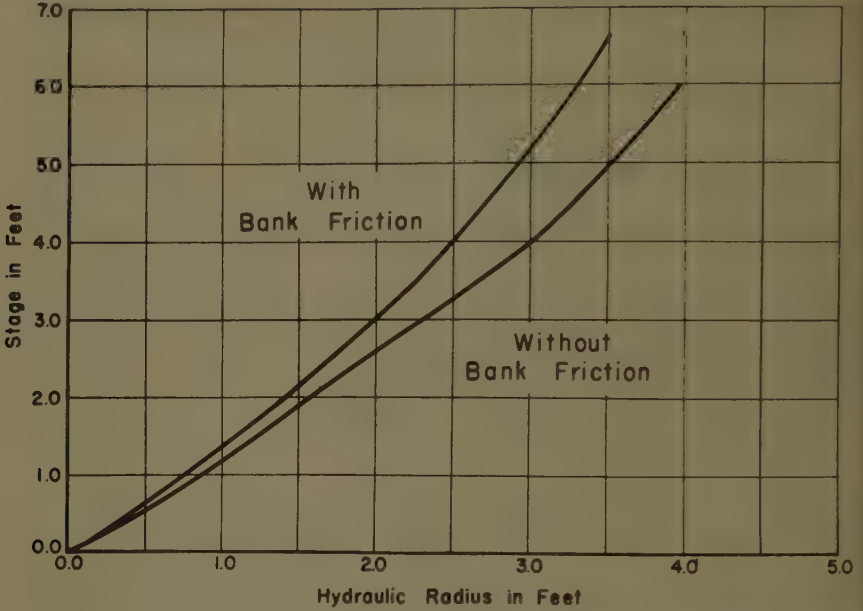


Figure 5 - Stage-Hydraulic Radius Relationship for Money Creek

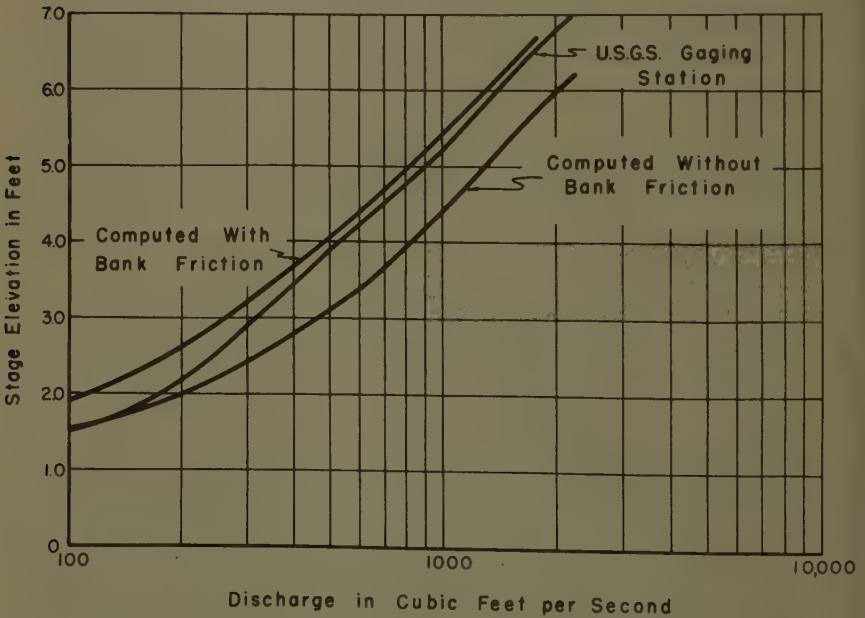


Figure 6 - Stage Discharge Relationship for Money Creek

width of 30 feet was arbitrarily chosen to represent the width of bed for the reach of Money Creek under consideration.

Computations of hydraulic properties need to be made only up to a stage corresponding to the highest flood that had occurred in this creek. This stage of seven feet was the maximum utilized in determining all hydraulic properties.

Bed-Sediment Samples

Since the bed-load formulas used in this study relate the grain-size composition of the bed material with the flow of the channel it is necessary to obtain representative samples of the bed material. A total of 18 samples of sediment was taken along the active channel and the flood plain of Money Creek. Samples were obtained by means of an auger or a pipe sampler and were taken to a depth of about 1.5 feet, the estimated depth of scour or active bed movement. The flood plain samples indicated 90 percent by weight to be finer than 50 microns, and it was concluded that these finer particles were deposited during the recession of flood flows. Consequently the flood plain samples were abandoned and five samples were chosen to represent the bed material in the active channel. The size distribution of this bed material based on these samples is shown in Table 2.

The data from Table 2 are plotted in Fig. 8, from which can be noted the characteristic grain sizes. The size which enters the Einstein equation of transport is $D_{35} = 0.195 \text{ mm} = 0.000639 \text{ feet}$ (grain size of which 35 percent is finer). The size characteristic for friction $D_{65} = 1.22 \text{ mm} = 0.0040 \text{ feet}$.

The sediment transport was calculated for grain sizes between 9.4 millimeters and 0.050 millimeters which represents 67 percent of the bed material. It is important to recognize however that 12 percent of the bed material is coarser than 9.4 millimeters. These gravel-size particles do not move for normal flows although an extremely small rate of transport may occur at high flood stages. Twenty-one percent of the bed material is finer than 0.050 millimeters. As much as 15 percent of this size may be expected to be a part of wash-load particles lodged behind the coarser grains. This can generally be neglected. No adjustments were made since a large percent of these finer materials were found in the bed. Though included in the bed material size distribution, no bed-load function exists for these finer particles. Calculations were made for individual sieve fractions using as representative the average grain sizes varying from 7.3 to 0.073 millimeters as shown in Table 2.

Calculation of Bed Material Deposited in the Lake

One of the most critical phases of the present investigation was the determination of the total quantity of sediment deposited in Lake Bloomington which was of the size moved as bed-material-load through the tributary creek, Money Creek. The quantities of sediment measured in the lake survey contained principally fine material which was undoubtedly moved into the lake as wash load. The 16 sediment samples taken during the 1948 and 1955 lake surveys were considered to be sufficient in number to indicate the sediment nature in the various segments of the reservoir. These samples were subjected to size distribution analyses. The locations of these sediment samples are shown in Fig. 2.

All particles of sizes 0.050 millimeters (50 microns) and more were considered as bed-load and particles of sizes smaller than 0.050 millimeters, in

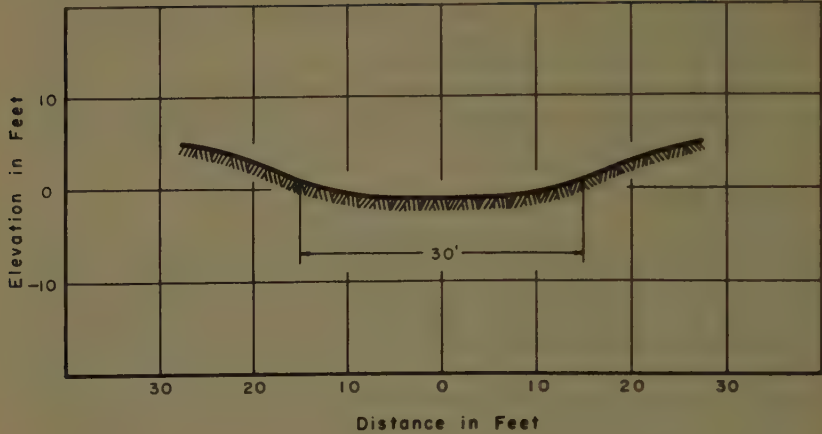


Figure 7 - Money Creek Average Cross Section

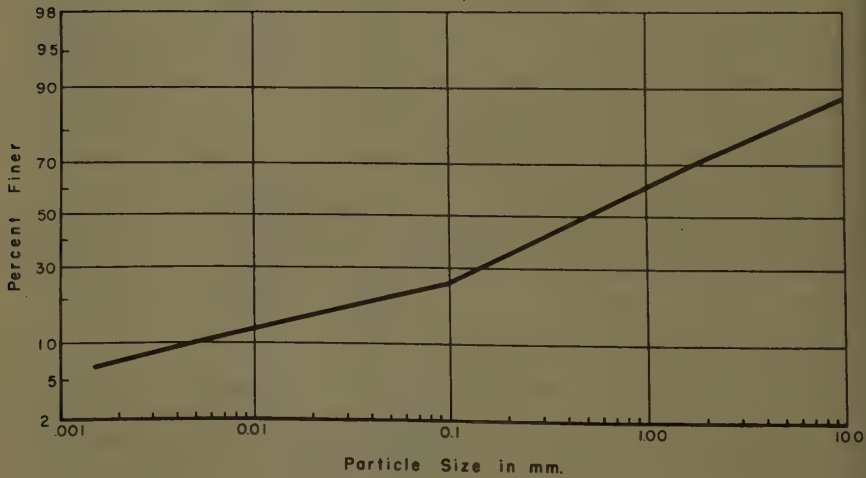


Figure 8 - Average Size Distribution of Bed Material Samples

Table 2. Average Size Distribution of Money Creek Bed Material Based on Five Samples

Grain Size mm	Per Cent by Weight	Mean Diameter mm	Feet
Less than 0.050	21.0	-----	-----
0.050 to 0.097	4.0	0.073	0.000239
0.097 to 0.19	9.5	0.144	0.000472
0.19 to 0.37	10.7	0.28	0.000918
0.37 to 0.72	11.3	0.545	0.00179
0.72 to 1.4	10.7	1.06	0.00348
1.4 to 2.7	8.8	2.05	0.00672
2.7 to 5.2	7.0	3.95	0.01295
5.2 to 9.4	5.0	7.3	0.02393
Greater than 9.4	12.0	---	-----

Table 3. Sand Content of Lake Sediment Samples

Sample No.	Per Cent Sand By weight (Diameter > 50 microns)
1	97
2	53
3	22
4	33
5	17
6	11
7a	0.5
7b	0.5
8	0.5
9a	2.0
9b	7
10	2.5
11	1.0
12a	3.0
12b	2.5
13	18
14	2.5
15a	1.0
15b	0.5
16	1.0

"a" Samples from upper portion of sediment deposit
 "b" Samples from lower portion of sediment deposit

the range of silt and clay, were considered wash load. Table 3 presents the results of these analyses, showing for each sample, the total percent by weight of material having a diameter greater than 50 microns. In only two of these samples was there material having a diameter in excess of 9.4 millimeters and in each of these cases the percentage was extremely small.

The sediment samples at the 16 locations in the lake were utilized to compute the total quantity of sediment in tons in each segment of the lake. The locations of the sediment samples and the lake segments are shown in Fig. 2. Table 4 shows the results of these calculations.

Reference to Figs. 1 and 2 shows that Money Creek is tributary to that portion of the lake containing segments 5 through 15 and Hickory Creek contributes the flow to segments 16 through 21. The two arms of the lake come together to form that portion of the lake containing segments 1, 2, 3 and 4. The tonnage of sediment as calculated in Table 4 for these four segments (1 through 4) was calculated by proportioning the total tonnage coming from Hickory Creek and from Money Creek. The drainage area of the Money Creek above the lake is 51.9 square miles and the drainage area on Hickory Creek above the lake is 10 square miles. The proportion of these two drainage areas was used to calculate the tonnage of bed material sediment deposited in these lower four segments of the reservoir. It will be noted from Table 4 that the total quantity of bed material, which can be assumed to have moved down Money Creek and into Lake Bloomington during the period 1929-1955, amounts to 60,527 tons.

Flow Duration Data

Computation of the bed load by any of the three formulas developed a relationship between sediment discharge in tons per day and water discharge in cubic feet per second. To determine the total quantity of material moved through this reach of the stream as bed load, it was necessary, therefore, to construct flow duration curves. It was desired that such data be available for each of the three periods during which sediment deposition was measured in Lake Bloomington. Water discharge data from the stream-gaging station on Money Creek were complete in this respect except for the period 1929 to 1933 and for the year 1941. To complete the flow record, the discharge at Money Creek was synthesized for these missing years.

Stream-gaging records were available for the neighboring Mackinaw River for the missing periods of record as well as for the complete period of record for Money Creek. The two drainage basins were assumed to be homogeneous in regard to their general flow characteristics. Flow duration curves for the two rivers were drawn based on the same period of records, namely 1934 through 1940 and 1942 through 1954. These were used to synthesize the missing records at Money Creek based upon the actual flow measurements on the Mackinaw River using a method described by Mitchell.⁽⁶⁾ The actual flow records of Money Creek which is in the Mackinaw River basin have been published by the United States Geological Survey in their Water Supply Papers.⁽⁷⁾

To determine the bed-load quantity, the flow duration data for each of the three different periods were compiled as described above and shown in Table 5. Only flows above 110 cubic feet per second have been considered. This assumes that the quantity of bed material moved by lesser flow is negligible. Table 5 shows the duration of the high flows which have occurred at the Money

Table 4. Total Tonnage of Sand and Larger Material Deposited in Lake Bloomington

Segment	Sediment Tons	Samples	Per Cent Sand (> 50 microns)	Total Sand Tons	
				Hickory Cr. Arm of Lake	Money Cr. Arm of Lake
1	10,881	12a,12b	2.75	54	245
2	32,735	12a,12b	2.75	163	737
3	46,828	11	1.0	85	383
4	42,238	10,11	1.75	134	605
5	28,117	10	2.5	--	703
6	33,945	9a,9b	4.5	--	1528
7	49,294	9a,9b	4.5	--	2218
8	41,323	8	0.5	--	207
9	56,245	7a,7b,8	0.5	--	281
10	71,130	6	11	--	8594
11	99,630	5	17	--	16,937
12	41,840	3,4	27.5	--	11,506
13	27,527	2,3	37.5	--	10,323
14	5,061	1,2	75	--	3796
15	2,541	1	97	--	2464
16	45,285	16	1.0	453	---
17	16,407	16	1.0	164	---
18	11,960	15a,15b	2.75	329	---
19	15,182	14,15a,15b	2.17	329	---
20	16,477	13,14	10.3	1697	---
21	10,027	13	18	1805	---

60,527 Tons

Table 5. High Flow Duration During Lake Sedimentation Periods

Money Creek Gaging Station

Mean Discharge cfs	Duration in Days			Total
	1st Period Dec. 1929 to Aug. 1948	2nd Period Sept. 1948 to Aug. 1952	3rd Period Sept. 1952 to July 1955	
110	376	124	59	559
165	199	58	20	277
245	103	34	11	148
355	58	18	6	82
520	31	10	3	44
760	11	2	--	13
1100	3	1	--	4

Creek gaging station during the three periods for which sedimentation was measured in Lake Bloomington. Discharges considered are mean values of incremental discharge ranging from 110 cubic feet per second to 1100 cubic feet per second.

Sediment Transport Calculations

The Einstein Procedure

H. A. Einstein developed and published in 1950 a complex procedure for computing the quantity of bed material transported by a stream.⁽¹⁾ This bed load function was applicable to an alluvial channel in an equilibrium state, which moves the material through which it flows.

The approach was based on the probability of movement of a particle of a particular diameter in the "bed layer." Movement in this layer was considered to occur by rolling and sliding on the bed or by making a series of short hops and was termed "surface creep." The thickness of the bed layer was postulated to be twice the grain diameter. The movement of particles was considered to be governed by statistical laws of probability and was so related to the flow. The average distance traveled by a particle between periods of deposition was assumed to be 100 diameters.

The concentration of particles having a particular diameter at the top of the bed layer is assumed to be equal to the concentration of suspended particles of the same diameter at this same boundary. This concentration is then related to the concentration of similar particles at any elevation in the vertical. By integration of the function the total sediment load of this diameter, per unit width, was determined at a representative vertical in the stream cross section at a given discharge. Load was calculated for a number of grain-size categories based on the samples of bed material. In calculating the total load of a mixture of particles, corrections were introduced for the "hiding factor" or interference of the larger grains with the smaller. A later publication by Einstein⁽⁸⁾ improves this correction.

The principal relationships utilized by Einstein in the bed load function are as follows:

$$q_s = \int_a^d c_y \bar{u}_y dy \quad (1)$$

$$c_y = c_a \left(\frac{d-y}{y} \frac{a}{d-a} \right)^z \quad (2)$$

$$z = \frac{v_s}{ku_*} \quad (3)$$

Where,

q_s = Rate of transportation of suspended load

d = Water depth

\bar{u}_y = Velocity at distance y above bed

c_y = Sediment concentration, weight per unit volume, of the fluid-sediment mixture at distance y above the bed

c_a = Sediment concentration at distance a above bed

v_s = Settling velocity of a sediment grain in still water

k = Universal constant of von Karman

u_* = Shear velocity at the bed

Einstein⁽¹⁾ considered the velocity distribution in open-channel flow over a sediment bed as being best described by the logarithmic formula based on von Karman's similarity theorem with the constants as proposed by Prandtl and von Kármán.⁽⁹⁾ He gave the vertical velocity distribution including the transition between the rough and smooth boundaries as:

$$\frac{\bar{u}_y}{u_*} = 5.75 \log_{10} \left(30.2 \frac{y x}{k_s} \right) \quad (4)$$

$$= 5.75 \log_{10} \left(30.2 \frac{y}{\Delta} \right)$$

wherein x is given as a function of k_s/δ

\bar{u}_y = the average point velocity at the distance y from the bed

$$u_* = \sqrt{\tau_0 / s_f} = \sqrt{S_e \cdot R \cdot g} \quad (\text{the shear velocity}) \quad (5)$$

s_f = the density of the water

S_e = the slope of the energy grade line

R = the hydraulic radius

g = the acceleration due to gravity

y = the distance from the bed

k_s = the roughness of the bed

x = a correction parameter

$$\Delta = k_s / x \quad \text{the apparent roughness of the surface} \quad (6)$$

$$\delta = \frac{11.6}{u_*} \quad \text{the thickness of the laminar sublayer of a smooth wall} \quad (7)$$

ν = the kinematic viscosity of the water

The value of k_s for uniform sediment equals the grain diameter as determined by sieving. The representative grain diameter of a sediment mixture is given by that sieve size of which 65 percent of the mixture by weight is finer.

The total rate of sediment transportation is the sum of the suspended and bed-load transport rate and is given by Einstein in Equation (63) of Reference (1) as,

$$i_T q_T = i_B q_B (P I_1 + I_2 + 1) \quad (8)$$

where:

i_T = Fraction of total load in a given size range

q_T = Total transport rate, weight per unit time and width

i_B = Fraction of bed load in a given size range

q_B = Bed load transport rate

I_1 = Integral value (Evaluation tables furnished by author)

I_2 = Integral value (Evaluation tables furnished by author)

P = Parameter of total transport

and,

$$P = \frac{1}{0.434} \log_{10} \left(\frac{30.2 x}{k_s / d} \right) \quad (9)$$

In the evaluation of sediment movement through the reach of Money Creek considered in this paper, the hydraulic character of the channel was computed in accord with the methods reported by Einstein. Detailed computations are not presented here but the resultant effects of bank friction are shown in Figs. 4 to 6 of this report. The computations of sediment movement are based on these hydraulic computations including the bank friction.

The relationship of sediment discharge to water discharge for Money Creek as determined by the Einstein procedure is tabulated in Table 6 and is shown graphically in Fig. 11. Table 6 shows the utilization of this relation and the flow duration data to determine the total bed material movement into Lake Bloomington during the sedimentation periods under consideration. Total transport calculated by this means amounts to 196,477 tons.

Schoklitsch Bed-Load Formula

The sediment movement in Money Creek was calculated by utilization of the Schoklitsch formula for uniform sand.

$$G = \frac{86.7}{\sqrt{d}} S^{1.5} B (q - q_0) \quad (10)$$

$$q_0 = \frac{0.00532 d}{S^{1.33}} \quad (11)$$

and the bed load for a mixture

$$G_t = a G_a + b G_b + c G_c \dots + m G_m \quad (12)$$

where

G = Bed load in tons per day

G_t = Total bed load for a mixture of particles

G_a = Quantity of bed load of a particular diameter

a = Percent weight of a particular diameter in a mixture

m = Number of size-gradation divisions in a mixture

d = Diameter of particle, inches

S = Hydraulic slope

B = Bed width, feet

q = Discharge, cfs

q_0 = Critical discharge at which movement of particle of diameter d , begins

The Schoklitsch⁽¹⁰⁾ formula serves to compute that portion of the total load solids in the river which is transported (not in suspension) along the river bed by the tractive force of the stream. The Schoklitsch formula is based mainly on the classic flume experiments of G. K. Gilbert besides additional experimental data collected by Schoklitsch. It was developed for uniform grain material but there can be no valid objection to its being applied to mixtures as well. It has been verified and found to agree closely with the measurements in the River Danube and the Terek River.

In the application of this formula to a natural stream it was stated by Schoklitsch that the reach studied be relatively straight and the depths of water as uniform as possible in order that the width of the stream change as little as possible with stage. Table 7 shows the relation of area and width of Money Creek at the various discharges considered.

Table 8 summarizes the movement of bed-load material in Money Creek calculated by the Schoklitsch formula. The relationship of sediment discharge to water discharge is plotted in Fig. 11. Table 8 shows the product of sediment discharge rating and flow duration information converted into total quantity of bed-load movement in tons for the various periods. Total transport by this method amounts to 79,065 tons.

DuBoys Formula

The sediment transport in Money Creek has been calculated by the DuBoys formula.

$$q = C_s \tau (\tau - \tau_c) \quad (13)$$

Table 6. Money Creek Sediment Discharge by Einstein Bed Load Function

For particles 0.05 mm to 9.4 mm

Water Discharge cfs	Sediment Discharge Tons/Day	1st Period		2nd Period		3rd Period		Sediment Tons
		Duration Days	Sediment Tons	Duration Days	Sediment Tons	Duration Days	Sediment Tons	
110	94	376	35,344	124	11,656	59	5,546	2,546
165	145	199	28,855	58	8,410	20	2,900	40,165
245	232	103	23,896	34	7,888	11	2,552	34,336
355	335	58	19,430	18	6,030	6	2,010	27,470
520	550	31	17,050	10	5,500	3	1,650	24,200
760	920	11	10,120	2	1,840	--	-----	11,960
1100	1450	3	<u>4,350</u>	1	<u>1,450</u>	--	-----	<u>5,800</u>
Total			139,045		42,774		14,658	196,477

Table 7. Money Creek Area-Width Relationship

Discharge cfs	Stage Feet	Area Sq.Ft.	Width Feet
110	1.98	49.5	25.0
165	2.38	63.0	26.5
245	2.91	83.0	28.5
355	3.49	106.0	30.4
520	4.13	133.5	32.3
760	4.84	171.0	35.3
1100	5.63	226.5	40.2

and the bed load for a mixture

$$G = (a q_a + b q_b + c q_c + \dots + n q_n) \gamma S_s \quad (14)$$

and

$$\tau = \gamma y s \quad (15)$$

where

q = Transport rate of a particular diameter particle in volume per second per foot of width

C_s = Sediment parameter

τ = Intensity of bed shear

γ = Unit weight of water

y = Depth of flow

s = Hydraulic slope

τ_c = Value of τ for which q_s is zero

S_s = Specific gravity of sediment particle

a = Percent weight of a particle diameter in a mixture

n = Number of size-gradation divisions in a mixture

G = Bed load total for mixture, pounds per second per foot of width

The DuBoys formula was one of the earliest published to determine the bed transport of sediment. A great number of other formulas have been developed subsequently and have a similar nature. Johnson⁽¹¹⁾ tested a number of these and concluded that all formulas fitted equally well, thus indicating that the choice could be made on the basis of convenience. In order to utilize this formula, it was necessary to evaluate the parameters C_s and τ_c . The values summarized by Straub and published in Engineering Hydraulics⁽¹²⁾ were utilized. It was necessary, however, to extrapolate these relationships shown in Fig. 9 for the relation of C_s to particle diameter, and in Fig. 10 for the relation of τ_c to particle diameter.

In Table 9 is summarized the results of the calculation of bed-load movement in Money Creek by the DuBoys formula. The relation of sediment discharge to water discharge has been plotted in Fig. 11. Table 9 shows the computation of the total sediment movement throughout this reach based on the flow duration of Money Creek for the three sedimentation periods. It will be noted that the total quantity of sediment moved calculated by this means amounts to 529,944 tons.

Discussion of Results

General

In Fig. 11 is shown the sediment discharge versus water discharge for Money Creek as determined by the three different methods. Table 10 shows a comparison of the quantity of sediment measured in Lake Bloomington

Table 8. Money Creek Sediment Discharge by Schoklitsch Bed Load Formula

For particles 0.05 mm to 9.4 mm

Water Discharge cfs	Sediment Discharge Tons/Day	1st Period		2nd Period		3rd Period		Total Sediment Tons
		Duration Days	Sediment Tons	Duration Days	Sediment Tons	Duration Days	Sediment Tons	
110	33.6	376	12,622	124	4,163	59	1981	18,766
165	59.8	199	11,894	58	3,467	20	1195	16,556
245	98.0	103	10,090	34	3,331	11	1078	14,499
355	152	58	8,797	18	2,730	6	910	12,437
520	232	31	7,192	10	2,320	3	696	10,208
760	349	11	3,842	2	698	--	----	4,540
1100	515	3	<u>1,544</u>	1	<u>515</u>	--	----	<u>2,059</u>
Total			55,981		17,224		5890	79,065

Table 9. Money Creek Sediment Discharge by DuBoys Bed Load Formula

For particles 0.05 mm to 9.4 mm

Water Discharge cfs	Sediment Discharge Tons/Day	1st Period		2nd Period		3rd Period		Total Sediment Tons
		Duration Days	Sediment Tons	Duration Days	Sediment Tons	Duration Days	Sediment Tons	
110	282	376	105,855	124	34,910	59	16,610	157,375
165	408	199	81,180	58	23,661	20	8,159	113,000
245	657	103	67,647	34	22,330	11	7,224	97,201
355	921	58	53,402	18	16,573	6	5,524	75,499
520	1295	31	40,130	10	12,945	3	3,884	56,959
760	1679	11	18,465	2	3,357	--	-----	21,822
1100	2022	3	<u>6,066</u>	1	<u>2,022</u>	--	-----	<u>8,088</u>
Total			372,745		115,798		41,401	529,944

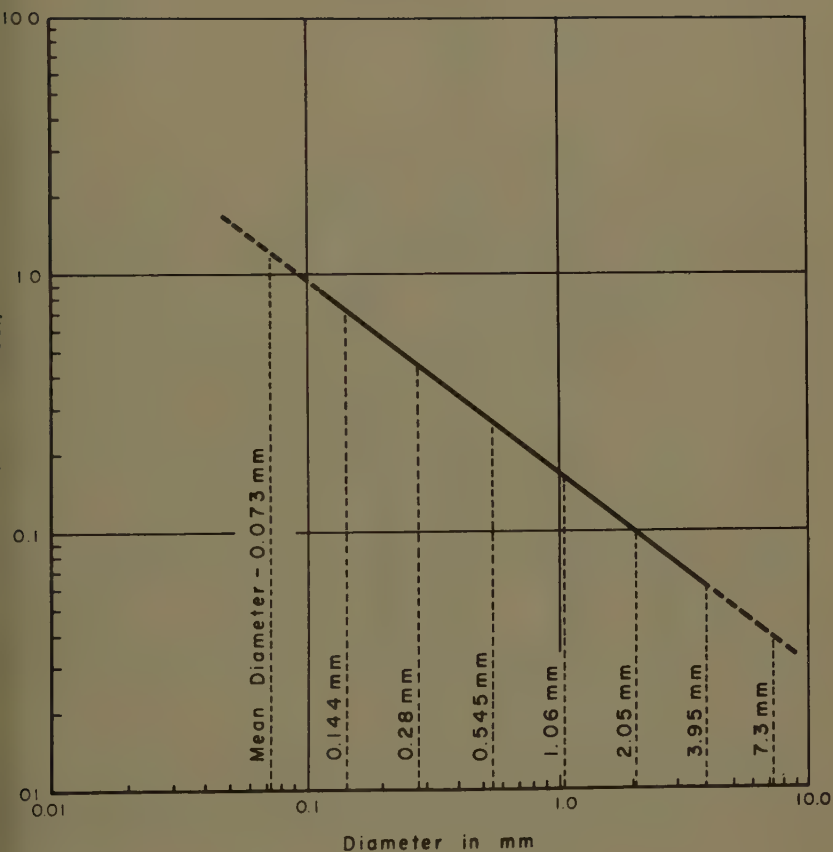


Figure 9 - Relationship of Sediment Parameter to Particle Diameter

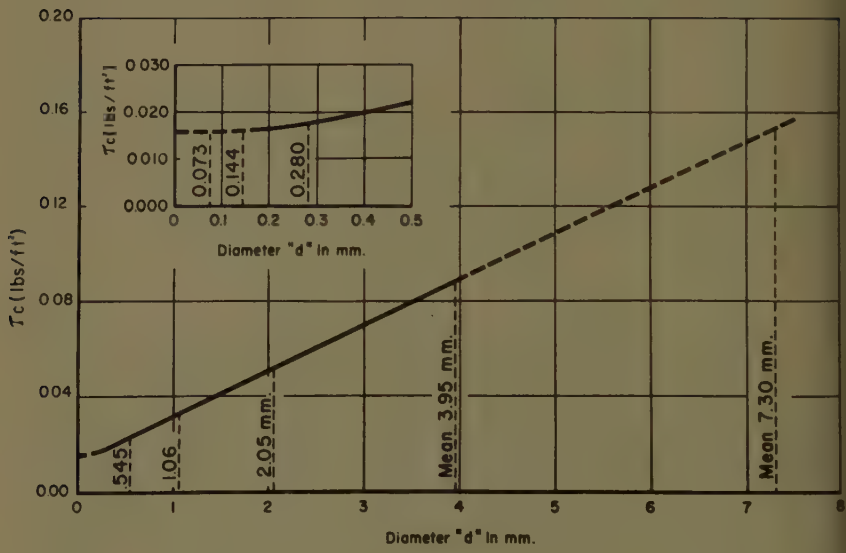


Figure 10 - Relationship of Critical Shear to Particle Diameter

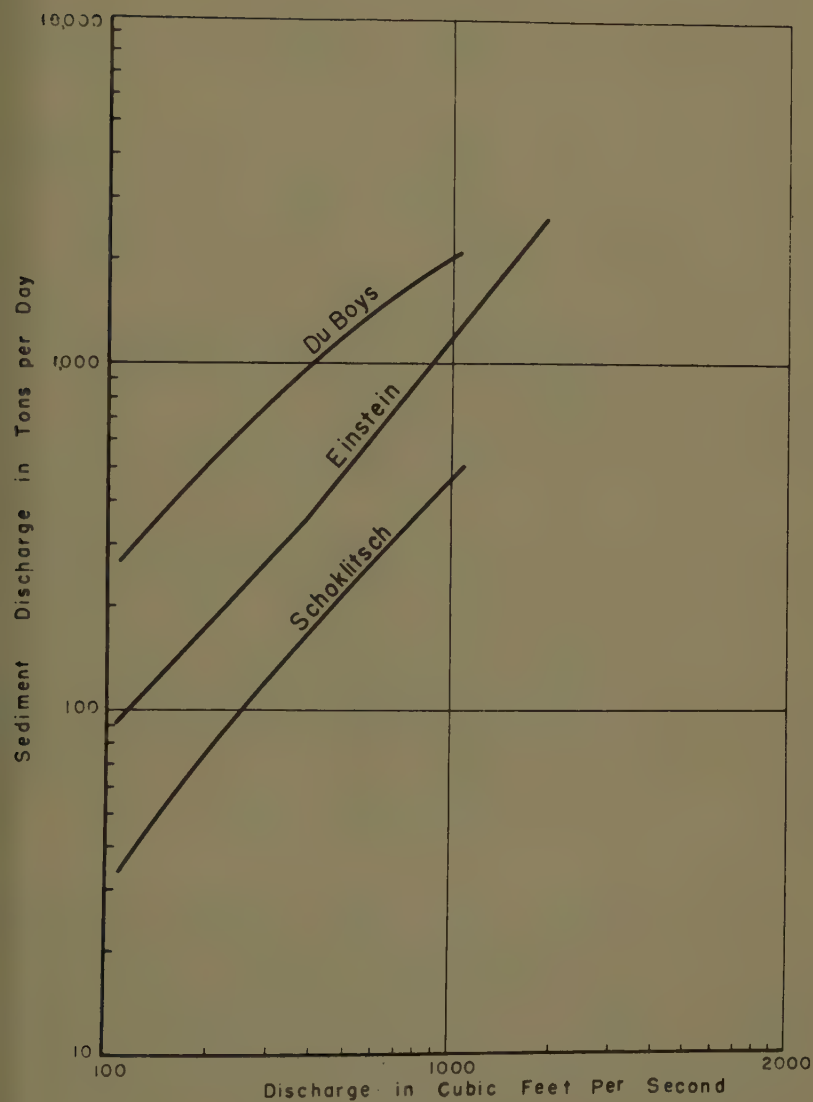


Figure 11 - Sediment Discharge Relation to Water Discharge

with the amount moved through the Money Creek reach, as computed by each of the three methods.

As shown in Table 10, the Schoklitsch formula gives results most nearly in agreement with the actual sediment measured in Lake Bloomington. For the total period of record, this formula gives results in tons only 31 percent greater than the measured quantity. In comparison the Einstein procedure gives results 225 percent too great, and the DuBoys formula, 776 percent too great.

The usefulness and limitations of the three methods utilized in this paper to compute sediment movement have been discussed in detail by Chien.⁽¹³⁾ Recognizing the limitations, these approaches merit continued study, trial, and improvement. These approaches were utilized on the Niobrara River near Cody, Nebraska⁽¹⁴⁾ in 1955. Results showed severe limitations to the Schoklitsch and DuBoys approaches and excellent results from the Einstein approach.

One recognized source of error in the use of a bed-load formula is the use of the water surface slope instead of the slope of the energy gradient. An accurate determination of the slope of the energy gradient requires the measurement of the velocity distribution at each end of the experimental reach. This observation is often eliminated and the resulting error involved in the slope determination is fairly large for the usual experimental conditions. It is of interest to note that Gilbert⁽¹⁵⁾ was undecided as to the proper value of slope to use and stated "I do not find it easy to decide which slope should be regarded as the true correlative of capacity for traction but as all of our laboratory data include the debris slope while the determinations of water slope are relatively infrequent the discussion of the results has adhered almost exclusively to the former. If the water slope is the true correlative then the use of the debris slope involves a systematic error."

Professor O'Brien and Lt. B. D. Rindlaub⁽¹⁶⁾ support Gilbert's selection in the statement "It is to be noted that the slope at the bottom is more nearly equal to the slope of the energy gradient than is the slope at the water surface and partly for this reason the data of G. K. Gilbert show less scattering than the data of more recent experimenters who have criticized Gilbert for not measuring the slope of the water surface in all of his experiments."

The Einstein Method

Sediment movement and river behavior are inherently complex since natural phenomena involve a great many variables. In applying the unified method presented by Einstein,⁽¹⁾ questions may arise such as: (1) Is it possible to obtain a truly representative bed material sample for size distribution characteristic curves? (2) What is the average (representative) diameter of the entire sediment mixture? (3) Is it possible to select an ideally uniform channel in nature? (4) Can the formulas for the hydraulics of the open channel be applied to such a complex problem as that of sediment transport phenomena? (5) If only one point of the size distribution curve is to be used for roughness height k_s , (D_{65}), how much confidence can the engineer have in its practical use? (6) Is the evaluation of bar resistance accurate and sufficient? (7) What is the lower limit in integrating suspended load? Many other questions may also arise. However, the engineer is warned against being discouraged by the absence of a better solution. In answer to the above questions it should be pointed out that the available information on the subject

Table 10. Bed Load Material Deposited in Lake Bloomington Compared to Computed Bed Material Movement in Money Creek.

Sediment	Tons			
	<u>1st Period</u>	<u>2nd Period</u>	<u>3rd Period</u>	<u>Total</u>
<u>Measured</u>				
Deposited in Money Creek Arm Lake Bloomington	48,176	10,725	1,626	60,527
<u>Computed</u>				
(Per cent error shown below each value in tons)				
Wastein	139,045 189	42,774 299	14,658 802	196,477 225
Hoklitsch	55,981 16	17,224 61	5,890 262	79,065 31
Boys	372,745 674	115,798 980	41,401 2,446	529,944 776

of hydraulics of open channel flow has been applied as closely as possible. Other information is rationalized through practical experience and field measurements.

Schoklitsch and DuBoys Formulas

Although these two formulas are essentially the same in structure, their application to Money Creek gives results at great variance. It will be seen that the results of the Schoklitsch formula are more nearly in agreement with the survey data. One reason for the high values in the case of DuBoys may be the limitations to the evaluations of the parameters C_s and τ_c . Since the sediment parameter C_s expresses the relative susceptibility of a given sediment to movement and since the shear terms τ and τ_c involve the complex system of forces exerted by the flow upon the bed, the evaluation of these parameters by means of suitable experimental methods determines the reliability of the results. The adaptation of the values, utilized as shown in Figs. 9 and 10, to conditions in Money Creek is therefore somewhat questionable.

The Manning formula permits DuBoys relationship to be written in the following alternative form.

$$q = C_s \tau (\tau - \tau_c) \quad (16)$$

$$= C_s \frac{r^2 s^{1.4}}{(1.49/n)^{1.2}} (q^{1.2} - q_0^{1.2})$$

The exponent of the slope is 1.4 in this relationship as against 1.5 in the Schoklitsch formula while the exponent of q_0 is 1.2 as compared with 1.0. Although this shows general agreement the disparity between the results of the two formulas is well accounted for. In addition to this, it is a recognized fact⁽¹²⁾ that the DuBoys formula was based on an incorrect assumption as to the sliding motion of the sediment particles in movement.

CONCLUSION

By utilizing the measured quantity of sediment of bed-material size in Lake Bloomington as a check on the computed sediment which has moved through Money Creek it is concluded that the Schoklitsch formula gives the most reliable results, being only 31 percent in error for the over-all period of the study. The Einstein procedure gave results 225 percent high and the classic DuBoys formula gave results 776 percent high.

REFERENCES

1. Einstein, H. A., "The Bed-Load Function for Sediment Transportation in Open Channel Flows," Technical Bulletin No. 1026, U. S. Dept. of Agriculture, Washington, D. C., 1950. (a) p. 10.
2. Eakin, H. M., "Silting of Reservoirs," U. S. Dept. of Agriculture Technical Bulletin No. 524. Revised by C. B. Brown, U. S. Government Printing Office, Washington, D. C., 1939, 169 pages.
3. Roberts, W. J., "Hydrology of Five Illinois Water Supply Reservoirs," Bulletin No. 38, State of Illinois, Water Survey Division, Urbana, Illinois, 19

- Chang, Y. L., "Laboratory Investigation of Flume Traction and Transportation," Transactions, ASCE, Vol. 104, 1939, pp. 1246-1313. Discussion by Johnson, pp. 1287-1293.
- Einstein, H. A., "Bed-Load Transportation in Mountain Creek," Technical Publication No. 55, SCS, U. S. Dept. of Agriculture, Washington, D. C., 1944.
- Mitchell, W. D., "Water Supply Characteristics of Illinois Streams," State of Illinois, Department of Public Works and Buildings, Springfield, Illinois, 1950.
- "Surface Water Supply in the United States, Part 5," Geological Survey, Water Supply Paper No. 925, pp. 365, 366, U. S. Dept. of the Interior, Washington, D. C., 1941. Also others in series.
- Einstein, H. A., and Chien, Ning, "Transport of Sediment Mixtures with Large Ranges of Grain Sizes," Missouri River Division, Corps of Engineers, Sediment Series No. 2, University of California, Berkeley, California, June 1953.
- Keulegan, G. H., "Laws of Turbulent Flow in Open Channels," National Bureau of Standards, Journal of Research, Vol. 21, 1938, pp. 701-741.
- Shulits, Samuel, "The Schoklitsch Bed-Load Formula," Engineering, London, June 21, 1935.
- "Laboratory Investigation of Flume Traction and Transportation," Discussion by J. W. Johnson, Transactions, ASCE, Vol. 104, 1939, pp. 1287-1293.
- "Sediment Transportation," Chapter XII, in "Engineering Hydraulics," edited by H. Rouse, p. 795, John Wiley & Sons, Inc., New York, N. Y., 1950.
- Chien, Ning, "The Present Status of Research on Sediment Research," Transactions, ASCE, Vol. 121, 1956, pp. 833-884.
- Colby, B. R., and Hembree, C. H., "Computations of Total Sediment Discharge—Niobrara River near Cody, Nebraska." Water Supply Paper No. 1357, Geological Survey, U. S. Dept. of the Interior, Washington, D. C., 1955.
- Gilbert, G. K., "The Transportation of Debris by Running Water," Professional Paper No. 86, Geological Survey, U. S. Dept. of Interior, Washington, D. C., 1914.
- O'Brien, M. P., and Rindlaub, B. D., "The Transportation of Bed-Load by Streams," Transactions, Am. Geophysical Union, Vol. 15, 1934, pp. 593-603.

Journal of the HYDRAULICS DIVISION

Proceedings of the American Society of Civil Engineers

FIELD INVESTIGATIONS OF SPILLWAYS AND OUTLET WORKS^a

Benson Guyton,¹ A.M. ASCE
(Proc. Paper 1532)

ABSTRACT

The Corps of Engineers hydraulic field testing program is coordinated by the U. S. Army Engineer Waterways Experiment Station, Vicksburg, Mississippi. Included are flood-control and multiple-purpose projects, river and harbor works, estuarine and wave problems. Test data discussed include spillway, conduit-intake, and gate-leaf pressures; air demand; and concrete conduit friction factors.

INTRODUCTION

This paper is limited to hydraulic field investigations of spillways and outlet works constructed and operated by the Corps of Engineers, particularly those in which the U. S. Army Engineer Waterways Experiment Station, located at Vicksburg, Mississippi, has played a part. We call the structure where field tests are made "the prototype" as opposed to a working model on which tests are made at a smaller scale. Usually more variables are studied in the model tests than in field tests because of the ease in control and lesser time and costs involved.

The main purpose of field tests is to obtain data for use in producing more economical designs. Frequently data are needed for conditions where model studies are not applicable, or the scale ratios are unknown. For example, simulating air-water mixtures is difficult in a model, and the scale ratios for cavitation and those involving high Reynolds numbers are not clearly understood. Another purpose of field tests is to investigate and evaluate the

Discussion open until July 1, 1958. A postponement of this closing date can be obtained by writing to the ASCE Manager of Technical Publications. Paper 1532 is part of the copyrighted Journal of the Hydraulics Division, Proceedings of the American Society of Civil Engineers, Vol. 84, No. HY 1, February, 1958.

Presented at Jackson Convention of the American Society of Civil Engineers, February 18-21, 1957.

Chief, Prototype Section, Hydraulic Analysis Branch, Hydraulics Division, U. S. Army Engineer Waterways Experiment Station, Vicksburg, Miss.

performance of the prototype, usually for some phase of performance in which operating difficulties are occurring. Also tests have been made to verify model indications, and in some instances field tests have been necessary to obtain data for designing or operating the model.

Within the Corps of Engineers field tests are made either by the District operating the project or by the Waterways Experiment Station in conjunction with District personnel. District personnel make tests involving conventional equipment such as current meters and stage recorders, take discharge measurements for rating gates, and make river and harbor soundings. Some extensive tests involving pressure measurements, vibration, and hoist forces are also made by Districts. However, most of the extensive tests requiring the use of special equipment are made by the Waterways Experiment Station and Districts cooperating.

The Experiment Station is the coordinating agency for hydraulic prototype testing in the Corps of Engineers. In this capacity recommendations are made to the Districts concerned regarding collection of field data and installation of testing facilities such as embedment of piezometers or conduit for electric leads during construction. The Waterways Experiment Station is in a favorable position to carry out this assignment because of early association with new projects—sometimes through model tests during which the need for field tests may become apparent. Also the Experiment Station in discharging its responsibility of disseminating hydraulic design criteria to the Corps frequently sees the need of field tests. The presence of an Instrumentation Branch with a reservoir of electronic measuring equipment and instrumentation engineers adds much to the capabilities of the Station.

The scope of the Corps' hydraulic field testing program includes flood-control and multipurpose projects, river and harbor works, and estuary and wave-action problems. In recent years the program has been concentrated on multipurpose projects, particularly the spillways and outlet works of concrete and earth dams. The spillway tests have been primarily confined to the measurement of pressures and the collection of data for determining spillway discharge coefficients. Tests on outlet works have been of broader coverage.

Spillway Tests

In addition to the problems involved in the installation of facilities during construction, the problem of water availability for testing is more acute for spillways than for outlets. Obviously spillways cannot be operated until the reservoir level rises above the spillway crest. In many cases this does not happen for years. Some uncontrolled spillways on projects over 15 years old have not yet gone into operation. A severe limitation in testing controlled spillways is that large flows cannot always be tolerated downstream. This restriction hampered testing at Pine Flat Dam in June 1956. Nevertheless, a limited number of spillway tests have been made. This include velocity measurements in the chute of Fort Peck Dam in 1946; ogee crest pressure measurements at 19 per cent of the design head and the taking of water-surface profiles at Arkabutla in 1953; recording of crest and baffle pier pressures at 75 per cent of the design head at McNary² in 1954; and recording of crest, tangent, and flip-bucket pressures at Pine Flat at 57 per cent of

2. Walla Walla District, Corps of Engineers, Model-prototype Conformity, McNary Dam Spillway. June 1956.

the design head for gate openings up to 8 ft in 1956.

The most extensive tests yet made at a Corps spillway were at Chief Joseph Dam (see photograph 1) during the summer of 1956. Chief Joseph Dam is a 235-ft-high, concrete-gravity structure located on the Columbia River in eastern Washington some 50 miles downstream from Grand Coulee. Pressures both upstream and downstream from the tainter gate were measured with 23 piezometers, and pressure pulsations near the gate seat were measured with three electric pressure cells. At the time the field tests were made, only four power units were in operation; therefore, most of the 300,000-cfs discharge was passed over the 19-bay spillway. For test purposes the reservoir pool elevation was altered by changes in discharge during the preceding night. Thus testing at heads of 32.5, 37.5, 41.6, and 46.5 ft or 0.8, 0.9, 1.0, and 1.1 times the design head of 41.6 ft was possible. The piezometer lines were permanently installed in bay 9 during construction, as were inserts and conduit for the pressure cells. The cells themselves were installed just prior to testing. Piezometer pressures were observed from gages attached to a valve-bank manifold in the access gallery. Pressure-cell data were recorded on an oscillograph, also located in the gallery.

A section through bay 9 showing piezometers and pressure cells located along the bay center line is shown in Fig. 1. The crest conforms to the standard Corps of Engineers shape for overfall spillways. The rising portion of this shape is a compound curve with radii 0.2 and 0.5 times the design head. The falling portion of the curve conforms to the equation $x^{1.85} = 0.0 H_d^{0.85} Y$, where H_d is the head for which the crest shape is designed. In the case of Chief Joseph the crest shape is designed for a head of 41.6 ft whereas the head at maximum pool would be 55.4 ft. The practice of designing the crest shape for a head as low as three-fourths of the maximum expected head was advocated after model tests indicated that discharge coefficients would be substantially increased and negative pressures would not be excessive.

Pressure profiles at the design head of 41.6 are shown in Fig. 2 for gate openings of 5 ft, 10 ft, 20 ft, and free overflow. Pressures on the area downstream from the gate are about the same regardless of gate opening, being about minus one foot of water for the 10-ft opening and plus one foot for the 20-ft opening and for free overflow. These profiles were obtained with the adjacent gates closed. Tests were also made with the adjacent gates open full and at openings equal to those in the test bay with resulting changes in pressures being less than a foot or two of water. Furthermore, there was little difference in pressures measured along the center line of the spillway and along a parallel line one foot from the pier. However, for the free overflow condition positive pressures on the rising portion of the crest were considerably higher along the center line than near the pier.

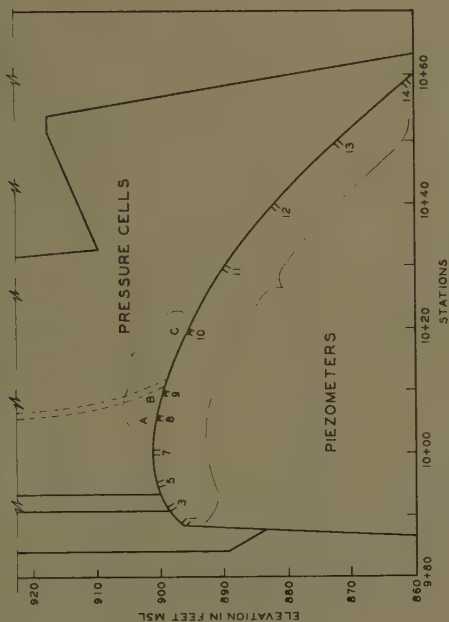
Comparisons of pressure profiles from model tests of the dam conducted at the Bonneville Hydraulic Laboratory and the prototype at 46.5-ft head, or 1.1 times the design head, are shown in Fig. 3 for 20- and 30-ft gate openings and for free overflow. Negative pressures did not exceed minus two feet of water. It is worthy of note that good correlation between model and prototype occurred for all comparable tests as would be expected from the Froude law. The pressure cells measured the magnitude and frequency of the pulsations on the crest. Oscillograms of the tests at design head are shown in Fig. 4. Cell A was located flush with the concrete surface five feet upstream from the gate seat. Cell B was one foot upstream and cell C was 9 feet downstream



Photograph 1. Chief Joseph Dam



Photograph 2. Pine Flat Dam



CREST PIEZOMETER AND PRESSURE CELL LOCATIONS

CHIEF JOSEPH DAM
CREST PIEZOMETER, PRESSURE
CELL LOCATIONS AND
SECTION THROUGH SPILLWAY BAY 9

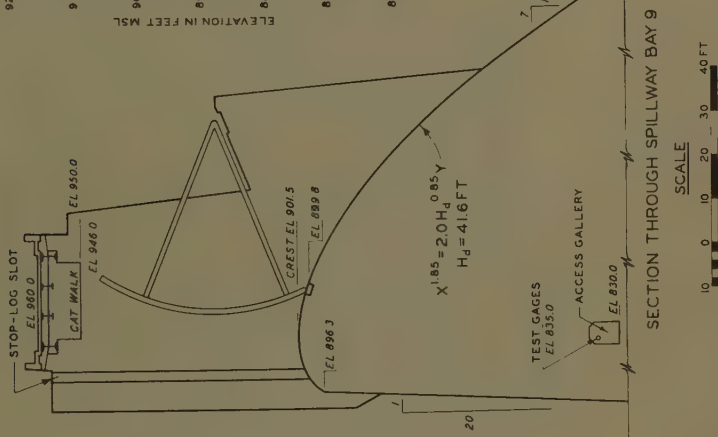
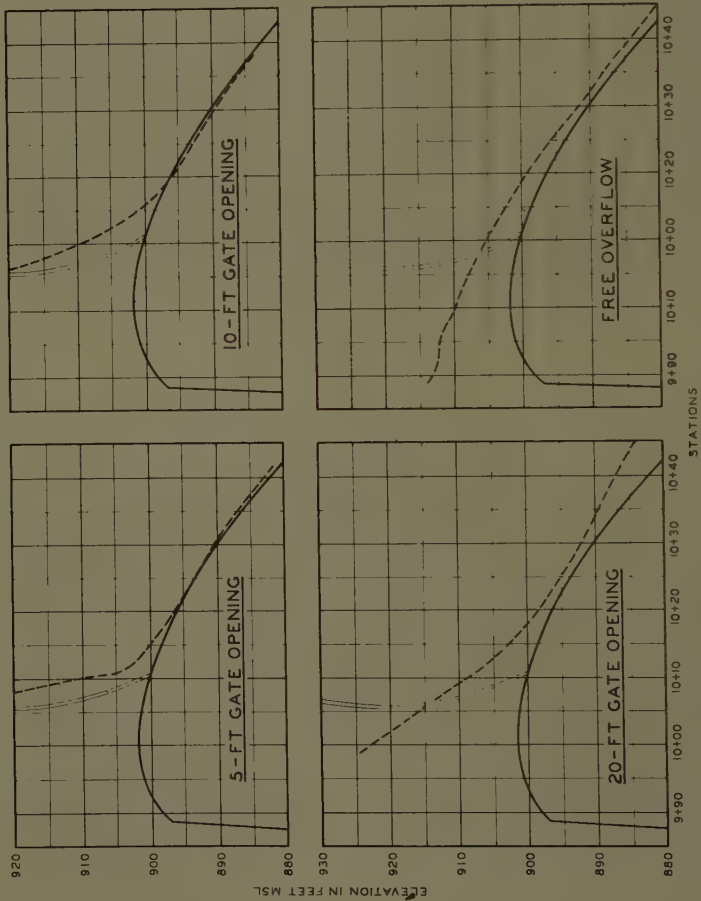
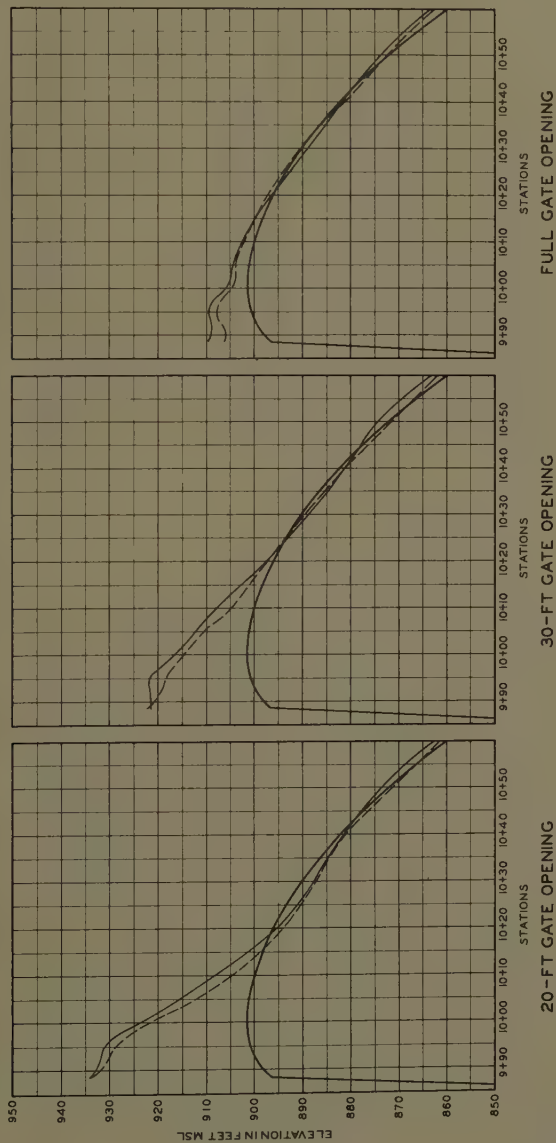


FIGURE 1



CHIEF JOSEPH DAM
SPILLWAY PRESSURES
POOL 943.6

FIGURE 2

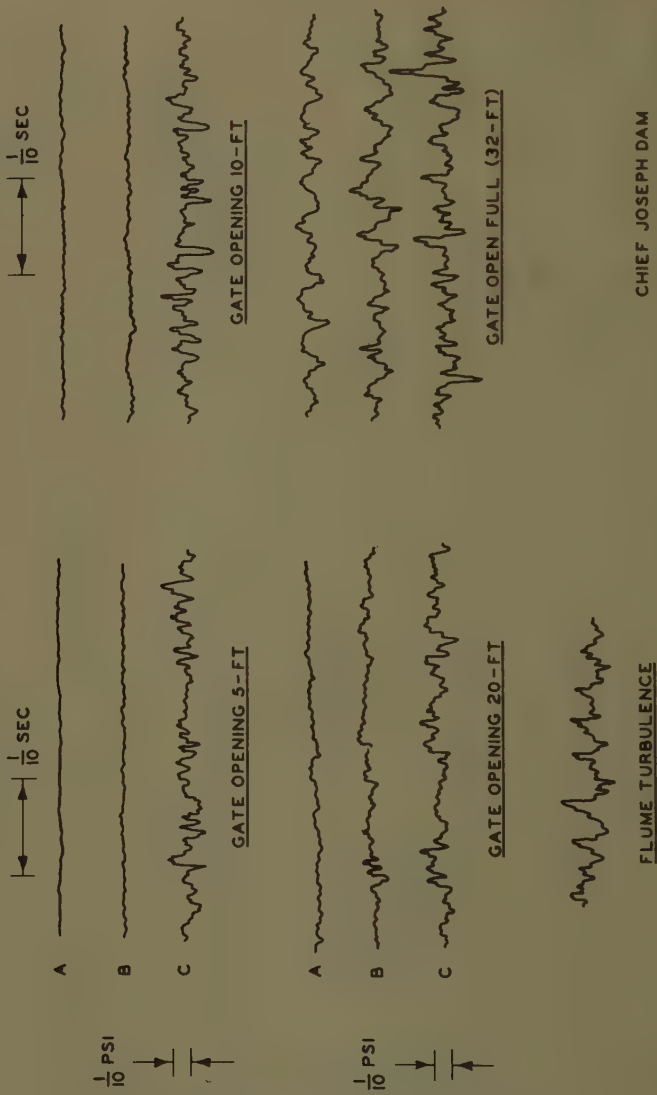


CHIEF JOSEPH DAM
SPILLWAY PRESSURES
 20-FT, 30-FT, AND
 FULL GATE OPENINGS

NOTE: ALL GATES OPEN EQUALLY
 POOL ELEVATION = 948

LEGEND
 --- MODEL
 --- PROTOTYPE

FIGURE 3



CHIEF JOSEPH DAM
CREST PRESSURE PULSATIONS
POOL 943 (H_d)

FIGURE 4

from the gate. The pressure pulsations were of small magnitude and irregular frequency varying from 0.1 to 1.1 ft of water at frequencies of 0.1 to 100 cycles per sec. It is interesting that the turbulence at cell C, downstream from the gate, was much greater at small gate openings than that at A or B, upstream of the gate. This is believed to be associated with the development of the turbulent boundary layer. As the gate opening increased, turbulence downstream from the gate seat also increased. At full gate opening (free overflow) turbulence was about the same at all locations. The pattern closely resembles velocity pulsations observed in flume studies.

The only condition at which any tendency towards uniform, sinusoidal pulsations occurred was at a 20-ft gate opening with the adjacent gates closed while testing at a head of 32.5 ft or 0.8 design head. At this particular head the jet broke loose from the gate at an opening of 25 ft. Therefore, flow conditions at the crest were extremely turbulent. In fact a violent roller alternately formed and broke against the gate. It is doubtful that operation would normally occur under these conditions since it could be eliminated by rather small changes in gate openings. It is to be noted that the maximum magnitude of the pulsations shown in Fig. 5 was about 1/4 psi at 8-sec periods. The periodic oscillations were damped after three or four cycles.

As far as the author knows the tests at Chief Joseph spillway are the first to be conducted at a head approaching the head for which the crest was designed.

Outlet Works Tests

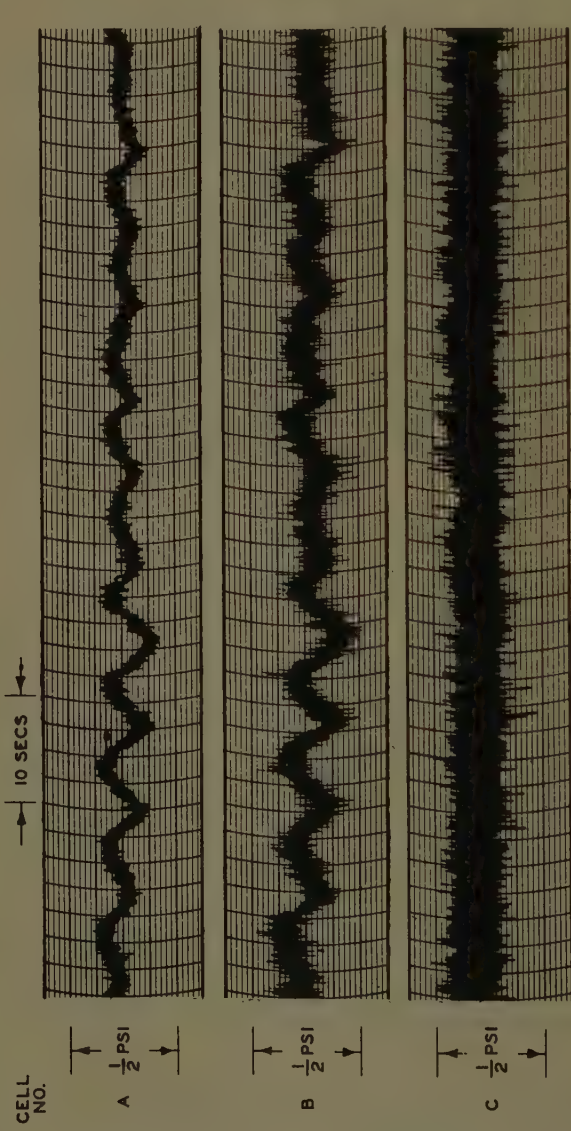
Outlet works have been tested more extensively than spillways because of more installed facilities and greater availability of water for test purposes. Tested outlets vary from 4-ft by 6-ft sluices to 25-ft-diam tunnels and tests include measurements of pressures in intake curves, gate liners, conduits proper, exit portals, buckets, and stilling basins. In addition pressures and vibration have been measured on a variety of control gates including hydraulically operated slide gates, cable-operated tractor gates, and tainter gates. Rather extensive field tests were made on the Fort Peck³ cylinder gate and control shaft to investigate pressures, vibration, and air demand. Our most extensive installation for testing sluices at high heads is at Pine Flat Dam (see photograph 2) located on the Kings River near Fresno, California.

This dam is a 440-ft-high, concrete-gravity structure with an upper tier and lower tier of five sluices each. A section through the spillway and sluices is shown in Fig. 6. Sixty-two piezometers have been installed in one of the 10-ft-wide by 9-ft-high lower sluices and 71 piezometers in an upper sluice. Fourteen series of pressure measurements have been made in the lower sluice at heads varying from 110 to 300 ft. Data from the closely spaced piezometers in the entrance curve have been reduced to pressure drop coefficients and compared with model data for similarly shaped elliptical intake curves based on the equation $\frac{X^2}{D^2} + \frac{Y^2}{(\frac{D}{2})^2} = 1$, where D is the dimension across

$$\frac{X^2}{D^2} + \frac{Y^2}{(\frac{D}{2})^2} = 1$$

3

³ Corps of Engineers, Waterways Experiment Station, Hydraulic Prototype Tests, Control Shaft 4, Fort Peck Dam, Missouri River, Montana. Technical Memorandum No. 2-402, April 1955.



CHIEF JOSEPH DAM
CREST PRESSURE PULSATIONS
20-FT GATE OPENING
POOL 934

FIGURE 5

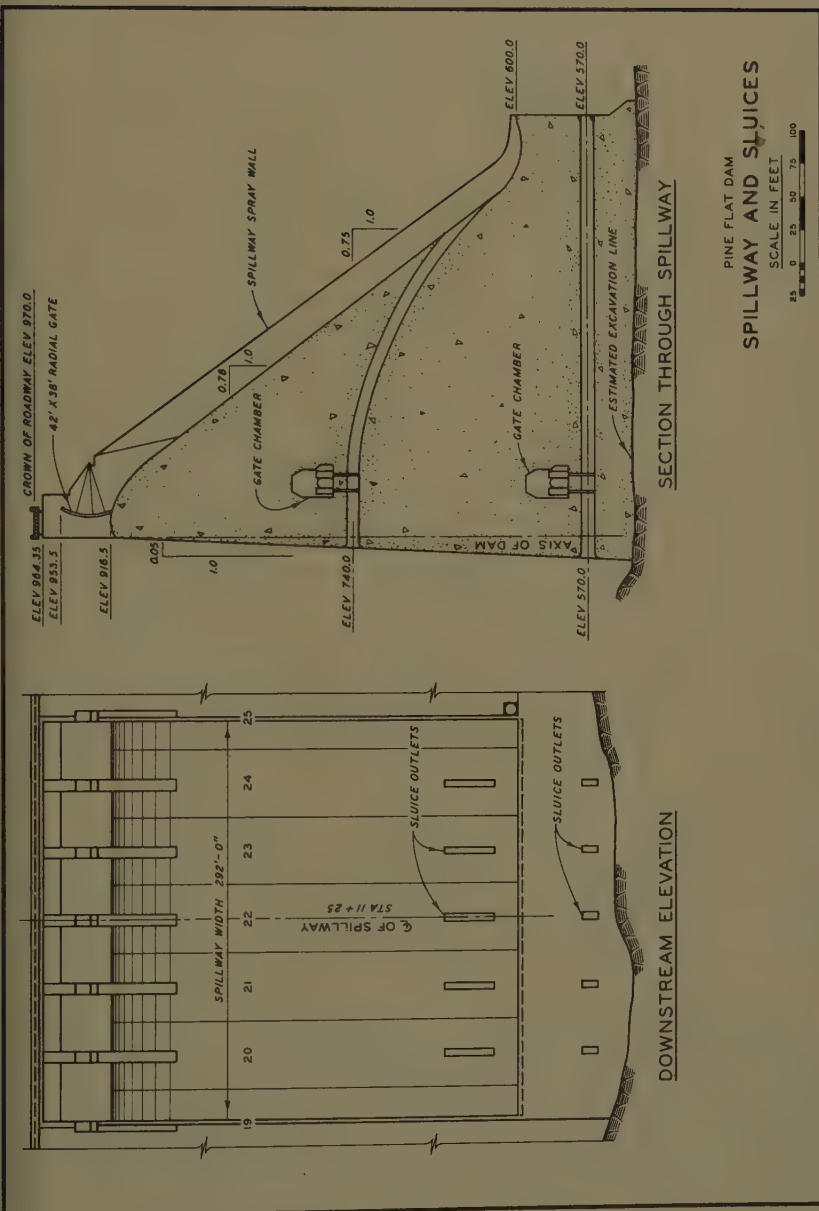


FIGURE 6

the conduit in the direction concerned. The prototype coefficients shown in Fig. 7 are averages obtained from the 14 tests just mentioned. The model coefficients are interpolated from model data on vertical and 10° sloping upstream face to correspond with the $2^\circ 52'$ sloping face at Pine Flat. The prototype data indicate slightly greater coefficients than the model.

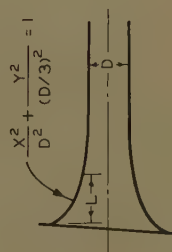
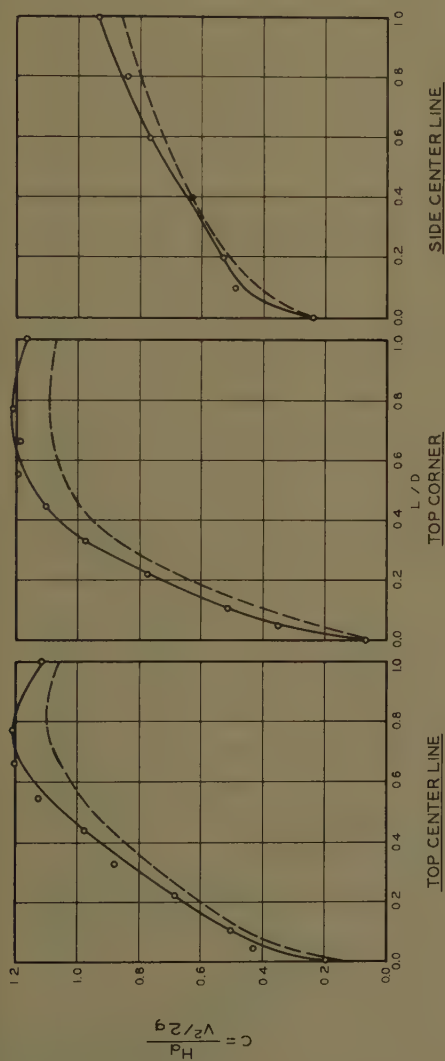
The superiority of the 45-degree lip over the old flat bottom for slide gates was demonstrated in model and prototype tests of the Norfork Dam⁴ gates. Tests were made at Pine Flat⁵ to measure vertical and flexural vibration of the 5- by 9-ft, 45-degree lip, slide gates. Acceleration measurements indicated stable vibration conditions for all gate openings. These gates have been operated for long periods of time at partial gate openings with no apparent damage. Piezometric measurements of pressures on the gate leaf have been made for heads ranging from 100 to 256 ft. Pressures for gate openings of 1 ft and 5 ft observed at heads of 105 and 256 ft are shown in Fig. 8.

Air is admitted to the sluices through a vent pipe joining the roof of the gate chamber just downstream from the gate. Velocities in the 30-in.-diam air vent have been measured for a range of heads varying from 92 to 370 ft. A plot of air demand vs gate opening in Fig. 9 shows peak demands at small openings and at about 60 to 80 per cent opening. This substantiates similar measurements at other projects including Norfork and John H. Kerr.

One of the earlier installations of prototype testing facilities is in a 20-ft-diam, cut-and-cover type conduit at Denison Dam.⁶ Piezometric pressure measurements have been made using the 47 piezometers installed during construction. Piezometer locations and the results of piezometric measurements at a 98-ft head are shown in Fig. 10. It is believed that the flat, uniform slope of the grade line in the downstream portion of the conduit is the friction gradient. The Darcy-Weisbach friction coefficient computed from this slope is 0.00644 at a Reynolds number of 120 million. These values when plotted on a chart for friction factors in concrete conduits fall about one-fourth of the distance between the smooth- and rough-pipe curves developed by Von Karman and Prandtl (see Fig. 11). Pressure-cell tests at the Fort Peck 24-ft-8-in.-diam concrete conduit indicated an "f" value of 0.0069 at a Reynolds number of 60 million.

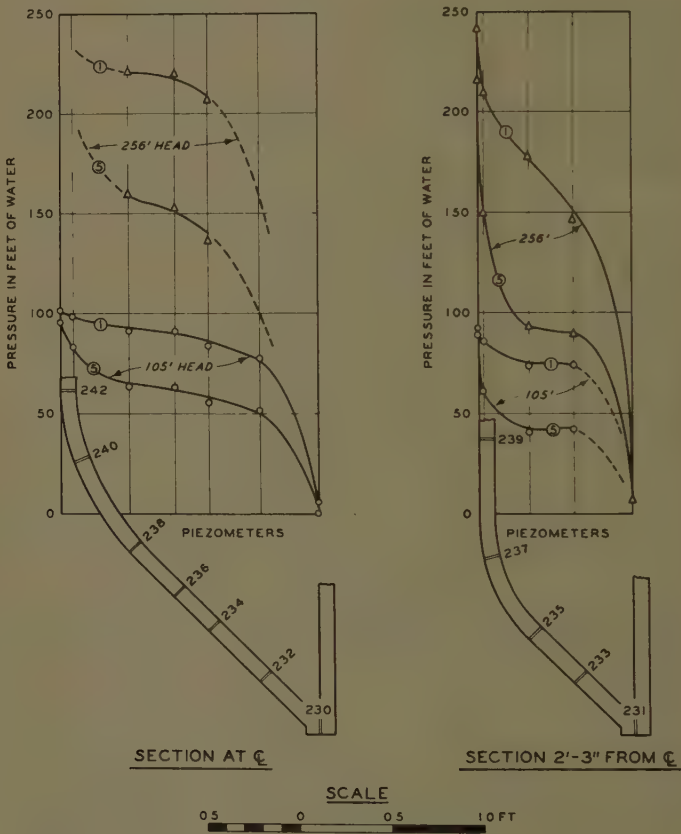
Discharges through tunnels of earth dams are frequently controlled by cable-operated tractor gates. Usually 2, 3, or 4 gates separated by piers are used. Pressure and vibration measurements were made on the 45-degree lip, 11- by 23-ft intake gates controlling flow into a 22-ft-diam tunnel at Fort Randall Dam,⁷ on the Missouri River. Vibration tests at heads of 79, 97, and 110 ft revealed no unstable oscillations that would indicate resonance with

4. Corps of Engineers, Waterways Experiment Station, Slide Gate Tests, Norfork Dam, North Fork River, Arkansas; Model and Prototype Investigations. Technical Memorandum No. 2-389, July 1954.
5. Corps of Engineers, Waterways Experiment Station, Vibration, Pressure and Air-demand Tests in Flood-control Sluice, Pine Flat Dam, Kings River California. Miscellaneous Paper No. 2-75, February 1954.
6. Corps of Engineers, Waterways Experiment Station, Pressure and Air-demand Tests in Flood-control Conduit, Denison Dam, Red River, Oklahoma and Texas. Miscellaneous Paper No. 2-31, April 1953.
7. Corps of Engineers, Waterways Experiment Station, Vibration and Pressure-cell Tests, Flood-control Intake Gates, Fort Randall Dam, Missouri River, South Dakota. Technical Report No. 2-435, June 1956.



INTAKE PRESSURE DROP
COEFFICIENTS

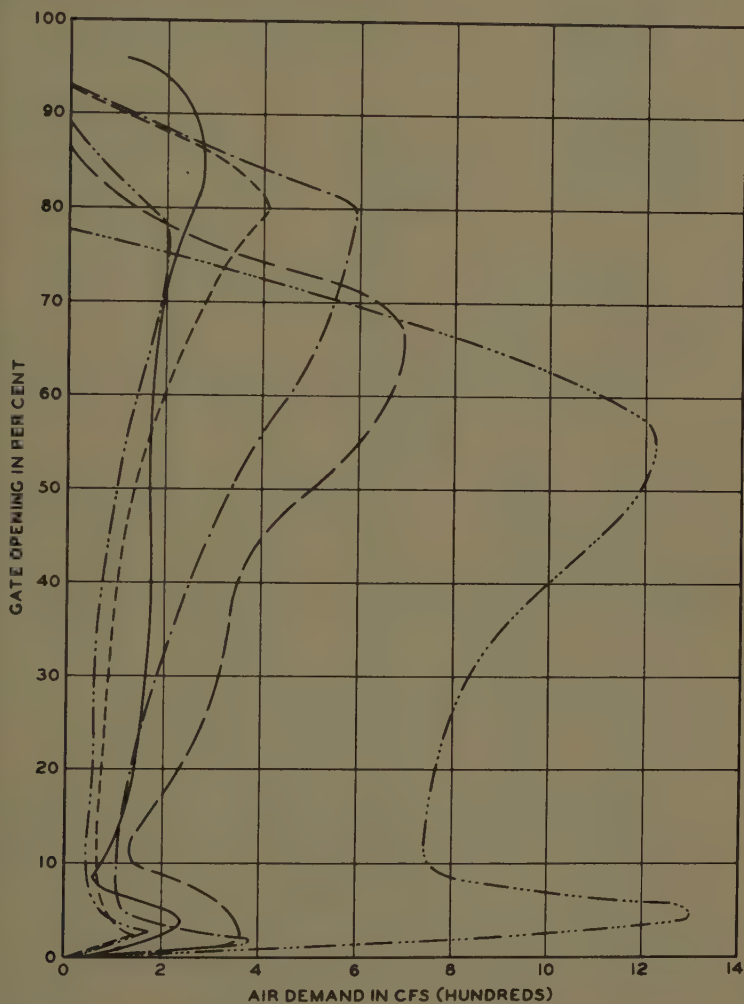
FIGURE 7



NOTE: ① AND ⑤ REFER TO GATE OPENINGS IN FEET.

PINE FLAT DAM
GATE LEAF PRESSURES
1 AND 5-FT GATE OPENINGS
105 AND 256-FT HEADS

FIGURE 8

**LEGEND**

PROJECT	SLUICE SIZE (FT)	VENT DIA (IN)	HEAD (FT)
----- PINE FLAT	5 X 9	30	92
----- PINE FLAT	5 X 9	30	254
----- PINE FLAT	5 X 9	30	370
----- JOHN H. KERR	5.7 X 10	30	73
----- JOHN H. KERR	5.7 X 10	30	95
----- NORFORK	4 X 6	20	157

AIR DEMAND

FIGURE 9

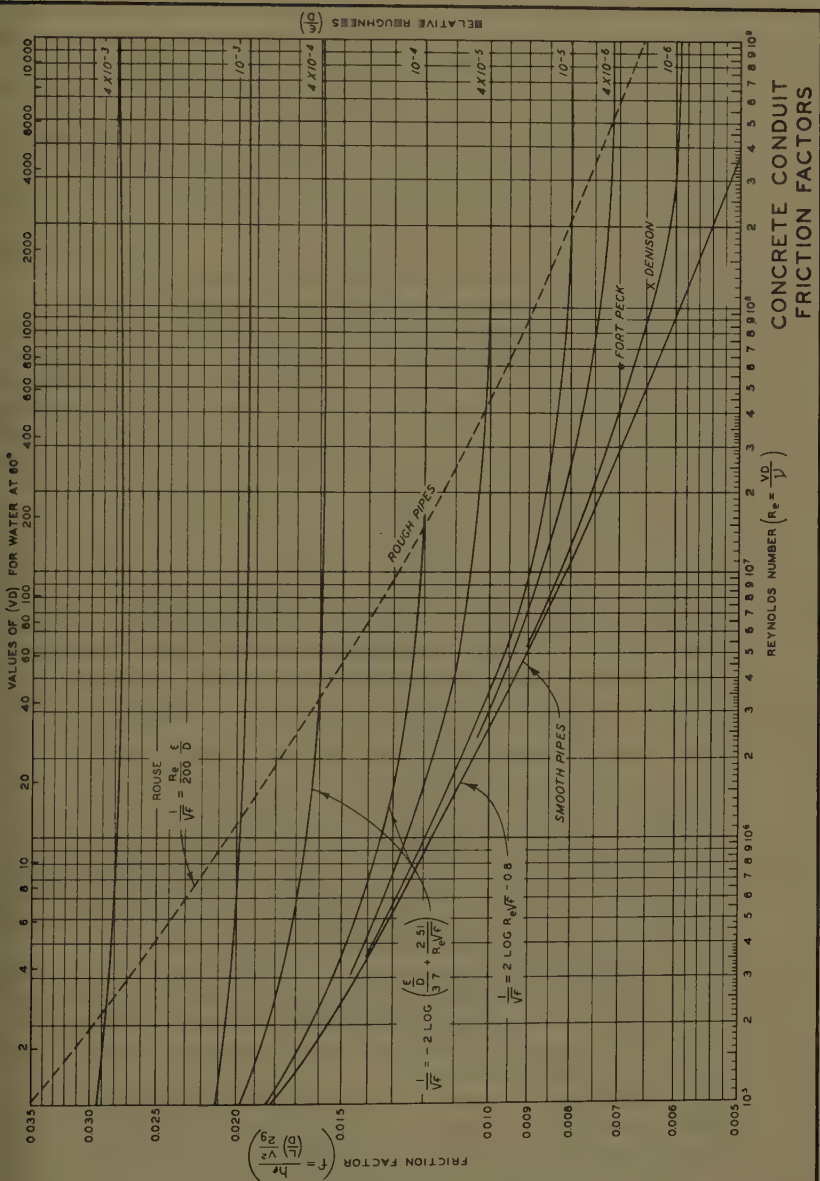


FIGURE 11

with a forcing frequency. Pressures along the gate center line and near the side measured with ten pressure cells were positive for heads of 97 and 110 ft. The ratio of the average pressure on the gate bottom to the height of pool above gate sill is shown in Fig. 12. The average pressures were determined for that part of the gate bottom within the conduit proper by integrating contoured plots of the measured pressures. The pressure-height ratios can be used to estimate pressures on the gate bottom for other pool elevations. Water-surface elevations in the gate well were measured with an electrode sounding device simultaneously with the pressure-cell tests. The ratio of the height of the column of water in the gate well above the tunnel roof to the pool-tunnel roof depth is shown in Fig. 13. The data in Figs. 12 and 13 are, of course, applicable only to the Fort Randall project or to systems geometrical-ly similar with respect to gate shape and gate-well clearances.

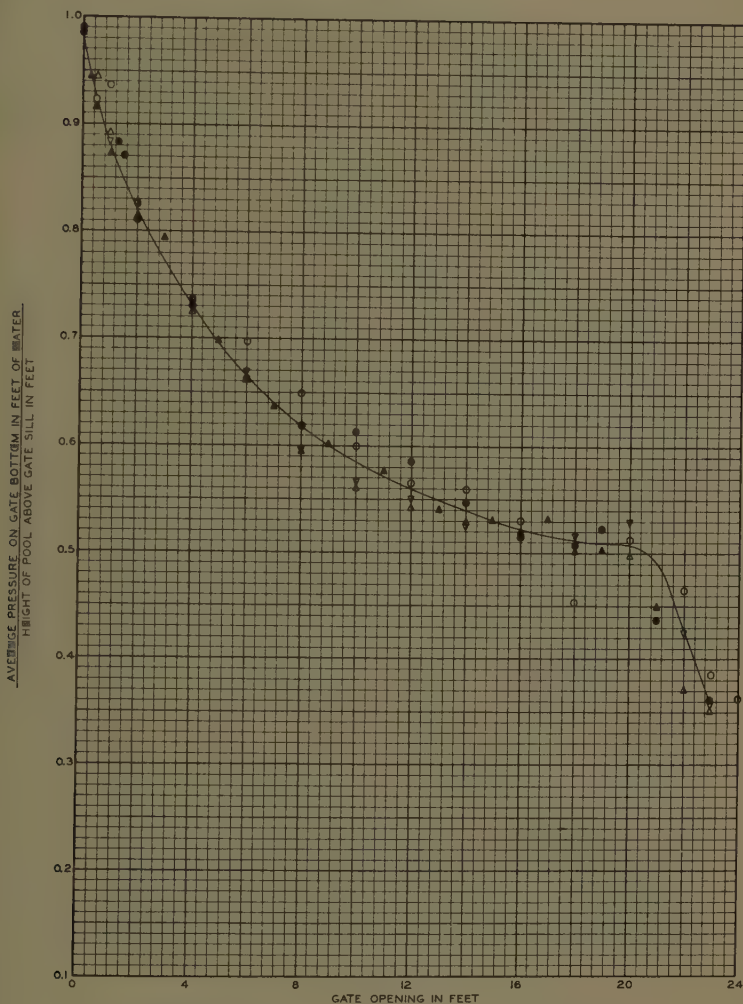
A discussion of spillways and outlets would not be complete without mentioning stilling action. Pressures in spillway and outlet buckets have been measured for nominal flow conditions at a few projects. Pressures were measured at two points on a baffle block at McNary. Prototype pressure-cell measurements on the elliptical-shaped steps of the Bull Shoals⁸ stilling basin revealed high-frequency pressures whose averages compared favorably with those obtained in the model. However, fast pressure drops to as low as -34 ft of water were indicated by the pressure cells. These low pressures occurred too fast to be indicated by model piezometric measurements. Considerable cavitation damage to the prototype concrete steps occurred. Perhaps the lesson to be learned is to be wary of piezometer indications where high-frequency, pulsating pressures might be expected such as in gate slots, baffle piers, and sudden changes in boundary shapes for high-velocity flows.

Without going into the details of testing equipment, the types of measuring equipment used in the field tests will be discussed briefly. Piezometer pressures are usually measured with a pressure gage or a manometer filled with mercury or some other fluid. Pulsating pressures are measured with electric pressure cells. Vibration is measured with accelerometers. Direct writing recorders are used with pressure cells or accelerometers when frequencies are less than 100 cycles per sec. Recorders using a photographic process are used for higher frequencies. Air demand has been measured with pitot tubes, velometers, and orifice plates. Water-surface elevations have been observed with the customary stage recorders and electrical-probe devices. Adaptations of some special testing equipment include deflection gages, electrical-resistance thermometers, and air-pressure cells.

The field testing program is a continuing one. Future tests will be made at many of the projects already mentioned as additional water for test purposes becomes available. Facilities have been installed or are now being installed at a number of projects where either water has not yet become available or construction is not completed.

In addition to extending the range of measurements that have just been described, investigations will be made of crest pressures and pressure pulsations on a low, ogee crest; velocity profiles and air entrainment will be measured on chute-type spillways and at a high overfall dam; pressure pulsations will be measured in the gate slots of a large tunnel; velocity

8. Corps of Engineers, Waterways Experiment Station, Pressure-cell Tests, Bull Shoals Dam Stilling Basin. Miscellaneous Paper No. 2-77, February 1954.



LEGEND

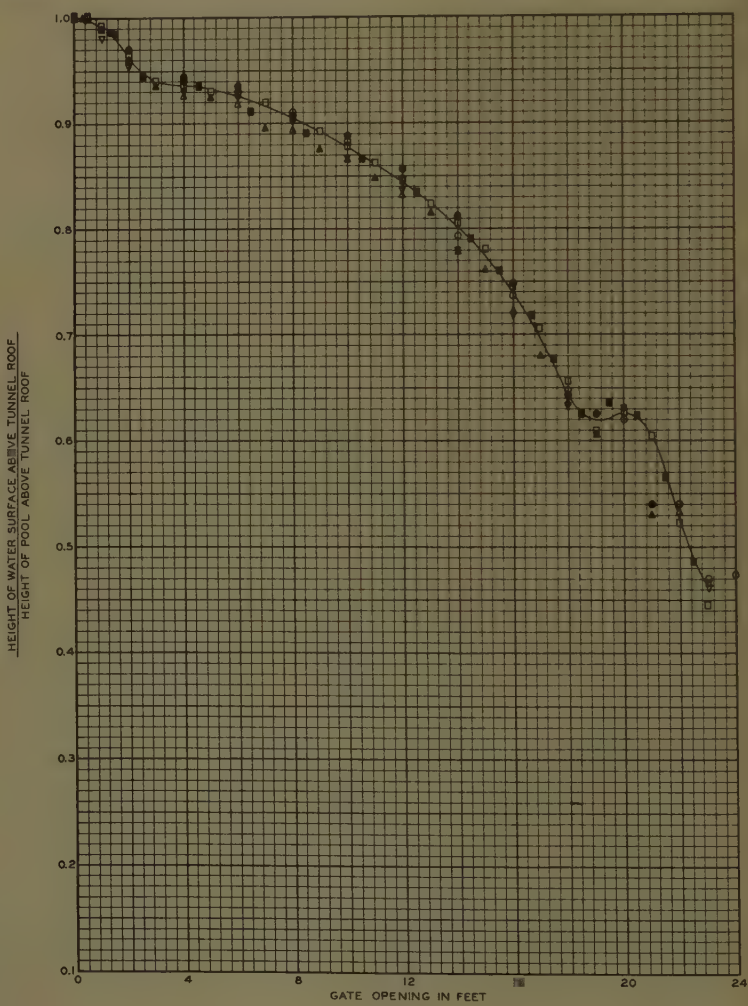
POOL ELEV	GATE OPERATION	
	STOPPED	MOVING
1339	OPENING ○	CLOSING ●
1326	OPENING △	CLOSING ▽

NOTE: AVERAGE PRESSURE IS FOR THAT PART OF GATE BOTTOM WITHIN CONDUIT PROPER.

FORT RANDALL DAM
AVERAGE PRESSURE
ON GATE BOTTOM
BOTH GATES SAME
OPENINGS

WES 5-56

FIGURE 12



POOL ELEV.	GATE OPERATION		
	STOPPED		MOVING
	OPENING	CLOSING	OPENING
1339	○	●	
1326	△	▲	▽
1308	□	■	

FORT RANDALL DAM
GATE WELL
WATER-SURFACE ELEVATION
BOTH GATES SAME
OPENINGS

WES 5-56

FIGURE 13

distribution and turbulence phenomena will be studied with a removable strut installed in a 22-ft-diam, steel-lined tunnel at Fort Randall Dam; and provisions for measuring sluice discharge by an ultrasonic method are being considered at a high-head concrete dam.

In conclusion, the hydraulic field investigations of the past few years have thrown considerable light on the understanding of many hydraulic problems. The increasing interest of design engineers in providing facilities for making tests is encouraging. The development of new equipment and new techniques will facilitate gathering data heretofore considered impossible. Our program of hydraulic field investigations should continue to be fruitful.

ACKNOWLEDGEMENTS

Most of the tests described in this report were conducted under the Corps of Engineers hydraulic prototype testing program, one phase of Civil Works Investigation 804, "Analysis of Hydraulic Experimental Data for the Development of Design Criteria." Mr. J. H. Douma of the Office, Chief of Engineers, has been instrumental in planning this work. The Waterways Experiment Station is assigned the responsibility of coordinating the testing program. Col. A. P. Rollins, Jr., CE, is Director and Mr. J. B. Tiffany is Technical Director of the Waterways Experiment Station. Chief of the Hydraulics Division is Mr. E. P. Fortson, Jr. The Prototype Section is a part of the Hydraulic Analysis Branch, of which Mr. F. B. Campbell is chief. The frequent advice of Mr. Campbell is gratefully acknowledged. Mr. H. A. Bell, Jr., of the Prototype Section has capably assisted in the preparation of this paper. The author is also indebted to many engineers of the Districts and projects of the Corps of Engineers as well as engineers of the Instrumentation Branch of the Waterways Experiment Station, who rendered valuable assistance in obtaining field measurements.

Journal of the
HYDRAULICS DIVISION
Proceedings of the American Society of Civil Engineers

CONTENTS

DISCUSSION
(Proc. Paper 1558)

	Page
Economic Aspects of Flood Plain Zoning, by Harry W. Adams. Proc. Paper 882, February, 1956. Prior discussion: 881. (discussion closed.)	---*
Open Exploratory Studies in Hydraulics, by Hunter Rouse. Proc. Paper 1038, August, 1956. Prior discussion: 1230. (discussion closed.)	
by Hunter Rouse (closure)	1558-3
Measuring Streamflow under Ice Conditions, by A. M. Moore. Proc. Paper 1162, February, 1957. Prior discussion: 1348. (discussion closed.)	
by A. M. Moore (closure)	1558-5
Frequency Analysis of Streamflow Data, by David K. Todd. Proc. Paper 1166, February, 1957. Prior discussion: 1283, 1288. Discussion closed.)	
by David K. Todd (closure)	1558-7
Butterfly Valve Flow Characteristics, by M. B. McPherson, H. Strausser, and J. C. Williams, Jr. (Proc. Paper 1167, February, 1957. Prior discussion: 1348. Discussion closed.)	
by M. B. McPherson, H. S. Strausser, and J. C. Williams, Jr. (closure)	1558-9
Mechanics of Sediment-Ripple Formation, by Hsin-Kuan Liu. Proc. Paper 1197, April, 1957. Prior discussion: 1417. (discussion closed.)	
by Vito A. Vanoni and Norman H. Brooks	1558-17
by E. Roy Tinney	1558-22
by M. L. Albertson, D. B. Simons, and E. V. Richardson	1558-23

(Over)

Proc. Paper 1558 is part of the copyrighted Journal of the Hydraulics Division,
Proceedings of the American Society of Civil Engineers, Vol. 84, No. HY 1,
February, 1958.

There will be no closure.

The Efficacy of Floor Sills Under Drowned Hydraulic Jumps, by Ahmed Shukry. (Proc. Paper 1260, June, 1957. Prior discussion: 1417. Discussion closed.) by Mushtaq Ahmed	1558-33
Is the Writing of Flood Insurance Feasible? by John F. Neville. (Proc. Paper 1202, October, 1957. Prior dis- cussion: 1417, 1456. Discussion closed.) by Mushtaq Ahmad	1558-39
Attenuation of Solitary Waves on a Smooth Bed, by Yoshiaki Iwasa. (Proc. Paper 1262, June, 1957. Prior discussion: none. Discussion closed.) by Yoshiaki Iwasa (corrections)	1558-41
A Study of Bucket-Type Energy Dissipator Characteristics, by M. B. McPherson, and M. H. Karr. (Proc. Paper 1266, June, 1957. Prior discussion: 1417. Discussion closed.) by Gale B. Dougherty	1558-43
Systematic Changes in the Beds of Alluvial Rivers, by Walter C. Carey and M. Dean Keller. (Proc. Paper 1331, August, 1957. Prior discussion: none. Discussion closed.) by T. Blench	1558-47
Synthetic Storm Pattern for Drainage Design, by Clint J. Keifer and Henry Hsien Chu. (Proc. Paper 1332, August, 1957. Prior discussion: none. Discussion closed.) by M. B. McPherson	1558-49
Characteristics of Flow over Terminal Weirs and Sills, by P. K. Kandaswamy and Hunter Rouse. (Proc. Paper 1345, August, 1957. Prior discussion: none. Discussion closed.) by F. V. A. Engel	1558-59
100 Frequency Curves of North American Rivers, by E. Kuiper. (Proc. Paper 1395, October, 1957. Prior discussion: none. Discussion open until March 1, 1958.) by H. C. Riggs	1558-61

SEVEN EXPLORATORY STUDIES IN HYDRAULICS^a

Closure by Hunter Rouse

HUNTER ROUSE,¹ M. ASCE.—Because of the evident limitations of class
e, none of the seven subjects reported upon in this summary paper was
pletely covered even in an exploratory manner. Nevertheless, it was felt
t some knowledge of value to the profession was contained in each study.
e tone of the discussion of the two studies supervised by Mr. Laursen would
tify this belief; it is hoped that the five which were not discussed have
ved equally interesting to the profession. The discussion by Messrs.
Pherson and Dittig serves to illustrate the complexity of the overfall
blem. It is readily apparent that the transitions from one regime of flow
another are especially in need of further investigation. Messrs. McPherson
l Dittig are correct in assuming that the nappe was not ventilated; in answer
their direct question, the brink depths which were measured were not con-
ered precise enough to be significant. The discussion by Mr. Paderi is
lcome because of the information that it provides regarding his own work
the free overfall.

Proc. Paper 1038, August, 1956, by Hunter Rouse.
Director, Iowa Inst. of Hydraulic Research, State Univ. of Iowa, Iowa City,
Iowa.

MEASURING STREAMFLOW UNDER ICE CONDITIONS^a

Closure by A. M. Moore

A. M. MOORE,¹ A.M. ASCE.—The writer should have covered more fully one of the points brought out by Professor Behlke. Obtaining a good record of stage is difficult during cold weather even when the temperature does not fall below 0° F. Inlet pipes may freeze or ice may form in the well. Where electricity is readily available engineers have prevented the formation of ice by leaving a 50- or 75-watt bulb burning in the gage well or by installing soil-heating cable in inlet pipes and wells. At many installations a ready source of power is not available and the engineer must rely on placing the inlets below the frost line and seating the float that controls registration of stage in a tank containing 5 or 10 gallons of oil. This pipe must be of such length and so located that there is little danger of the oil escaping at the bottom or top of the pipe as the stage fluctuates. The layer of oil must be thick enough so that the underlying water surface will be below the bottom of the ice in the well. As an added precaution subfloors are sometimes installed in the wells, below the frost line. At some stations, ground water several degrees above freezing is pumped into wells and supplies enough warmth to keep well and inlets free from ice. Usually such an occurrence is accidental but in at least one instance ground water was purposely piped into the well. But as Professor Behlke points out, in parts of Alaska and Canada the cold is so intense and prolonged that little or nothing can be done to insure a reliable record of stage during the winter months. The Geological Survey is currently experimenting with a radically different type of gaging station requiring no stilling well and with a recorder driven by a battery-operated motor. This may prove to have merit for cold-weather operation. Cold weather can also cause the oil in recorder bearings to congeal, and the added friction may cause clock stoppage. At least one manufacturer of zero-stage recorders is now trying out plastic bearings that require no oil. This may minimize one major cause of lost records during cold periods. The writer agrees with Professor Behlke that during prolonged periods when the temperature remains many degrees below zero, correlation on a day-by-day basis between air temperature and stream discharge is impossible. The showing of a dashed line representing effective gage height in Fig. 2 may have led Professor Kolupaila to believe that the author uses the "Stout" effective gage-height method exclusively. The dashed line was included in the figure merely to show the amount of backwater, and was obtained by backing backward from the adjusted discharge. The writer does use the

effective gage-height method, described in the reference quoted by Professor Kolupaila, for days when the effect of anchor ice is clearly visible on the recorder chart and sometimes for the first or last day of a period of backwater from surface ice. Some engineers of the Geological Survey use this method throughout the entire period of backwater from surface ice but merely as one of the tools. Actually neither the "Stout" method nor the "Lithuanian" method as such as used by the Survey. Both methods are given consideration along with many other factors and perhaps the most reliance is placed in records for adjacent gaging stations and weather records. When adjusted discharge and discharge corresponding to gage heights are plotted on the same logarithmic-scale graph the linear distance between the two graphs actually is the cologarithm of "K", the discharge ratio. Therefore, if during a period of relatively stable ice conditions the adjusted discharge graph is drawn to pass through the measurements and to follow the general shape of the unadjusted discharge graph, the Lithuanian method is essentially being used without the need for actually computing a value of "K".

The intent of the Paper was to identify the factors that are considered when winter records are computed by the survey, rather than to compare the relative merits of various technical details.

The writer does not comprehend the empirical formula for "K" ratio for Elbe River credited to Mr. H. A. Klein. This formula, as shown by Professor Kolupaila, is $K = 0.308 + .02T$, where T = number of days since ice cover was formed. Possibly the formula is intended as a guide for determining adjusted discharge after the ice has reached its maximum thickness; but it is difficult to imagine a hydrometeorological pattern that closely repeats itself each year. The formula indicates that after ice cover has formed the amount of backwater decreases with time and is completely gone 35 days later.

Professor Kolupaila clearly scored a point in his listing of references dealing with the effect of ice on stream-flow measurement.

The writer is greatly indebted to Professors Behlke and Kolupaila for their cogent comments and discussions that undoubtedly have gone far toward clarifying and supplementing the paper.

FREQUENCY ANALYSIS OF STREAMFLOW DATA^a

Closure by David K. Todd

DAVID K. TODD,¹ J.M. ASCE.—The discussions are a welcome supplement to this paper.

Mr. Foster's statements emphasize points brought out in the paper. His contributions and active interest in frequency analysis over many years have encouraged the proper application of these methods by engineers.

Mr. Benson's point that mathematically-fitted frequency curves are not superior to graphically-fitted curves is well taken. The basis for his statement follows from the fact that it is not possible to establish that a series of flood events must conform to a predetermined statistical distribution. Within the range of recorded floods on a stream, the two methods generally will yield similar results. Which method, then, is preferable? From an engineering standpoint it is the author's opinion that the mathematically-fitted frequency curve is superior. By fitting observed data with a curve based upon a specified statistical procedure, a consistent result, eliminating the factor of human judgment and completely reproducible, is obtained. This is important for planning and design work.

Mr. Benson questions fitting two straight lines to frequency data where floods are influenced by two distinct causes. It must be granted that in situations where the two types of floods extend over the same discharge range, frequency curves can only be fitted by separating the data and fitting curves to each population. More common, however, are situations where the two causes produce floods of different ranges which overlap, or merge, to a small extent. Here it is possible to fit two curves to the data, one for higher floods and one for the lower floods, but at the same time recognizing that a transition between the two types exists in the vicinity of the intersection of the curves. Examples have been reported within the last year by Potter² for a group of 70 watersheds and by Williams³ for trade-wind and hurricane floods in the West Indies.

Proc. Paper 1166, February, 1957, by David K. Todd.

Assoc. Prof. of Civ. Engr., Univ. of California, Berkeley, Calif.

Potter, W. D., Relations between low and high frequency peak rates of runoff, Trans. Amer. Geophys. Union, v. 38, p. 402, 1957.

Williams, G. R., Discussion of "The estimation of the frequency of rare floods", Proc. Amer. Soc. Civil Engrs., v. 83, HY 3, pp. 1283-11-1283-12, 1957.

BUTTERFLY VALVE FLOW CHARACTERISTICS^a

Closure by M. B. McPherson, H. S. Strausser and J. C. Williams, Jr.

M. B. McPHERSON,¹ A.M. ASCE, H. S. STRAUSSER,² A.M. ASCE, AND C. WILLIAMS, JR.,³ J. M. ASCE.—The outstanding classic mathematical development by Mr. Turgut Sarpkaya has more than offset the disappointingly small amount of additional data furnished by manufacturers.

The profile of the Rockwell 6-inch valve (at centerline) and measurements obtained with the two-dimensional apparatus appear in Table X. Values of C_Q calculated by means of these measurements compare quite well with the low test data given by Mr. Henry Voltmann.

Table XI compares free discharge values of C_Q from the 4-inch CDC valve low tests, from Mr. Sarpkaya's Fig. 5, and as calculated from the two-dimensional apparatus. Mr. Sarpkaya's theoretical treatment for free discharge is restricted to a blade of infinitesimal thickness and presumed that Z_L could not extend beyond the valve body. The two-dimensional results, where the centerline valve profile was used, are quite similar to those determined by Mr. Sarpkaya. This similarity, despite a lack of correlation of blade profile, suggests that the empirical adjustment of Eq. (8) by the authors might have corrected more for measurement errors in y than for disparities between the two and three-dimensional cases.

When this research was initiated the effects of installation, blade shape and closure angle were unknowns and consideration of a theoretical treatment (by others) was abandoned in favor of more general two-dimensional tests. Since the results of the program indicate a relative independence from blade shape, the theoretical analysis by Mr. Sarpkaya is now especially appropriate. Note in Tables VI, VII, and VIII of the paper the comparative constancy in area ratios for all types of installations. Therefore, the results obtained by Mr. Sarpkaya in considering a thin disk and a free jet should also be applicable to estimates for other installations. In Table XII are values of C_Q from low tests, compared with those determined by means of two-dimensional tests plotted in the authors' Fig. 1) and those calculated from Mr. Sarpkaya's Fig. 5 through use of Eqs. (7-a) and (7-b).

Although time did not permit of further study, it seems quite likely that the use of values of α and β , for the actual leading blade tips of the various valves, in Mr. Sarpkaya's equations should yield even closer estimates of actual coefficients, although some approximation would be inherent in such a

Proc. Paper 1167, February, 1957, by M. B. McPherson, H. S. Strausser, and J. C. Williams, Jr.

Research Engr., Philadelphia Water Dept., Philadelphia, Pa.

Assoc. Prof. of Civ. Eng., Univ. of Washington, Seattle, Washington.

Senior Project Engr., CDC Control Services, Inc., Hatboro, Pa.

TABLE I
6-IN. ROCKWELL VALVE - "CONTINUOUS PIPE"

α	C_D FROM FLOW TESTS (p. 1348-48)	FROM TWO-DIM. MEASUREMENTS		
		$\frac{D}{2\sqrt{A}}$	$\frac{A_v/A_j}{\text{VIA EQ. (8)}}$	C_D VIA EQ. (7-b) AND A_v/A_j
25°	0.78	2.20	2.36	0.82
30°	0.613	2.71	2.81	0.61
35°	0.48	3.26	3.28	0.49
40°	0.38	3.93	3.84	0.39
45°	0.31	4.88	4.60	0.31
50°	0.23	6.55	5.93	0.23
55°	0.17	8.34	7.28	0.18
60°	0.13	12.9	10.6	0.12
65°	0.08	22.2	16.7	0.07

BLADE PROFILE
TWO-DIMENSIONAL STUDY
6-IN. ROCKWELL
(REPRESENTS PROFILE AT $\frac{1}{2}$
OF PROTOTYPE - SEE FIG. 4)

TABLE XI

TWO-DIM. VS. THEOR. FLOW COEFFICIENTSFREE DISCHARGEL-IN. CDCFROM TWO-DIM. APP.

α	A_v/A_j (p.1167-23)	C_Q VIA A_v/A_j & EQ. (7-a)	C_Q SARPKAYA (p.1348-37)	C_Q FLOW TESTS (p.1167-12)
15°	1.96	0.567	0.58	0.635
20°	2.18	0.509	0.505	0.565
25°	2.51	0.443	0.43	0.490
30°	2.94	0.378	0.365	0.420
35°	3.53	0.314	0.30	0.355
40°	4.30	0.258	0.245	0.285
45°	5.37	0.207	0.195	0.223
50°	6.72	0.165	0.145	0.166
55°	8.72	0.127	0.105	0.120
60°	12.2	0.091	0.070	0.083
65°	19.4	0.057	0.045	0.053

TABLE XII
TWO-DIM. VS. THEOR. FLOW COEFFICIENTS

CONTINUOUS PIPE

1-IN. CDC

α	C_Q FLOW TESTS (p.1167-17)	SARPKAYA		TWO-DIM. TESTS	
		A_v/A_j VIA EQ. (7-a) and p.1348-37 (C_Q , FREE JET)	C_Q VIA EQ. (7-b) and A_v/A_j	A_v/A_j FROM p.1167-23	C_Q VIA EQ. (7-b) and A_v/A_j
10°	1.38	1.66	1.69		
20°	0.92	2.20	0.92	2.18	0.94
30°	0.592	3.04	0.54	2.92	0.58
40°	0.354	4.53	0.31	4.24	0.34
45°	0.272	5.69	0.24	5.28	0.26
50°	0.208	7.65	0.17	6.55	0.20
60°	0.106	15.9	0.074	11.7	0.10
65°	0.064	24.6	0.047	18.2	0.065

cedure, with two sets of angles involved.

Mr. Sarpkaya has compared his curve for $\beta = 90^\circ$ in his Fig. 6 with the Génissiat and Dow data and states: "The agreement between the theoretical and experimental results is excellent". Inasmuch as the Génissiat data are for a converging valve body, far from satisfying the parallel walls of Mr. Sarpkaya's analyses, and the Dow data are not necessarily for $\beta = 90^\circ$, the agreement must be considered as accidental. Otherwise the value of the analyses would be diminished by this rather loose conjecture.

The comments by Mr. Sarpkaya on the distribution of stagnation points (theoretical) are very interesting and deserve consideration by future researchers. The authors had begun to study the correlation of stagnation point with pressure distribution and hydrodynamic torque, but interest subsided as the torque problem diminished with the introduction of more modern actuators.

With reference to free discharge versus submerged characteristics, the authors wish to reiterate: "----, it would be logical to assume that the flow characteristics might not be identical even though the installations are quite similar." The comment "advocated as a panacea" by Mr. Sarpkaya is hardly consistent with the above originally suggested hypothesis. In fact, the conclusions reached in his reference 11 were based upon an acknowledged "exploratory study". Further, he implies a larger coefficient for the submerged case, when in Table II it is larger only for 10° to 30° . There is no argument whatever on the need for "further study and a better explanation" of submerged fluid flow characteristics.

The discussion by Mr. Ronald E. Nece was mostly confined to a consideration of continuous pipe installations. The introduction of another factor, K_L , does not add particularly to the clarity of the data presented.

The CDC, Rockwell, Netsch and Schulz, and Dickey and Coplen valves had smooth walls without "stops, recesses, or projections". Wall conditions for the others were not given. Mr. Nece quite properly points out the possibility of divergence in results, due to probable dissimilar wall conditions in prototype valves (particularly in the larger sizes) as opposed to the smaller valves normally tested.

In the paper it was stated that "a deduction from the overall loss had been made for equivalent pipe friction to and from the valve body for purposes of correlation". For the Netsch and Schulz data presented in Table IV, one-tenth of a velocity head was deducted for the flared conduit entrance, and a friction factor of 0.014 for the constant Reynolds number of their tests was used to apportion the conduit friction to and from the valve body. A sizable disparity could therefore be found in the Netsch and Schulz values of Table IV converted to Mr. Nece's table. Mr. Nece's Eq. (4) applies only to a circular valve; to obtain K_L for the square damper of Table IV the right side of this equation must be multiplied by $\left(\frac{4}{\pi}\right)^2$. Should the reader check against Mrs. Cohn's graphs, it is to be noted that her plot for Disk II is incorrect inasmuch as she did not use the "open area" in interpreting Fig. 14 of Dickey and Coplen, as stipulated. The head loss for the Dickey and Coplen data was stated to have been for the "damper only" and hence a deduction for conduit friction was not made for their data in Table IV.

In Table XIII are compared the theoretical "average C_c from von Mises" for free discharge by Mr. Nece and similar values from Mr. Sarpkaya's Fig. 6. Mr. Nece assumed, as an expedient approximation, that the flow was divided equally to each side of the blade. The exact theoretical values by Mr.

TABLE XIII
COMPARISON-COEFFICIENT OF CONTRACTION

α_0	"AVG. C_c (VON MISES 2-DIM.)" (NECE)	$(C_{c1} + C_{c2})/2$ $\beta=90^\circ$ (SARPKAYA)
0°	1.000	1.000
10°	0.862	0.741
20°	0.773	0.711
30°	0.716	0.689
40°	0.675	0.670
45°	(0.660*)	0.662
50°	0.657	0.655
60°	0.632	0.640
70°	0.618	0.629
80°	0.612	0.619
90°	0.611	0.611

(* Value of 0.660 from p.38, "Engineering Hydraulics", by Rouse⁽¹²⁾,

$\alpha_0 = 45^\circ$, $\beta = 90^\circ$, where unbalanced distribution of flow on each side of 2-dim. case was taken into consideration; used values from von Mises analysis).

Sarpkaya show this approximation to be too gross, particularly for the near-open values. A value of 0.660 at 45° using the von Mises figures, for equal jet velocities and hence unequal distribution of flow, is compared with the 0.662 from the Sarpkaya analysis. The Sarpkaya analysis is now superior to an adaptation for butterfly valves of the von Mises analysis because the latter is restricted to a β of 90° , while the former is solvable for any closure angle. Both have a failing as regards accounting for blade shape in determining theoretical contraction coefficients.

Mr. Nece's reference D-3 deserves a careful review by anyone interested in a comparison of flow characteristics between various types of valves.

Mr. Henry Johnson deplors the use of the two-dimensional tests because the quantitative results as compared with the prototypes were not perfect, and declares that "prediction of cavitation inception ----- on the basis of such tests would be meaningless". The implications of Table IX have escaped Mr. Johnson. The assumptions of Table IX include usage of Eq. (7-b) with prototype flow data and usage of an average jet velocity rather than a local velocity; the two-dimensional tests were not involved. The two-dimensional tests were presented mostly to enhance confidence in the equations for C_Q , particularly Eq. (7-a) and (7-b), and to suggest the possible value of comparative two-dimensional studies in the development or appraisal of a unique geometry. In recently reported gate valve cavitation tests,⁽¹⁴⁾ for positions up to 90% of full open, audible cavitation was obtained, as would be expected, at a lower total head at Station 1 than anticipated "based on Borda loss". Significantly, the cavitation index for audible cavitation was roughly equivalent to the anticipated indices plus a constant. Similar descriptions of cavitation tests for butterfly valves are noticeably absent from the literature; recourse to approximation methods is dictated by default.

Unfortunately, the authors' Eq. (1) for C_Q is useful only for a circular valve. An equitable comparison of the Dickey-Coplen circular Disk I and its counterpart, the square damper, can be made only by multiplying the C_Q values of the square damper by $\frac{\pi}{4}$ as shown in Table XIV. This comparison

adds further evidence to the correlation of two-dimensional relationships with circular valve, despite the opinion of Mr. Johnson to the contrary.

A description of the mechanical and operating features of butterfly valves, a summary of the reports of 1,100 users, has recently been presented.⁽¹⁵⁾

The intense interest in the subject displayed by all of the discussers and the quality of the material added by the discussions has been very gratifying.

REFERENCES

1. Ball, J. W., "Cavitation Characteristics of Gate Valves and Globe Valves Used as Flow Regulators Under Heads up to About 125 Feet", Trans. ASME, Vol. 79, No. 6, August 1957.
2. Mahon, Ross L., "Hydraulic Butterfly Valves", Civil Engineering, pp. 52-57, October 1957.

TABLE XIVFLOW COEFFICIENT, C_D -CONTINUOUS PIPECOMPARISON OF VALVE SHAPE IN TERMS OF AREA RATHER THAN D^2 (DATA FROM TABLE IV)

<u>α</u>	<u>DICKEY-COPLIN DISK I (THIN)</u>	<u>SQUARE-DAMPER DICKEY-COPLIN (TIMES $\frac{7}{4}$)</u>
10°	1.87	1.85
20°	1.00	1.01
30°	0.63	0.60
40°	0.39	0.44
50°	0.22	0.21
60°	0.120	0.116
70°	0.062	0.054
80°	0.028	0.022

MECHANICS OF SEDIMENT-RIPPLE FORMATION^a

Discussion by Vito A. Vanoni and Norman H. Brooks

VITO A. VANONI,¹ M. ASCE and NORMAN H. BROOKS,² J.M. ASCE.—The author has presented an interesting paper on an important subject, reviewing the various explanations for the occurrence of dunes and ripples on the beds of streams, and developing an analogy between sand-ripple formation and instability of an interface between two liquids of differing density. His analogy depends on the basic assumptions that (a) a sand bed behaves like a dense fluid, and (b) sand waves and interfacial waves are basically caused by the same fluid forces.

The writers find this analogy difficult to accept. At low velocities when ripples are just forming, the sand bed does not move or deform like a fluid. Ripples are built up through the rolling and sliding of sediment particles over the surface, with the particles being entrained at some places and stopped at other places. During this process only the grains at the very surface are free to move; hence, near the critical velocities the growth of ripples may be extremely slow.

By contrast, waves at an interface between two fluids may be quickly generated because the denser fluid may deform as a continuous mass. A lowering of the interface at one point results immediately in a corresponding rise elsewhere because the whole dense fluid layer may flow in response to differential normal stresses. On the other hand a sand bed, being firm, does not respond to normal stresses at all, and the particles are constrained to tangential motion of the surface only. (These conditions prevail, of course, only when the sediment is just starting to move, and not at high velocities when the sediment transport rate is large and the dunes are obliterated again.) Consequently, the writers believe a theory for ripple formation must take into account the granular properties of the bed, which cannot be adequately represented as a dense liquid.

To derive Eq. (10), it is actually not necessary to use stability theory for an interface, as dimensional analysis will suffice. Whether or not ripples will form in a flat sand bed depends on a critical relation between the following variables: T , the bed shear stress; ρ , the mass density of the fluid; d , diameter of particles; μ , the fluid viscosity; and w , the settling velocity of the particles. For simplicity, shape and size-distribution factors are not considered. A straightforward analysis immediately yields the dimensionless numbers U_*d/w and U_*d/ν and Eq. (10) for the criterion of ripple formation.

Proc. Paper 1197, April, 1957, by Hsin-Kuan Liu.

Prof. of Hydraulics, California Inst. of Technology, Pasadena, Calif.

Asst. Prof. of Civ. Eng., California Inst. of Technology, Pasadena, Calif.

The quantity U_*d/ν is simply a type of Reynolds number (sometimes called the bed Reynolds number) and need not be considered as an "instability index". In fact, it is hardly appropriate to call this an instability index when the criterion for ripple formation is practically independent of it when U_*d/ν is greater than 100 in Fig. 9 or greater than 10 in Fig. 11.

The five variables listed above embody all the important components of the problem, i.e., applied force (T), fluid properties (ρ, μ), and sediment properties (w, d). In regard to the latter, it should be noted that w, d, ρ , and μ uniquely determine the submerged unit weight of the particles because it is the only unknown in the drag formula

$$\frac{\pi}{6}(\gamma_s - \gamma)d^3 = C_D \frac{\pi}{4}d^2 \frac{1}{2}\rho w^2 \quad (11)$$

wherein C_D , the drag coefficient for spheres, is determined from the value of $w d \rho / \mu$ (by an experimental curve found in any fluid mechanics textbook). In fact, if it is preferred to use $(\gamma_s - \gamma)$ as the fifth variable instead of w , the result in place of Eq. (10) is

$$\frac{T}{(\gamma_s - \gamma)d} = \phi_3\left(\frac{U_*d}{\nu}\right) \quad (12)$$

The author presents the experimental data in Fig. 9 in the form of Eq. (10) whereas Fig. 11 is in the form of Eq. (12). Although there is more scatter of points in Fig. 12, it does not necessarily mean that Eq. (12) is not as good as Eq. (10), as implied by the author in the last paragraph before the summary, inasmuch as

$$\frac{T}{(\gamma_s - \gamma)d} = \frac{T}{3/4 C_D \rho w^2} = \frac{4}{3 C_D} \frac{U_*^2}{w^2}$$

by Eq. (11) and the definition of the shear velocity U_* . Thus the ordinate in Fig. 11 is essentially the square of that in Fig. 9, and the scatter of points should, accordingly, be about twice as great on a logarithmic graph, as is the case.

The present writers are particularly interested in Figs. 10 and 11 which show the Shields' curve for beginning of motion of sediment and the curve for the beginning of ripples. These two curves coincide for bed Reynolds numbers in excess of 100, but for smaller Reynolds numbers the curves indicate that ripples start at higher values of U_* than are required to start motion of the sediment. The writers have wondered if the two curves should, perhaps, not coincide over the entire range, thus indicating that ripples always start as soon as motion of the sediment starts.

In suggesting this, it is realized that there is the danger of being accused of flying into the face of fact in the form of experimental data. However, it is also realized that there is appreciable uncertainty in the results of sediment-transport experiments, especially when the transport rate is very low, as it is in the experiments reported by the author. Under these circumstances it takes considerable time to move enough sediment to determine if a ripple pattern is developing, and the natural tendency is to err in the direction of obtaining values of U_* for beginning of ripples that are too large. An example of

such a difficulty is presented by the author in describing the experiments in which the sand waves of Fig. 6 were obtained. As an example of the slowness with which bed ripples develop, the writers cite one of their experiments,⁽¹⁾ made at low velocity in a flume 33.5 inches wide with a fine sand bed which was made level at the beginning of the run. When the flow was started, ripples started forming slowly in several spots and finally after about 30 hours of continuous running the bed reached its steady state configuration of dunes. During this development stage the slope, bed shear stress, and friction factor all gradually increased. Pertinent data for this run are given in two columns of Table 2, one for 5.1 hours after the start of the run (when the first good slope determination was made), and the other at the end of the run, 55.3 hours after starting. Although no concentration measurements were made during the period of dune growth, visual observations indicated that the concentration increased as the dunes developed; after reaching equilibrium the total transport concentration was only 3.3 ppm.

In experiments of this kind, the shear velocity U_* increases considerably from its initial value for the same depth and velocity because of the increased roughness. The run cited above (Table 2) is a good illustration, showing a change in U_* from 0.037 fps near the beginning of the run to 0.078 fps at the end of the run. The corresponding changes in the dimensionless parameters U_*d/ν , U_*d/ν , and $T/(\gamma_s - \gamma)d$ are also indicated in Table 2; if these data are plotted on Figs. 9 and 11, it is apparent that the development of dunes in the course of a run moves the data points considerably up and to the right. It seems likely that this effect may have contributed to a fictitious divergence between the curves for initiation of sediment movement and ripple formation on Figs. 10 and 11, especially in the case of data from the other sources. Most of the data plotted in Fig. 11 are not available to the writers, so it is difficult to judge their precision. It would be of considerable assistance to readers if the author would give the specific references from which these data were taken. Without more knowledge of the data used, the writers would still be inclined to move the curve for beginning of ripples, in Fig. 11, downward because of the natural tendency to obtain too large values of U_* in the experiments for the reasons discussed above. It might not be unreasonable to move this curve down so it fitted the lowest points, in which case the curve for beginning of ripples and the Shields' curve would be quite close. It is obvious that this question cannot be settled with the information at hand, but that it will be necessary to make more of the tedious and time-consuming experiments of the kind performed by the author before the matter can be settled.

The formation of dunes from a flat bed is indeed a puzzling phenomenon. The writers do not concur with the author in the opinion that turbulence and small irregularities of the bed are not primary causes of ripple formation. Although the pattern which develops may be quite regular, the natural turbulence in the stream may still be the instigator. When U_*d/ν becomes small, it is believed that the frequency with which eddies penetrate the laminar sublayer decreases but that the sublayer never becomes a perfect "insulator" for the bed even for $U_*d/\nu < 4$ as suggested by the author. When an eddy sweeps down to the bed, particles on the bed are disturbed. Where the particles are lifted a few grains higher than the initial surface, a small wake develops which makes the particles immediately downstream more likely to be entrained. The effect of these leeside eddies carries downstream only several times the height of the obstruction, so sand may accumulate to form another tiny ridge.

Another wake is formed and so on, with a regular ripple pattern developing from a random turbulent motion, as described by the author's quotation from Inglis.

It is easily observed in a flume that the initial ripples have the shortest wave length, and that as time passes the wave length increases as the height increases, as would be expected according to the above explanation. After a sufficiently long time some equilibrium height and wave length are reached, the values of which probably depend principally on the grain size, depth, settling velocity and flow velocity. When the dunes are fully developed the turbulence characteristics are certainly altered, but this fact does not a priori exclude turbulence as a major cause. On the other hand, the writers concur with the author that the occurrence of ripples or dunes does not depend on there being a free surface. This fact is conclusively demonstrated by observations of dunes in pipes by Ismail⁽²⁾ and Craven.⁽³⁾

In regard to the author's experiments, several points are of interest. First of all it should be noted that, with the exception of Run 1-4, the depths are exceeding small, ranging from 0.010 ft (1/8 in.) for Run 1-3 to 0.040 ft (1/2 in.) for Run 1-6. Even apart from the problem of accurately maintaining and measuring such small depths, the validity of the results is open to question because of the very low Reynolds numbers. With the aid of a Stanton-Moody pipe-friction diagram, it may be estimated that for Run 1-3 the friction factor $f = 0.04$, $V =$ mean velocity $= 0.75$ fps and Reynolds number $4Vd/\nu = 3000$; for Run 1-6 the corresponding estimates are $f = 0.05$, $V = 1.05$ fps and $4Vd/\nu = 15,000$. If turbulence is an important factor in ripple formation, then the lack of fully developed turbulence, as indicated by the low Reynolds numbers for all but Run 1-4, must exert an important but undetermined effect on the results.

The ripple photographs in Figs. 6 and 8 lead the writers to believe that the ripples observed by the author may not have been typical. The shape of the dunes in Fig. 8 appear more like antidunes⁽⁴⁾ than true ripples; the crests appear to be quite rounded and the profile rather symmetrical. On the contrary, the writers have observed that small ripples are characterized by gentle upstream slopes, sharp crests, and steep downstream faces. From Fig. 8 the wave length appears to be about 2-1/4 inches or about 18 times the mean depth, a ratio which is more plausible for antidunes than ripples. If the Froude number is near or above the value one, then antidunes should in fact be expected. It is estimated that the Froude number for this illustration (Run 1-3) is $V/\sqrt{gd} = 1.3$. It would not be surprising if the height of the antidunes was of the same order as the mean depth.

Likewise, in Fig. 6 the oblique crests do not appear typical of ripples occurring at low velocities. They are perhaps similar to the sand fronts described by Brooks⁽⁵⁾ which occur at an advanced stage of transport when the dunes are about to disappear and the bed to become flat.

The condition of beginning of ripples is an interesting one, but in fact it occurs seldom, if ever, under natural conditions. An alluvial river produces ripples or dunes on its bed at low stages and may completely obliterate or appreciably change them at higher stages. However, when the stage drops after a flood, dunes with re-form. If the stage drops to the point where sediment motion is about to cease, (i.e., to the point where dunes would be expected to start forming if the bed were initially flat), dunes already exist and represent the stable condition for the existing flow. If the flow or stage were

TABLE 2

Summary of Data for Run 2-12 (A)

Hours since beginning of run		5.1	55.3
1, Median sand size,	mm	0.137	0.137
Mean depth,	ft	0.539	0.541
Mean velocity,	fps	0.81	0.80
Slope,		0.00011	0.00039
Bed friction factor (adjusted for wall friction)		0.017	0.076
U_* , Bed shear velocity (adjusted for wall friction) fps		0.037	0.078
Temperature,	$^{\circ}\text{C}$	23.3	24.6
T , Bed shear stress,	psf	0.0027	0.012
w , Settling velocity,	fps	0.053	0.054
$\frac{U_*}{w}$		0.70	1.45
$\frac{U_* d}{\nu}$		1.7	3.6
$\frac{T}{(\gamma_s - \gamma) d}$		0.057	0.25

reduced still further, sediment motion would cease and the dunes would remain unchanged. This idea is borne out by the presence of dunes in ephemeral streams during their dry period. Hence the writers do not concur with the author in the first paragraph on pp. 1197-19, where he indicates that dunes will disappear when the flow conditions fall below the curve in Fig. 9.

Other dune problems, even more interesting than that of initiation, are (a) how they are modified as the velocity increases, and (b) at what velocity are they obliterated. Such changes in the bed configuration of a stream appear to be responsible in large part for loops in stage-discharge curves for rivers (for example Ref. 6) and for large fluctuations in roughness coefficients, which are accompanied by variations in sediment transport rate. Hence these dune problems are intimately related to the whole problem of sediment movement. Their importance has been recognized widely as evidenced by the attention devoted to it by workers in this field.⁽⁷⁾

REFERENCES

1. Brooks, Norman H., Closure to "Mechanics of Streams with Movable Beds of Fine Sand", ASCE Journal of Hydraulics Div., Vol. 83, No. HY 2, April 1957, pp. 1230-7, Table 8, Run 2-12.
2. Ismail, Hassan M., "Turbulent Transfer Mechanism and Suspended Sediment in Closed Channels", Trans. ASCE, Vol. 117, Paper No. 2500, 1952, pp. 409-34.
3. Craven, John P., "The Transportation of Sand in Pipes - 1. Full-Pipe Flow", Proc. 5th Hydraulics Conf., State Univ. of Iowa, Studies in Engineering, Bul. 34, No. 426, 1952, pp. 67-76.
4. Langbein, W. B., "Hydraulic Criteria for Sand-Waves", Trans. Amer. Geophysical Union 1942, Part II, p. 615.
5. Brooks, N. H., loc. cit., pp. 10-11.
6. Carey, Walter C., and Keller, M. Dean, "Systematic Changes in the Beds of Alluvial Rivers", ASCE, Journal of Hydraulics Div., Vol. 83, No. HY 4, August 1957, paper 1331.
7. "Hydraulic Research in the United States", U. S. Bureau of Standards, 1957.

E. ROY TINNEY,¹ J.M. ASCE.—The physical explanation provided by Mr. Liu for the mechanics of ripple formation is both interesting and helpful. Such an attempt to attack the complex problems of sediment transportation by the latest concepts of fluid mechanics is highly commendable. The writer feels, however, that the data and analysis presented by the author do not convincingly verify his plausible verbal description of the mechanics of ripple formation.

In particular, the data presented in Fig. 9 shows that for all values of U_*d/ν greater than about 120

1. Head, The R. L. Albrook Hydr. Lab., Div. of Industrial Research, State College of Washington, Pullman, Wash.

$$\frac{U_*}{w} = 0.13 \quad (1)$$

$$T_c = 0.0169 w^2 \quad (2)$$

is equation is remarkable similar to formulae for critical tractive forces at initial movement. Such a similarity between the formulae makes it extremely difficult to present a clear distinction between the two phenomena. Therefore a convincing argument for the mechanics of ripple formation can be made, it will be necessary to present data for the beginnings of ripple formation at moderate values of the bed load rather than at the beginning of bed movement.

Furthermore, the value of $U_* d/\nu = 120$ agrees extremely well with the value $d/\delta' = 10$ (since $U_* d/\nu = 11.6 d/\delta'$) for the lower limit of "rough" boundaries. The only conclusion that can be drawn from the data on the right of Fig. 9 is that for "rough" boundaries ripples form as soon as motion of the sediment begins. Just why ripples form on a "rough" bed remains as an unverified hypothesis.

One interesting point with regard to Fig. 9 is that the lowest value of $U_* d/\nu$ for which data are given is 3.0. This corresponds to $d/\delta' = 0.258$ which is almost identical with the upper limit of "smooth" boundaries. If the author could find no ripples for values of $U_* d/\nu$ less than 3.0 it could be concluded that ripples do not form on "smooth" boundaries, a point that would strongly support the author's laminar sub-layer instability explanation for incipient ripple formation.

With regard to critical tractive force formulae, the writer presents the following graphs of several critical tractive force functions for small sediment sizes. Note that the critical tractive force concept is supported by Einstein's theory for bed load particularly for small grain sizes if the critical tractive force is defined as the tractive force required for negligibly small movement, say $G = 1$ to 5 lbs. per ft./hour. For sediment sizes over 0.03 ft. several experimenters, namely Shields, Straub, Lane and Carlson, and others, find that the equation

$$T_c = 0.06 (\gamma_s - \gamma) d \quad (3)$$

fits the available data reasonably well.

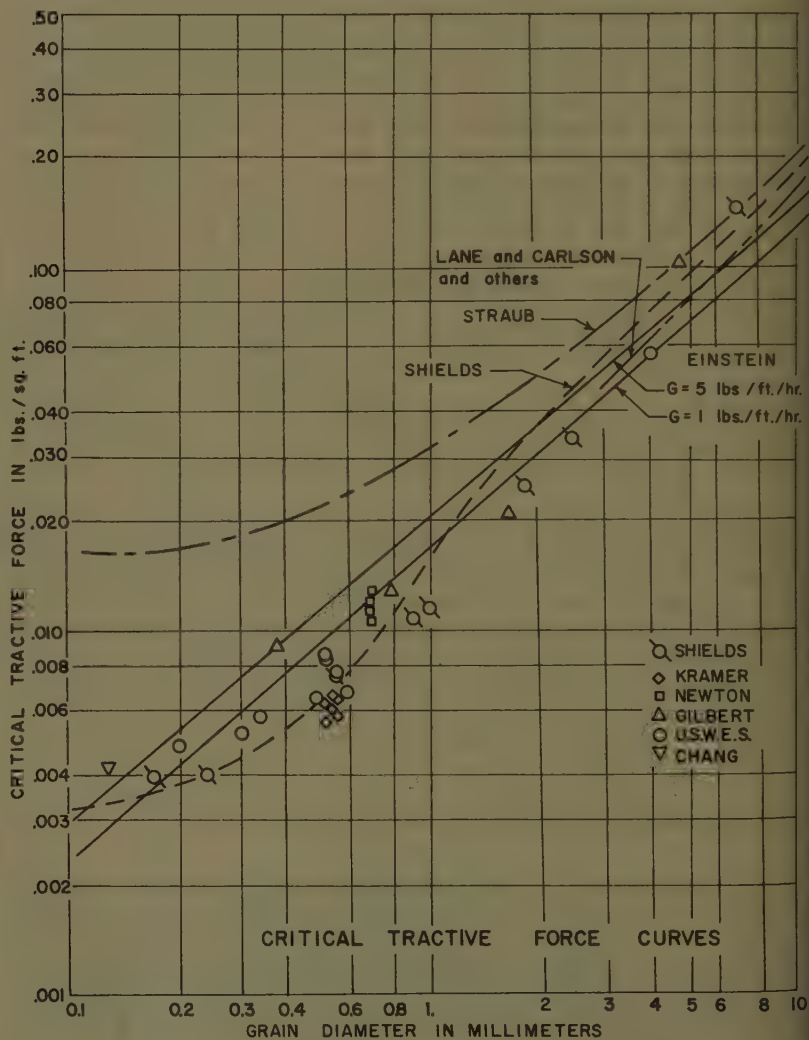
M. L. ALBERTSON,¹ M. ASCE, D. B. SIMONS,² A.M. ASCE, and E. V. CHARDSON,³ J.M. ASCE.—Mr. Liu is to be commended for his excellent summary of the salient literature on the subject of stability of an interface. Furthermore, he has related very logically this literature and applied it to the generation of ripples in alluvial streams. He has clearly demonstrated that there is a definite relationship between the formation of waves at the interface of two liquids, at the interface of sand and air, and at the interface

re: Published with the approval of the Director of the U. S. Geological Survey.

Director of Research Foundation and Prof. of Civ. Eng., Colorado State Univ., Fort Collins, Colo.

Research Engr., U. S. Geological Survey, Fort Collins, Colo.

Research Engr., U. S. Geological Survey, Fort Collins, Colo.



E. ROY TINNEY

sand and water. By this means considerable information already available has been brought to bear on the subject of ripple formation. In the opinion of the writers he has made a major contribution to this subject.

Mr. Liu has climaxed his research with the formation of a single plot which shows clearly the conditions under which movement of sediment is initiated and ripples are formed. His criterion for sediment ripple formation is a real milestone in the struggle to understand the mechanics of sediment transport. Mr. Liu quite logically uses a ratio of the shear velocity to the fall velocity of the sediment as his dependent variable and the shear velocity Reynolds number as his independent variable. The scatter of the data in this plot is quite small compared with the usual scatter of data involving sediment transport. Furthermore, data which have been taken more recently by Plate⁽¹⁾ and a theoretical development which he has made under Mr. Liu's direction prove even more conclusively the general validity of Fig. 9.

Despite the excellence of Fig. 9 and the discussion preceeding its development, the writers believe further interpretation of this figure would be helpful. The shear velocity Reynolds number for some purposes (and the writers believe this is one of them) can be represented more significantly as a ratio of the sediment diameter d to the thickness of the laminar sublayer by the equation for the thickness of the laminar sublayer $\delta' = 11.6 \frac{\nu}{U_*}$ which

can be inverted and both sides multiplied by d to give $11.6 \frac{d}{\delta'} = \frac{U_* d}{\nu}$ which means that the magnitude of $U_* d/\nu$ is nearly 12 times as great as the ratio d/δ' . If the assumption is made that the sediment size d is approximately equal to the size of the sand grain roughness k used by Nikuradse in pipes, the initiation of ripple formation might logically be related in some way to the transition from a smooth boundary to a rough boundary in rigid-boundary fluid mechanics.

Fig. 9 is particularly significant in that it shows a transition from one regime of flow to a second regime of flow. The significance can be understood more completely from the following observations:

1. Ripple formation is definitely dependent upon the ratio U_*/w . As the particle size increases, the shear velocity must increase in direct proportion if ripples are to be formed. Since the shear velocity is proportional to the square root of the shear, the shear must be increased 4 times if the fall velocity of the bed material is doubled.
2. For small $U_* d/\nu$ -values a much greater magnitude of the ratio U_*/w is required for ripples to form than for the larger $U_* d/w$ -values. The entire range of U_*/w -values is particularly significant when associated with the ratio d/δ' . In other words, the formation of ripples is very closely related to the size of the sediment d relative to the thickness of the laminar sublayer.

This concept is logical and quite in keeping with Dr. Liu's hypothesis that the laminar sublayer is intimately involved in the phenomenon.

3. At the minimum $U_* d/\nu$ -value for which there are data, $U_* d/\nu = 3$ and the shear velocity U_*/w required to form ripples is approximately 5 times that required at $U_* d/\nu = 50$. The reason for this is understood more clearly when the ratio d/δ' is used instead of $U_* d/\nu$. At $U_* d/\nu = 3$, d/δ' is approximately 0.26, which is significantly approaching the point in rigid-boundary fluid mechanics where the transition begins from a smooth boundary to a rough boundary for Nikuradse's data using sand

grains of uniform size. The data presented by Mr. Liu, however, were taken from experiments involving both sediment having a relatively narrow size-range and sediment having a wider size-range.

4. At $U_*d/\nu = 80$, where U_*/w becomes independent of U_*d/ν , $d/\delta' = 7$ which is approximately the value of k/δ' where a rigid boundary becomes completely rough based upon the data of Nikuradse and the curve of Colebrook-White. Apparently, the protective effect of the laminar sublayer is lost and the magnitude of U_*/w necessary to form ripples decreases from 0.6 to 0.12 as the sublayer is destroyed in the transition from smooth to rough boundaries.
5. Once the laminar sublayer is destroyed ($U_*d/\nu > 80$), the formation of ripples no longer takes place. Evidently, then, Dr. Liu has demonstrated that ripples cannot form without a laminar sublayer existing and Tison⁽⁶⁾ has shown that ripples do not form if the flow is laminar. The very significant conclusion can now be drawn that ripples form only if the flow is turbulent and the boundary is smooth or in transition from smooth to rough—that is, only when a laminar sublayer is in existence. This supports Dr. Liu's contention that ripple formation is somehow related to instability at the laminar sublayer.
6. In view of the foregoing analyses, the writers are inclined to believe that the formation of ripples is somehow associated not only with instability but also with the turbulence in the stream above the laminar sublayer and sand bed. Such turbulence in turn, is directly related to the instability of the laminar sublayer. In other words, turbulence and instability of the laminar sublayer are intimately related and cannot be separated. In rigid-boundary fluid mechanics the boundary transition (that is, the transition from a smooth boundary to a rough boundary) is initiated when periodic fluctuations in velocity caused by overhead turbulence (or eddies caused by instabilities of the interface) penetrate the laminar sublayer to the point where they encounter roughness projections. Under these conditions a part of the resistance to flow is being contributed by the form drag caused by the roughness projections. As the above turbulence becomes effective, the laminar sublayer is made thinner, and the boundary becomes rougher. Hence the local velocity caused by the turbulence encounters the roughness projections a greater percentage of the time until finally, when the boundary is completely rough, there is no laminar sublayer acting as a protective blanket and (in an alluvial bed) ripples can no longer be formed.
7. When the boundary is completely rough, the drag is due entirely to form drag around the roughness projections. The drag coefficient then becomes independent of the viscous effects. With a smooth boundary (in contrast to a rough boundary) the laminar sublayer acts as a protective blanket which completely covers the roughness projections and the resistance to flow is a function of the relative viscous effects as reflected by U_*d/ν or the ratio k/δ' or d/δ' .

The fact that ripples form only in the smooth to rough boundary transition region leads one to wonder what the difference might be in the nature of the ripples which form with a completely smooth boundary (if at all), with a boundary in transition, and with a boundary that is nearly rough.

The fact that Figs. 9 and 10 show clearly the conditions under which sediment movement begins and ripples are initiated led the writers to speculate

the possibility of similar relationships for other types of sand waves such as dunes, bars, antidunes, and the plane bed. Therefore, Fig. A was prepared using data from several sources where adequate information was available. In this figure it is clearly evident that, in general, dividing lines can be drawn to separate the regimes of ripple formation, dune formation, transition, and antidune formation. Furthermore, Fig. 9 is extended more than one cycle to the left by means of the data of Kalinske and Hsia⁽²⁾ and it is extended more than one cycle to the right by the data of Lane and Carlson.⁽³⁾ For purposes of comparison, the transition function from a smooth to a rough boundary is also included in Fig. A. It should be noted that although the abscissa is the same for both plots, the ordinate scales are entirely different and unrelated. Nonetheless, plotting the boundary transition function permits direct comparison of the data and curves representing alluvial channels with the beginning of the Colebrook-White transition, the beginning of the Nikuradse transition, and the ends of each transition. In this figure a temperature of 20° C was used to determine the fall velocity and kinematic viscosity where temperature was not available. The scatter among the points for Laursen,⁽⁴⁾ Brooks,⁽⁵⁾ Horton,⁽⁶⁾ and the USGS-CSU⁽⁷⁾ data is the result of temperature variation. Lines of constant temperature can be drawn for these data at an angle of 45 degrees. It is also noteworthy that for almost any transition line, a change in temperature for a given size of bed material could result in a change of regime.

The following are observations regarding Fig. A which may have significance.

1. Kalinske and Hsia⁽²⁾ reported ripple formation although they did not record the conditions under which movement began and the conditions under which ripples were initiated. The minimum value of d/δ' for their data is approximately at the same point that the Colebrook-White transition begins—that is, where the Colebrook-White curve connects with the smooth boundary curve. To the left of this point the boundary is completely smooth and no influence of the overhead turbulence is felt at the boundary. In other words, the laminar sublayer is a completely protective blanket. This fact leads one to wonder if it is possible for ripples to form under these conditions. In any event, the writers have been unable to locate any data for smaller values of d/δ' . It may be that the rather explosive nature of the fine materials makes it difficult to determine definitely when movement begins and ripples begin to develop.
2. The curves describing the regimes of bed roughness are rather clearly defined and are nearly parallel for $d/\delta' < 10$. In Fig. A it is apparent that Lui's curve is not parallel to the foregoing family of curves in this range, whereas the Shield's curve turns up at the left end more nearly in accordance with them. Based on the rather definite and systematic orientation of the regime curves and Shield's curve, it is possible that Liu's curve should be lowered in the vicinity of $d/\delta' = 1$. This results in a curve, see Fig. A, which more nearly conforms with the curves defining the other regimes of flow. Such a minor adjustment might also be justified by a careful study of the effect of size distribution of the sediment.
3. For increasing values of d/δ' (the laminar sublayer becoming relatively thinner and thinner) the influence of viscosity becomes less and less for

each type of bed formation. Ripples do not form beyond $d/\delta' \approx 10$ and dunes cease to exist beyond $d/\delta' \approx 40$. Apparently, the data are sufficiently complete to permit these approximate conclusions regarding both ripples and dunes. For the transition regime of bed formation, however, the data are not sufficiently complete for any conclusion to be drawn about whether the transition ceases to exist beyond some large value of d/δ' . Gilbert⁽⁸⁾ made observations which indicate that antidunes can form in large size bed material, although as far as the writers know only qualitative observations are available to support this conclusion.

4. Because of the extreme surface waves and irregularities for both the antidune regime and certain types of transition flow, the Froude number no doubt plays a very important part. No attempt has been made as yet to relate the Froude number beyond that done in the table in Fig. A.
5. Although the two variables U_* / w and $\frac{U_* d}{\nu}$ are shown by Fig. A to be of primary importance, there is some question about the significant third variable which will correlate the data in a quantitative manner as now done in a qualitative way by the terms: ripples, dunes, transition, and antidunes. The Froude number has some significance, as shown in the table, in defining the regimes of ripples and dunes, but there is considerable question whether it will prove to be as significant in these regimes as in the antidune regime. The drag coefficient C_D is essentially a constant for each size of bed material and hence is not a logical third variable except perhaps in establishing the points where the regimes, such as ripples and dunes, cease to exist. The remaining variables which might be significant are the slope S , the size of bed material d relative to the depth of flow D , the concentration of total load C_t , the Chezy discharge coefficient C/\sqrt{g} , and the parameter used by Shields $\tau_* / d \Delta \rho g$. Which of these would be most significant depends, at least to some extent, upon the use of the plot.
6. Fig. A shows that as d/δ' increases the existence of two of the regimes of flow are eliminated. When $d/\delta' > 7$ and sediment is moving, the possibility of the first regime (movement without bed waves) is eliminated. When $d/\delta' > 10$, ripples will no longer form and when $d/\delta' > 40$, dunes cannot exist. For the combination of water and sediment having specific gravities of 1.0 and 2.65 respectively, Fig. A shows that these changes in regime are related approximately to the size of sediment—the limiting size for the existence of sediment movement without bed waves, ripples, and dunes being approximately 2 mm, 2.5 mm, and 8 mm respectively. In the transition regime beyond $d/\delta' = 40$ several bed configurations are possible—such as a plane bed and a bed with symmetrical undulations of various sizes. The limiting conditions for the transition regime and antidunes are not established. In fact, they may not be in the realm of practical possibility.

Although the causes of these limits are not certain, they are no doubt related at least in part to the relative influence of viscosity as expressed by d/δ' . However, the limits may also be related to the gravitational forces relative to the forces creating the sand waves, the drag coefficient, the size of the sand waves relative to the size of bed material, and the Froude number. Perhaps both ripples and dunes disappear when the size of the grain roughness approaches the same order

of magnitude as the size of the dunes and ripples.

7. The form of the bed in the transition regime is very unstable and subject to frequent changes with respect to both time and distance. At times two or more types of flow may exist simultaneously side by side within a given reach. The following types of bed roughness and water surface conditions have been observed by experimenters in the transition regime:
 - a. A plane bed with no visible sand waves of any kind and a very smooth water surface. Based upon flume studies, this condition is unstable and is difficult to reproduce, particularly as the length of flume is increased beyond 75 ft.
 - b. An extremely rough pattern of sand waves of the form typical of the dune regime. The water surface above this type of bed is very turbulent and strong boils are visible at the surface.
 - c. Symmetrical standing waves of low amplitude which form and gradually disappear. Unlike antidunes these surface and bed waves have no tendency to migrate upstream or break and shear off. The bed may have symmetrical undulations; a diagonal dune pattern cross-laced like shoe strings; a washed-out dune pattern; sand bars or any combination of these.

The data indicate that the transition regime occurs when $0.6 < F_r < 1.2$. This variation of F_r may account for the instability of this regime.

That is, a small local increase or decrease in depth changes F_r and may change the local conditions from those favorable for one bed configuration to another. In rigid-boundary flow, a marked instability with respect to depth and wave formations also exists at $F_r \approx 1.0$. The instability of this regime, especially with the occurrence of sand bars and two distinctly different types of flow side by side, may be aggravated also by width depth ratios which are too large with respect to slope—that is, three dimensional flow.

8. As d/δ' increases beyond the transition regime, the stationary bed undulations (which are rather similar to sine waves) increase somewhat in size and antidunes, which travel upstream, are formed. For increasing values of d/δ' , the formation of antidunes is related to the size of the bed material, and as both d/δ' and U_*/w are increased the formation of antidunes is a function of the Froude number. As pointed out by Gilbert, the antidunes occur in coarse material of a size even greater than that for which data have already been taken.

Fig. A has considerable usefulness for design. Typical examples of design uses are tabulated as follows:

1. As demonstrated by the data of Lane and Carlson, the horizontal line at $U_*/w = 0.12$ is the limiting condition for which no movement of sediment will occur in a channel. In other words, this line can be used to compute the maximum flow which can be introduced in a given channel before movement of bed material begins. Such a fact can be very useful in the design of stable channels and in the design of channel modifications, such as cutoffs, for natural channels. If desired, a design could be made for somewhat larger values of U_*/w without moving appreciable quantities of sediment.

2. By using the concentration of total load of sediment as the third variable, it is possible (within reasonable limits of accuracy) to design a channel in a given size of bed material to carry a desired load of sediment.
3. A channel can be designed to have the desired regime of sand waves.
4. Where channel stabilization is the problem, and coarse non-cohesive materials are available, the size of the coarser material needed to construct a stable armorcoat for the bed and/or banks can be estimated. The size of material required to stabilize the banks is a special problem, however, because of the influence of gravity and angle of repose on the stability of material placed on an inclined plane.

Although Fig. A offers many possibilities for shedding light on the fundamental mechanics of flow in alluvial channels and on the design of alluvial channels, there are a number of aspects of these problems for which conclusions cannot be drawn without further information. Therefore, further research and study apparently are needed as follows:

1. Additional field data should be plotted on Fig. A to prove whether the conclusions reached using the flume data apply to field conditions.
2. The influence of size distribution of bed material has not yet been included in Fig. A. It is possible this will have considerable influence for some types of flow—especially for small d/δ' -values and for initiation of movement.
3. In an open channel the shear is not distributed uniformly across the channel. Hence the shear velocity U_* as used in Fig. A is simply an average. For certain flow conditions this non-uniform distribution may have appreciable influence upon the particular flow regime which will take place. Furthermore, certain shifting and sorting of the bed and bank material may occur. These factors need special study to obtain additional refinement.
4. There is no doubt some relation between sediment transport by water and sediment transport by wind. Data from wind studies also should be applied to Fig. A.
5. There is considerable evidence that the height of a sand wave is limited not only by the depth of flow but also by other factors such as C_D . These should be investigated.
6. Data should be taken for very fine material to extend those data of Kalinske and Hsia to the extreme limits—the initiation of movement and the formation of antidunes.
7. Studies should be made for various coarse materials to establish the transition and antidune regimes where $d/\delta' > 40$.
8. The magnitude of d/δ' at which ripples will no longer form and dunes will no longer form should be firmly established.

REFERENCES

1. Plate, E. J., "Studies of Sediment Ripple Formation," Thesis (1957) Colorado State University, Fort Collins, Colorado.
2. Kalinske, A. A. and Hsia, C. H., "Study of Transport of Fine Sediments by Flowing Water," Bulletin 29, 1945, University of Iowa, Iowa City.

Lane, B. W. and Carlson, E. J., "Some Factors Affecting the Stability of Canals Constructed in Coarse Granular Material," 1953 Proceedings, Minneapolis International Hydraulics Convention.

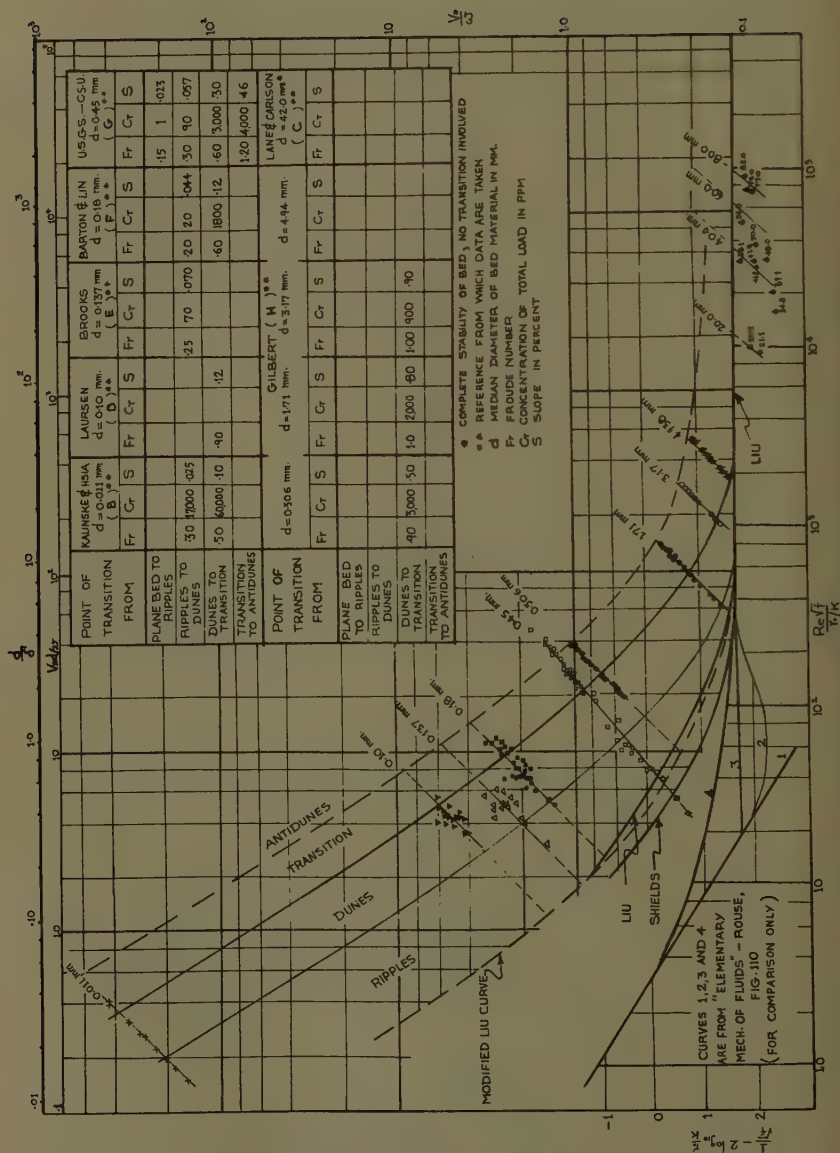
Laursen, E. M., "An Investigation of the Total Sediment Load," Iowa Institute of Hydraulic Research, 1957, State University of Iowa, Iowa City, Iowa.

Brooks, N. H., "Closure to Mechanics of Streams with Movable Beds of Fine Sand," ASCE Proc. Paper 1230, 1957.

Barton, J. R. and Lin, P. L., "A Study of the Sediment Transport in Alluvial Channels," 1955, Dept. of Civil Engineering, Colorado State University, Fort Collins, Colorado.

Unpublished data on Roughness in Alluvial Channels collected by D. B. Simons and E. V. Richardson, U. S. Geological Survey, 1957, Colorado State University, Fort Collins, Colorado.

Gilbert, G. K., "The Transportation of Debris by Running Water," Professional Paper 86, 1914, U. S. Geological Survey.



THE EFFICACY OF FLOOR SILLS UNDER DROWNED HYDRAULIC JUMP^a

Discussion by Mushtaq Ahmad

MUSHTAQ AHMAD.¹—The author has presented results of experiments on low head barrages working under drowned conditions of flow. He has tried to determine the efficiency of the sills against bed erosion by using the vertical velocity distribution as a criterion. The writer had the opportunity of experimenting for the last 15 years on a number of models of low head weirs, barges, and canal falls. In the alluvial plains of Indus, in West Pakistan, hydraulic structures are built on fine erodible sand and scour depths varying from almost zero to as much as 60 feet have been experienced at the works. The writer has always felt and advocated⁽¹⁾ that apart from the length characteristics of hydraulic jump and visual observations of flow conditions, the velocity distribution and comparative studies of scour should be taken as criteria for the proper design of stilling basins and scour prevention devices, especially for those built on highly erodible material.

If the vertical velocity distribution in and below the normal and drowned jump without and with scour control devices are examined (Fig. 1, a, b, and c), it will be noted that:

1. In a normal jump, the shooting flow continues as a live stream under the roller of the jump and then expands in the vertical direction. With normal velocity distribution, such as occurs in a natural stream, the velocities are maximum at or near the surface decreasing towards the bottom, but immediately below the normal jump, the distribution is just the reverse; that is, the maximum velocity filaments are near the bed and the velocity decreases as we move upward.
2. For maximum scour control, the designer must attempt to attain the normal velocity distribution within the confines of the stilling basin by moving the line of maximum velocity upward by means of sills or staggered baffle piers.
3. For a drowned weir or barrage of the type tested by the author, the real hydraulic jump does not form at all; the fast moving jet continues to expand as it goes into the stilling basin, thereby determining the velocity distribution pattern: The efficacy of sills or staggered blocks in the stilling basin in correcting velocity distribution or controlling scour has been found to be very low when the high velocity jet persists on the surface (see Fig. 1c) under conditions of a high drowning ratio.⁽²⁾ No

Proc. Paper 1260, June, 1957, by Ahmed Shukry.

Hydr. Officer, Head of Hydr. Laboratories Irrigation Research Inst., Lahore, Pakistan. Now on a visit to Bureau of Reclamation Laboratories U.S.A. as observer.

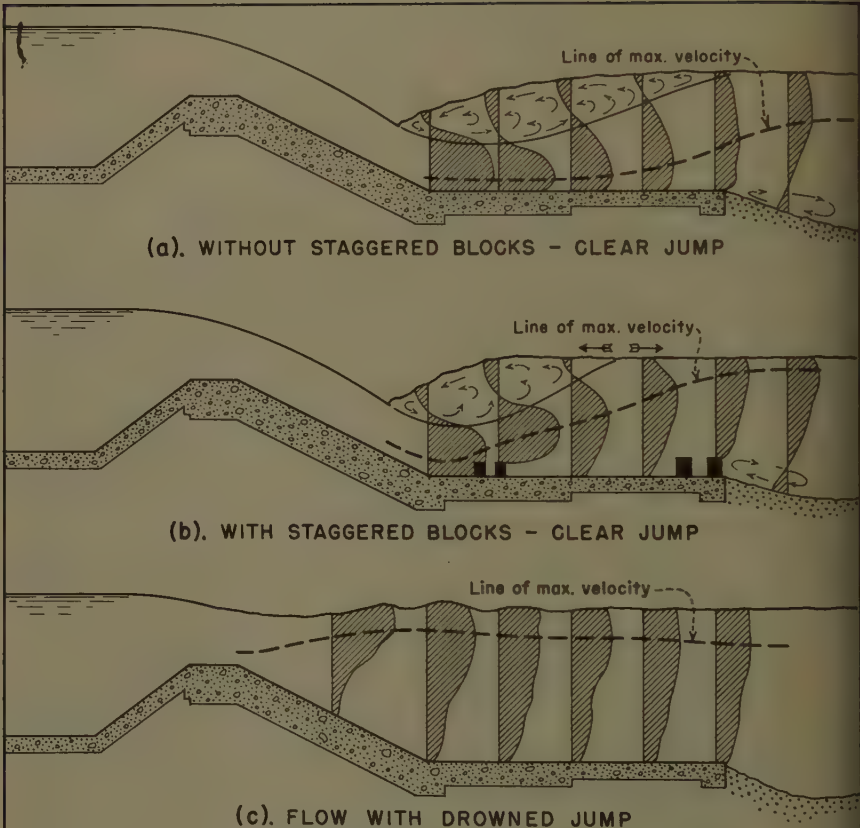


FIG.1. TYPICAL VELOCITY DISTRIBUTION IN STILLING BASIN

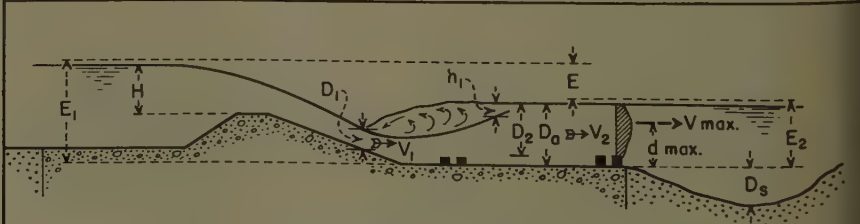


FIG.2. SYMBOL AND NOTATION SKETCH

hard and fast rules can be laid down about the best position of the sill for such conditions of flow, as variation in discharge, drop, downstream depth, etc., can change the length of the surface and bed rollers and thereby change the velocity distribution pattern. Such highly drowned structures shall always have to be tested on a model.

The author has obtained a relation for the bed shear but has not actually used it anywhere in the analysis of his data. $\frac{V_{\max}}{V_o}$, $\frac{V_b}{V_o}$, and L_f/Y_o have been

chosen by the author as dimensionless variables for the study of scour control devices below low head hydraulic structures, but there are many others that enter the problem. A functional relationship of the type given below, with perhaps even more variables added, needs a thorough study.

$$\frac{D_s \cdot g^{1/3}}{9^{2/3}} = f \left(\frac{V_1}{gD_1}, \frac{D(\text{actual})}{D_2}, \frac{L_f}{D_2}, \frac{d_{\max}}{D_2}, \frac{V_s}{V_2}, \frac{V_2 D_2}{\gamma}, \frac{V_{\max}}{V_2}, \frac{V_b}{V_2}, \frac{h_1}{H} \right)$$

where V_s is the fall velocity of the sand particles and other symbols are shown in Fig. 2.

Unfortunately, the author has been working in a region of flow where there is no hydraulic jump formation in the real sense and where there are many difficulties in generalizing results. The writer working on low head weirs and structures with a real hydraulic jump has made comparative studies of the scour depth in terms of $D_s/9^{2/3}$ (where D_s is scour depth below stilling basin floor) against L_f/D_2 (the optimum length of stilling basin), $D(\text{actual})/D_2$ (the optimum depth of the stilling basin, h_1/H (the drowning ratio) and V_b/V_2 , with and without sills and baffle piers or staggered blocks. The conclusions are given below:

1. When a hydraulic jump forms, two rows of staggered rectangular or cubical blocks of height between $1/10$ and $1/7 D_2$ placed at the point where the live stream under the roller starts expanding or at about $2.5 D_2$ below the upper end of the jump gives best results to move the line of maximum velocity upwards without causing hurdling or extra disturbances.⁽³⁾ Another row of staggered blocks of height between $1/5$ to $1/7 D_2$ near the downstream end of the stilling basin helps to create a bed roller and pile up bed material against the toe wall.
2. A length of stilling basin greater than $6 D_2$ does not help in proportional reduction in scour.
3. Scour control devices help to move the line of maximum velocity upward to obtain normal velocity distribution within the confines of the stilling basin of length 4 to $5 D_2$.
4. Two rows of staggered blocks as recommended in (1) above are better scour control devices than continuous sills or streamlined blocks.
5. As the weir becomes more and more drowned, the efficiency of staggered blocks as a device for changing velocity distribution and controlling scour decreases. The staggered blocks have to be made higher and have to be shifted downstream from their normal position in order to make them effective.

Mechanics of Energy Dissipation in the Stilling Basin and Function of Scour Control Devices

The author has discussed the changes in the size of the surface and bed

vortices with the variation in the position of the sill and also the efficiency of different types of sills as corrective measures for velocity distribution and scour control. It is admitted by the writer that the hydraulic jump is the best energy dissipation device. The visualization of the mechanism or physical process of energy dissipation in a jump can explain some of the above and more results obtained by the writer.⁽⁴⁾ It is well known that the energy per pound of flowing water at any point is measured by $\frac{\bar{U}^2}{2g}$ where \bar{U} is the mean

velocity. Apart from this, there is additional energy due to the fluctuating velocity vector and the total kinetic energy is equal to their sum. In a hydraulic jump, at the interface of the high velocity jet and the overlying mass of rolling water, lies a region of high shear stress where the kinetic energy is transformed into heat, partly caused by the shear and partly by the creation of vortices, eddies, and rollers. Each of the eddies formed and shed off from the region of high stress carries a certain amount of rotational energy in addition to its energy of translation. These eddies diffuse into the body of the liquid in the direction of flow. These small rotating masses of fluid in contact with each other cause instantaneous changes in velocity and create surfaces of high local shear; thus, the energy of turbulence is slowly dissipated through viscous action into heat. From the mathematical treatment of energy dissipation for isotropic turbulence, G. I. Taylor⁽⁵⁾ showed that the rate of energy dissipation per unit volume is:

$$\frac{\overline{W}}{\lambda^2} = 15 \mu \frac{\bar{U}^2}{\lambda^2}$$

where \bar{U}^2 is the mean square root of fluctuating velocity component and λ is the scale of turbulence or the average size of the eddies. The equation though not quantitatively applicable to nonisotropic turbulence, gives an important clue on the factors affecting rate of dissipation of kinetic energy. It shows that the rate of turbulent energy dissipation will increase as, λ , the size of the eddies, decreases for a given intensity of turbulence. This means that to get maximum energy dissipation, the high velocity jet should be broken into as small vortices as possible and as early as possible in the stilling basin.

This is what the hydraulic jump does and staggered blocks or sills, etc., are supposed to do. Anyone who has seen the process of scour formation in a fine material below a model in glass flume must have noticed how sediment is picked at irregular intervals and with varying force as vortices of different strength pass over the material. To control scour, therefore, the decay in vorticity should take place within the confines of the stilling basin to such an extent that vortices moving along the bed are not strong enough to lift the same particle in excess of those tending to settle down. To achieve this, it is necessary to push the line of maximum velocity near the surface and to decrease bed velocity.

To summarize, the energy dissipation and scour control measures in a stilling basin would comprise:

- a. Form hydraulic jump
- b. Break the high velocity jet into a large number of as small vortices as possible and as early as possible in the stilling basin to ensure maximum energy dissipation
- c. Use scour control devices in the stilling basin to help obtain the

above objective by moving the line of maximum velocity towards the top and obtaining normal velocity distribution within the stilling basin. The bed velocity and strength of vortices moving near the erodible bed then decreases

The above physical concepts of the phenomenon also incidentally explain that:

1. Staggered blocks are better scour control devices than a continuous sill which gives a continuous roller.
2. Any scour control device in a supercritical jet which causes hurdling but no breaking of the jet into a large number of small individual eddies, is not effective as a scour control device.
3. Streamlined baffle piers or those with the upstream face sloping or stepped are less effective than ones with vertical upstream faces.
4. If the height of the blocks or sills is increased beyond a particular limit, in relation to the depth of flow in the stilling basin, the scour depth increases again because of additional disturbances and vortices.

REFERENCES

Mushtaq Ahmad, "Some Aspects of the Design of Weirs and Canal Falls in Relation to Scour." Proceedings of Punjab Engineering Congress Lahore, Pakistan, 1950.

Uppal and Mushtaq Ahmad, "Some Aspects of Design of Canal Falls," Proceeding, Central Board of Irrigation Technical Report, Annual 1944, India.

Blench, T., Mushtaq Ahmad, and Nazir Ahmad, "Scour in Alluvium Below Falls," Report on the second meeting of IAHR, Stockholm, 1948.

Mushtaq Ahmad, "Hydraulic Design of Spreading Floor Type Canal Falls," Pakistan Journal of Scientific Research, Volume II, No. 3, July 1950.

Taylor, G. I., Proceedings of Royal Society, A 151, 1934.

IS THE WRITING OF FLOOD INSURANCE FEASIBLE?²

Closure by John F. Neville

JOHN F. NEVILLE.¹—Messrs. Laursen and Toch question the writer's conclusion that "insurance against the peril of flood applicable to fixed property cannot successfully be written" by suggesting means by which the amounts to be paid under a so-called insurance program could be reduced or limited. None of these suggestions alters or contradicts the writer's basic conclusion regarding the insurability of the peril of flood. In considering the insurability of the peril of flood, certain fundamentals of insurance should not be overlooked, particularly the requirements that any insurance plan must be self-supporting, that the protection offered must be sufficiently attractive to be feasible, and that enough property owners would in fact buy the type of protection offered to give the insurance company the spread of risk needed to permit the orderly working of the law of averages, and that the plan would not encourage selection against the insurance carrier. Another practical aspect of insurance is that over a long period premiums must necessarily be greater than losses due to the cost of acquiring and servicing business and of maintaining the insurance mechanism, notwithstanding the comment of Messrs. Laursen and Toch that "there is no advantage in having insurance against floods of frequent occurrence since the premiums must necessarily be greater than the 'losses' due to those floods."

The discussion of damage by frequent floods as a factor in annual costs of maintenance of the property presented by Messrs. Laursen and Toch has considerable merit. Where the structure involved is located on the flood plain subject to frequent inundation, it may be feasible to fill in the site or place suitable equipment at a higher elevation so as to eliminate damages from these frequent floods. This has actually been done in certain cases. The actual cost of such changes in location or design of structure may prove to be less than the theoretical average annual flood loss. It would obviously be to the advantage of the owner to incur such additional construction expense rather than to buy flood insurance with its necessary expense loading, even if such insurance were commercially available. Prevention of flood damage appears to be a sounder long-range approach to this problem than to seek to provide indemnity for flood losses by means financially unsound even though theoretically quite attractive.

Proc. Paper 1202, October, 1957, by John F. Neville.
Secretary, American Insurance Assn., New York, N. Y.

ATTENUATION OF SOLITARY WAVES ON A SMOOTH BED^a

Discussion by Yoshiaki Iwasa

YOSHIAKI IWASA.—As a result of errors in the author's calculation for parabolic flow, several equations in this paper should be corrected. As a result of the miscalculation in the shear distribution acting along the boundary for parabolic flow in Part III, the following correction may be expressed.

Location	Error	Correction
right hand of Eq. (18b)	$-\frac{30Y}{5C-2U_0}$	$-\frac{60Y}{5C-2U_0}$
right hand of Eq. (19b)	$+\frac{30}{\sqrt{3}R_c} \dots$	$+\frac{60}{\sqrt{3}R_c} \dots$
right hand of Eq. (20)	$\pm \frac{6}{\sqrt{3}R_c} \dots$	$\pm \frac{12}{\sqrt{3}R_c} \dots$
right hand of Eq. (21)	$\frac{8}{\sqrt{3}R_c}$	$\frac{16}{\sqrt{3}R_c}$
expression in p. 10	$\sigma_c \approx \frac{4}{\sqrt[4]{27}}$	$\sigma_c \approx \frac{4\sqrt{2}}{\sqrt[4]{3}}$
expression in	$\frac{8}{\sqrt{3}R_c}$	$\frac{16}{\sqrt{3}R_c}$

Therefore, the rate of energy dissipation dE/dt for parabolic flow, calculated by the laminar boundary layer thickness, should be divided by $\sqrt{2}$. Finally, the relation (26) of attenuation becomes

$$\lambda_0^{-\frac{1}{4}} \left[1 - 0.8062\lambda_0 - 1.6348\lambda_0^2 - 5.0970\lambda_0^3 - \dots \right] - \lambda_i^{-\frac{1}{4}} \left[1 - 0.8062\lambda_i - 1.6348\lambda_i^2 - 5.0970\lambda_i^3 - \dots \right] = 0.10602R_c^{-\frac{1}{2}} \left(1 + \frac{2y_0}{B} \right) \left(\frac{4}{y_0} \right)$$

us, the ordinates of the theoretical curve in Fig. 2 should be multiplied by and Fig. 3 may be corrected as follows.

Evidently the corrected curves in Fig. 3 indicate the behaviours of attenuation for low solitary waves with more accuracy. However, for high waves, the present first approximation for the influence of side walls will become incomplete.

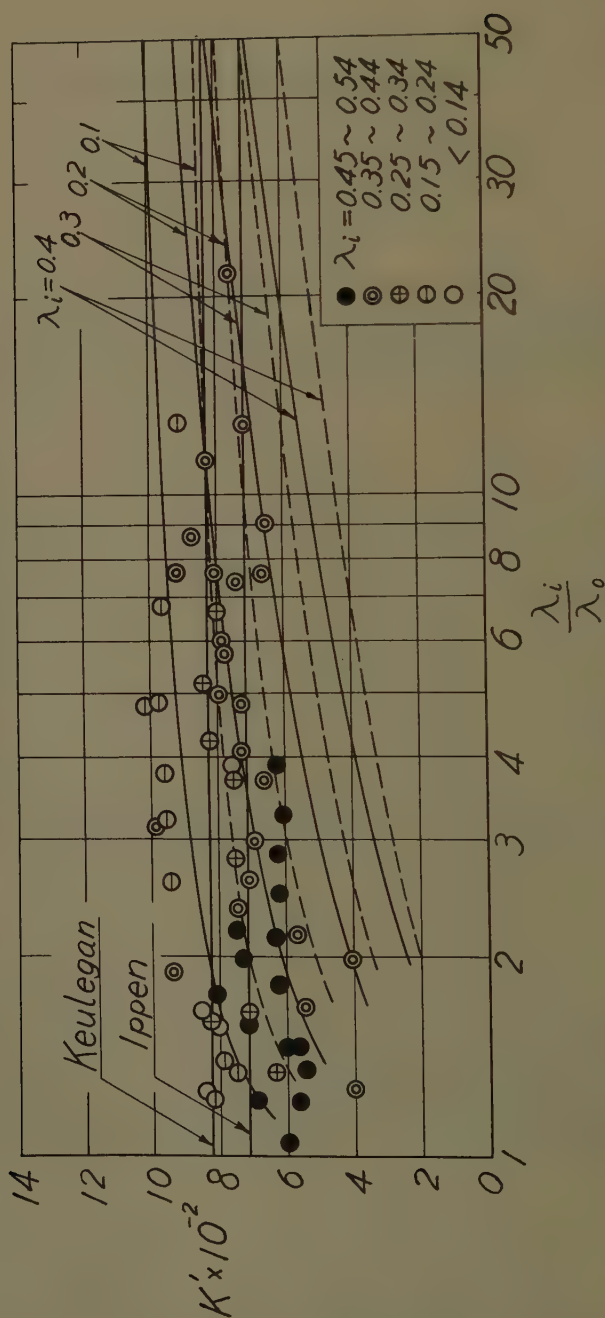


Fig. 3 Relation between K' and λ_i/λ_0

STUDY OF BUCKET-TYPE ENERGY DISSIPATOR CHARACTERISTICS

Discussion by Gale B. Dougherty

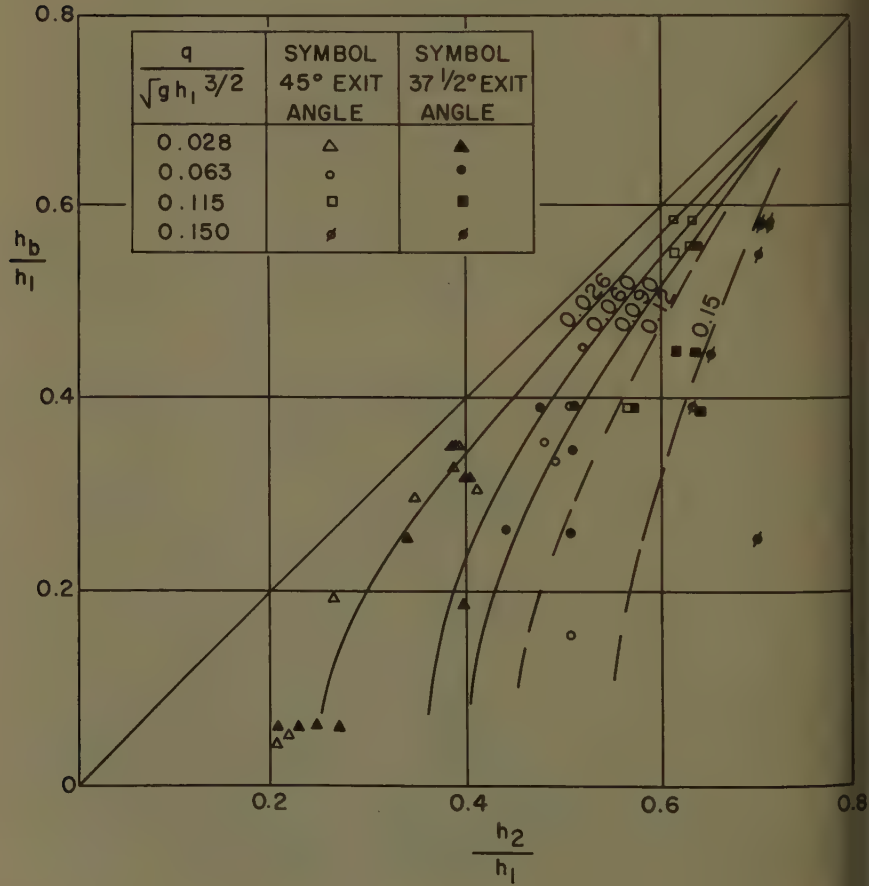
GALE B. DOUGHERTY,¹ A.M. ASCE.—The authors and the sponsoring firm are due the gratitude of the profession for making these data available for design use. Some recent studies in connection with the design of Weiss Dam for the Alabama Power Company provide data which confirm some of the results obtained by the authors. Several different buckets were tested in connection with a 1:48 scale standard crest spillway model. These tests were made in the Fluid Mechanics Laboratory of the University of Alabama and sponsored by the Alabama Power Company. The model consisted of a center bay flanked by two half bays. The bay width was 40 feet and the piers were 8 feet thick with ogive noses. The crest was 45 feet above the bucket invert. All tests were made with an upstream energy grade line 77 feet above the bucket invert. Discharges were controlled by radial gates except for the largest which was free discharge. The erosion bed consisted of 1/4 to 3/8 inch gravel and for most tests was placed 5 feet above the bucket invert. The exit angle buckets tested had radii of 15, 25 and 40 feet. One 40-foot radius bucket had a tangent lip added to place the end sill 10 feet above the bucket invert.

Fig. 1 shows a comparison of the data obtained for the Weiss Dam to the authors' curves (Fig. 3 of the original paper) for height of bucket roller. The data were taken from plotted water surface profiles after the erosion had stabilized. The correlation, while not conclusive, is indicative. No check was obtained for the surge height relationship. As the discharge increases, the plotted points fall below and to the right of the curves. This is attributed to the effect of the flow over the crest. It was noted that the surface of the bucket roller was not horizontal, but was depressed on the upstream end. This resulted in decreasing the value h_b .

The authors indicate that a 45° exit angle was used because others had found it to be the most effective under a variety of service conditions. At the University of Alabama, a 25-foot radius bucket with a 37-1/2° angle was tested with lip elevations, 5, 7.3 and 10 feet above the bucket invert. The results of these tests indicated that in general the erosion results were comparable to those for 45° exit angles. The addition of a tangent section to increase the elevation of the bucket lip had a beneficial effect for the 37-1/2° exit angle bucket. For intermediate discharges, the 37-1/2° exit angle bucket had better erosion characteristics than the 45° bucket for the same lip elevation.

The authors' conclusion with regards to placement of the invert with relation to the channel is perhaps a good starting point, but should be used with

CHARACTERISTICS OF BUCKET-TYPE ENERGY DISSIPATORS WITH ENTRANCE ANGLES OF 45°



caution. From Fig. 2 (authors') it appears that the conclusion was based on having a turbulence chamber downstream of the bucket with a stream bed at a significant height above the bucket invert. A proper evaluation of the erosion patterns by the reader would require some information as to the size of material used in the study and the model scale. With a horizontal bed, in the University of Alabama tests, erosion to a depth lower than the bucket invert elevation occurred in the relatively large material. A smaller size material in the erosion bed would have shown greater depths of erosion. Model studies can only give qualitative indications of erosion and erosive tendencies. The stable roller formed under the jet may not cause much erosion in the model, but it provides ample opportunity for ball mill action. This could produce a deep scour hole in any prototype stream bed material if given sufficient time.

With regards to the surge height, the authors suggest that this be used as a guide in determining the top elevation of training or spray walls. This implies that these walls will be above the surge height. The question is, must they be high? A designer who has no recourse to model studies must arbitrarily, in order to be conservative, answer, yes. The writer does not remember seeing any experimental data that proved that the training walls had to be above the surge height. Model tests should be used to determine the required training wall height with a definite possibility that the walls could be lowered with a saving in construction cost. The writer knows of model tests in a government laboratory which showed that the training walls for the project could be reduced to one-third of the maximum tailwater depth without adverse erosive action and the project was so constructed. While this was a baffle apron and not a bucket, it is the writer's conviction that similar results could be justified with the bucket dissipator.

SYSTEMATIC CHANGES IN THE BEDS OF ALLUVIAL RIVERS²

Discussion by T. Blench

T. BLENCH,¹ M. ASCE.—This set of observations of dunes in a sand-bed river is a valuable new addition to the collection of quantitative field studies of rivers (e.g. Refs. 1-9) that has been growing in the last few years. With the quantitative facts of canal and river regime now established from field observations, in dynamically satisfying form,⁽¹⁰⁾ the next step in field work was to be the collection and analysis of quantitative data on fluctuations about regime and on the details of transport of which bed-wave movement is a major demonstration; the laboratory, though of specialised value, can hardly provide more than the bottom point on an adequate correlation of natural phenomena, while theoretical speculations based on rigid boundary occurrences seem unlikely to be of more than academic interest till observed facts are established.

The writer initiated a set of similar observations in 1950 but was not in a position to have them published; a library copy exists.⁽¹¹⁾ The main object of the observations was to provide a set of occurrences to be copied by a model if the model was to be useful for predicting rates of scour. Daily sonic soundings were made on a couple of miles of navigation path for a dozen days before and after a large flood of about 400,000 cusecs peak with a tidal addition of the order of $\pm 100,000$ cusecs. The river bed was sand, and the average bed-load charge was of the order of a couple of hundred thousandths by weight. At the low discharges of the observations bed waves were small and travelled in groups at some 20 feet a day; at peak flood they had grown to 15 feet high, and 500 feet long, travelling at 250 feet per day; they decayed very much according to the way they grew. Plots of wave number per thousand feet against discharge at three locations in the run gave good and similar correlations. The results would hardly be typical of a nontidal river, since the water level was controlled closely by proximity to the ocean; with the nontidal river the water surface would vary with discharge and the phenomena would probably be less accentuated.

In company with the authors the writer hopes their example will interest organizations with the facilities in conducting further observations. He suggests that quantitative science would benefit if observations aimed at correlating bed-wave dimensions and speed with fluid discharge, bed-load constitution (median and dispersion about the median), and bed-load charge. A proper set of observations would require a full description and record of relevant river properties, viz. sectional form, slope, meander pattern in the zone of slope measurement, water levels relative to the sections, mechanical analyses of bed material, suspended load observations with load analyses, temperature of

water, and duration curve of discharge (i.e. frequency with which various discharges exceeded on long term); calculation from these data would give an approximate idea of bed-load charge, which is not measureable but is highly relevant to bed-wave form.

Generally the writer finds himself in agreement with the opinions in the paper, and able to endorse its facts from his own experiences.

REFERENCES

1. Leopold, L. B. and Maddocks, T., Jun. "The hydraulic geometry of stream channels and some physiographic implications." Prof. Paper. U.S.G.S. 252, 1953.
2. Wolman, M. G. "The natural channel of Brandywine Creek, Pennsylvania. Prof. Paper. U.S.G.S. 271. 1955.
3. Leopold, L. B. and Miller, J. P. "Ephemeral streams. Hydraulic factors and their relation to the drainage net." Prof. Paper. U.S.G.S. 282-A. 1956.
4. Leopold, L. B. and Wolman, M. G. "River Channel Patterns, braided meandering and straight." Prof. Paper. U.S.G.S. 282-B. 1957.
5. Wolman, M. G. and Leopold, L. B. "River flood plains. Some observations on their formation." Prof. Paper. U.S.G.S. 282-C. 1957.
6. Leopold, L. B. and Wolman, M. G. "Floods in relation to the river channel." Publication 42 of the International Association of Hydrology. 1956.
7. Sundborg, Ake. "The river Klaralven. A study of fluvial processes." University of Uppsala (Sweden) Dept. of Geography. Ser. A. No. 115. 1956.
8. Shulits, Sam. "Graphical analysis of trend profile of a shortened section of river." Trans. American Geophysical Union. Vol. 36, Number 5. August 1955.
9. Blench, T. "Regime theory equations applied to a tidal river estuary." Proc. International Association for Hydraulic Research. Minneapolis Convention. 1953.
10. Blench, T. "Regime behaviour of canals and rivers." Butterworths Scientific Publications. London. 1957. (available Butterworths (Canada), Toronto).
11. Pretious, E. S. and Blench, T. "Final report on special observations at Ladner Reach during 1950 freshet." Report to National Research Council, Ottawa, available from National Research Council Library, or from Civil Engineering Department, University of British Columbia, Vancouver, Canada.

SYNTHETIC STORM PATTERN FOR DRAINAGE DESIGN^a

Discussion by M. B. McPherson

M. B. McPHERSON,¹ A.M. ASCE.—The Water Department of the City of Philadelphia is currently investigating the suitability of the hydrograph method for the design of some extensive storm sewer improvements. This investigation is relatively modest compared with the efforts expended and the results obtained by Chicago. The authors are to be commended for their clear exposition of a new approach to a very controversial area of hydrology. The writer holds several major reservations insofar as the efficacy of the described synthetic storm is concerned. However, most of this discussion will be restricted to a modification in the use of the data set forth and a comparison with similar modified data for Philadelphia and Baltimore. A comparison with Baltimore data is desirable in view of the extensive overall hydrologic study which is in progress there.⁽¹⁾

With regard to intensity—duration—frequency curves, the U. S. Weather Bureau data⁽²⁾ provides a common basis of comparison between the three cities. Two—and five-year frequency (or return period) values of intensity for sample durations are set forth in Table D-I. The values listed were taken from 3x enlargements of the U.S.W.B. graphs, by scaling, and are accurate to within about ± 0.05 inches per hour. The data from which the curves were obtained ("maximum value for each year") covered the following periods:

Baltimore	- 1903 to 1951, incl.
Chicago	- 1905 - 1912 and 1926-1951, incl.
Philadelphia	- 1903 to 1951, incl.

The Eltinge and Towne equation was adopted "about 1944" by Chicago according to reference 4 of the authors. Independently determined curves were obtained by Chow⁽³⁾ with Chicago Weather Bureau data for 1913 to 1947 inclusive; the values he obtained on the basis of annual maximums have also been listed in Table D-I. For a city without a first-order station, the comparable approximate values taken from Yarnell's⁽⁴⁾ graphs may be of interest for available records to and including 1933, for most of the U. S.). Appraisal of means of the curves given by Hathaway,⁽⁵⁾ based upon the one-hour graphs of Yarnell, would yield similar results. The Philadelphia and Chicago values are quite similar. The Baltimore intensities are somewhat higher. There is no significant difference between the Weather Bureau, Eltinge and Towne, and the values for Chicago. The equations given by the authors could be used for the Philadelphia U.S.W.B. 5-year curve.

The authors have used 81 station-rainfalls in their Table I, for 27 storms.

Proc. Paper 1332, August, 1957, by Clint J. Keifer and Henry Hsien Chu.
Research Engr., Philadelphia Water Dept., Philadelphia, Pa.

The intensities for the various durations represent a wide range of frequencies. In an effort to segregate the data, six storms for Station 14 were selected which have 15-minute intensities closest to the 5-year values: June 20-21, 1937; June 12, 1944; August 9, 1946; July 3, 1954; August 18, 1954; October 10, 1954. In Table D-II are given the computed values of "r" for the four durations of Table I, and for only the 15-, 30-, and 60-minute durations, on the basis of both antecedent time and antecedent mass. (The reason for excluding the 120-minute will be given later.) The selected six-storm group values of "r", for all four durations, are not appreciably different from those computed by the authors for all 81 station-rains. The comparative values, with and without the 120-minute duration are also reasonably consistent, considering the type and extent of the samples.

As stated previously, the six storms for Station 14 were selected as representing most closely the 15-minute, 5-year frequency. In Table D-III are given the approximate frequencies of all four durations (based on the U.S.W.B. curves for Chicago). As would be expected, no single storm has a consistent frequency for more than two durations.

Intensity-duration-frequency curves are derived for each duration by taking maximum excessive rainfalls, regardless of where the critical duration occurs in each record, and arranging intensities by rank for statistical analysis. In this way the various durations of a frequency curve represent a series of unrelated values from a variety of storms; a frequency curve thus gives intensities on the average, which are for a rarer occurrence than indicated. The use of frequency-curve data for drainage design, by any method, thus becomes highly empirical. The method of transposition of actual storms, usually employed for larger watersheds, would be preferable. However, two restrictions, or reservations, confound usage of that method: (1) the difficulty in arriving at criteria for selecting a "typical" or design storm based on either infrequency, pattern or resulting discharge, and (2) even if an actual storm is used, point rainfall remains the source of data and there would be no particular correlation with the design area in the transposition. If the authors cannot adapt the transposition technique to Chicago, with the unique availability of seventeen private automatic recording rainfall gages, the prospect appears rather poor for other cities. In any event, the attempt by the authors to divorce themselves as much as possible from the illogical facets of the so-called "rational" method is indeed noteworthy.

In Table D-II the antecedence values of "r" for Chicago are similar with regard to both time and mass of rainfall. The authors stated that the Chicago results "might not be suitable in other localities." The authors have used data which is not publicly available. Also, they did not define the basis for selecting the antecedent mass. It is assumed that "excessive rainfall" as used follows the U.S.W.B. definition, of a depth in inches equal to or greater than the sum of one one-hundredth of the duration in minutes plus two-hundredths of an inch. All U.S.W.B. data published since 1936 have included the maximums for given durations but not the actual record of excessive rates with respect to time, as was the practice prior to 1936.

In order that data for the three cities could be equitably compared, the records for 1896 to 1935 were searched for each of the three cities, in the corresponding issues of the "Annual Report of the Chief of the W.B." Nine storms for each city were selected on the following arbitrary bases: (1) 15-minute duration precipitations nearest the 5-year U.S.W.B. value, and (2) a

Report tabulation including at least 30 minutes of rainfall. Only 15, 30 and 60-minute durations were considered; there are very few storm records which extend as long as 120-minutes. The writer could see no practical value in extending the record by the "extended duration" procedure. The data for these storms are given in Tables D-IV-B, D-IV-C and D-IV-P. The calculated values of the advance proportion "r" for these storms are as follows:

<u>City</u>	<u>By Peak 5-Min.</u>	<u>By Antec. Mass</u>
Baltimore	0.399	Approx. 0.071
Chicago	0.294	0.546
Philadelphia	0.494	0.667

The 0.294 for Chicago based on the peak 5-minutes compares with the corresponding three duration value of 0.299 in Table D-II, but the 0.546 based on the antecedent mass far exceeds all values given in Table D-II. The figures for Baltimore show the greatest disparity. It was noticed in searching the Baltimore data that large antecedent masses occurred with storms of higher frequency (and lesser intensities). The Baltimore value of 0.071 is approximate since a modified Eq. (13) was used. Philadelphia would appear to have an "r" of about one-half; the high value of 0.667 was influenced substantially by storm P-7. The approximate frequency in years for each duration of each storm using U.S.W.B. curves is given in Table D-V. The usual inconsistency in frequency values for different durations, as noted previously in Table D-III, is apparent.

From the above data there does not appear to be any outright correlation between an "r" calculated on the basis of an antecedent time and on the basis of an antecedent mass. In the opinion of the writer, the values 0.386 and 0.376 of the paper are characteristics of the specific sample used and their nearness in magnitude should be considered fortuitous. In the case of Baltimore, there was no conceivable combination of storms that would have raised the antecedent mass value of "r" much above one-tenth. Therefore, the premise of the authors is correct: the Chicago values are definitely "not suitable for other localities." Although the writer has used the method of the authors in determining the value of "r" from mass antecedent rainfall, he can find no basis or reason given by the authors to justify the assumption that the antecedent portion of their synthetic hyetograph should have the same trend or shape as the part after the peak.

The authors have advised the writer, by correspondence, that they are developing a program for storm sewer runoff analysis by means of a digital computer. Although evaluation and allocation of the factors involved in the overland flow method of surface routing would become much more complicated, why could not actual storms be used? Programming would become more involved, but the basic program would remain unchanged. Using the same storm pattern for both branch sewers and main sewers seems to be somewhat inconsistent. Perhaps design could be based upon the routing of several moderately infrequent storm patterns, in which different storms might well be critical for different sewers in the system. It is recognized that a basis for selecting the proper storms presents a formidable stumbling block. However, the method of storm evaluation proposed by the authors retains too many of the fallacies and empiricisms inherent in the "rational" method to recommend its principle for general use by others. The pioneering effort of

the authors is not to be underrated; perhaps no better solution will be achieved for some time to come.

The value 0.410 on p. 1332-12 should read 0.416.

The writer was capably assisted in this study by Robert E. Wenzinger, Drexel Institute of Technology, Student Chapter ASCE, and recent cooperative program employee of the Philadelphia Water Department.

REFERENCES

1. Bock, Paul, "Progress Report on the Storm Drainage Research Project," The Johns Hopkins University, Department of Sanitary Engineering and Water Resources, June, 1956.
2. "Rainfall Intensity—Duration—Frequency Curves," U. S. Department of Commerce, Weather Bureau, Technical Paper No. 25, December, 1955.
3. Ven Te Chow, "Frequency Analysis of Hydrologic Data with Special Application to Rainfall Intensities," University of Illinois Eng. Exp. Sta. Bulletin No. 414, p. 48, July, 1953.
4. Yarnell, David L., "Rainfall Intensity—Frequency Data," U. S. Dept. of Agriculture Misc. Public. No. 204, August, 1935.
5. "Military Airfields; A Symposium," ASCE Trans., Vol. 110, 1945, pp. 699-703. (The same graphs and curves are given by Elwyn E. Seelye, "Data Book for Civil Engineers—Design," Vol. One, Second Edition, John Wiley and Sons, 1951).

TABLE D-I: Comparison of Frequency Data.

(Tabulated Figures are Intensity in Inches Per Hour).

City and Data Source	DURATION - MINUTES			
	15	30	60	120
<u>For Five-Year Return Period:</u>				
Baltimore: Weather Bureau	4.70	3.20	1.95	1.15
Yarnell	4.2	3.0	1.9	1.1
Chicago: Eltinge & Towne	4.00	2.78	1.77	1.05
Ven Te Chow	4.04	2.82	1.81	0.99
Weather Bureau	4.05	2.80	1.80	1.10
Yarnell	3.9	2.6	1.7	1.0
Philadelphia: Weather Bureau	3.95	2.70	1.70	1.00
Yarnell	4.2	2.8	1.9	1.1
<u>For Two-Year Return Period:</u>				
Baltimore: Weather Bureau	3.45	2.30	1.42	0.83
Yarnell	3.5	2.4	1.5	0.8
Chicago: Ven Te Chow	3.12	2.12	1.29	0.71
Weather Bureau	3.10	2.15	1.35	0.80
Yarnell	3.3	2.1	1.3	0.7
Philadelphia: Weather Bureau	3.05	2.05	1.30	0.75
Yarnell	3.5	2.3	1.4	0.8

TABLE D-II: Chicago Data - Paper 1332, Table I,
Comparison of Values of "r".

	By Peak 5-Min.	By Antec. Mass
81 Sta.-rains; 15, 30, 60, 120-min.	0.376	0.386
81 Sta.-rains; 15, 30, 60-min.	0.387	0.350
Sta. 14, Six storms; 15, 30, 60, 120-min.	0.356	0.251
Sta. 14, Six storms; 15, 30, 60-min.	0.299	0.254

TABLE D-III: Chicago Data - Paper 1332, Table I; Six Storms, Station 14.

Equivalent Return Period, or Frequency, Years

15-Min.		30-Min.		60-Min.		120-Min.	
Max. Mass	Freq.	Max. Mass	Freq.	Max. Mass	Freq.	Max. Mass	Freq.
1.14	10.0	1.56	8.3	1.83	5.0	1.92	3.1
0.97	4.1	1.00	1.7	1.04	1.2	1.43	1.4
0.92	3.4	1.22	3.0	1.35	2.0	--	--
0.91	3.3	0.96	1.6	1.02	1.2	--	--
0.90	3.1	1.60	9.8	2.49	35.	2.66	14.
0.90	3.1	1.17	2.6	1.25	1.7	1.54	1.7

TABLE D-IV-B: Nine Approximately 5-year Return Period Storms - Baltimore -
U.S. W.B. Records 1896 to 1935 Inclusive.

D A T E	15-MIN. DURATION			30-MIN. DURATION			60-MIN. DURATION			DURAT. OF EXCESS RATE
	Ante-	Peak	Five Min.	Ante-	Peak	Five Min.	Ante-	Peak	Five Min.	
	Max.	cedent		Max.	cedent		Max.	cedent		
	Mass	Mass		Mass	Mass		Mass	Mass		
B-1 7/18/07	1.43	0.61	2	2.20	0.01	4	--	--	--	45 min.
B-2 7/25/01	1.18	0	2	1.85	0	2	--	--	--	35
B-3 8/6/19	1.04	0.04	3	1.30	0.04	3	--	--	--	27
B-4 7/7/05	1.03	0.21	2	1.28	0.14	3	1.41	0.01	5	41
B-5 8/27/02	1.02	0.10	2	1.24	0	3	--	--	--	25
B-6 8/12/34	1.01	0.09	2	1.05	0.09	2	--	--	--	12
B-7 9/1/10	0.98	0.01	2	1.39	0.01	2	--	--	--	36
B-8 6/13/15	0.94	0.01	3	1.25	0.01	3	--	--	--	38
B-9 8/25/05	0.91	0.01	2	1.20	0.01	2	--	--	--	25

TABLE D-IV-C: Nine Approximately 5-Yr. Return Period Storms - Chicago -
U.S. W.B. Records 1896 to 1935 Inclusive

A T E	15-MIN. DURATION			30-MIN. DURATION			60-MIN. DURATION			DURAT. OF EXCESS RATE
	Ante- Peak			Ante- Peak			Ante- Peak			
	Max. cedent Mass	Five Mass	Min.	Max. cedent Mass	Five Mass	Min.	Max. cedent Mass	Five Mass	Min.	
C-1 25/96	1.17	0.18	2	1.30	0.10	3	--	--	--	17 min.
C-2 20/28	1.16	0.23	1	1.70	0.23	2	2.30	0.01	2	60
C-3 7/21	1.10	0	1	2.03	0	1	--	--	--	34
C-4 15/06	0.97	0.23	2	1.26	0.01	4	--	--	--	30
C-5 14/09	0.90	2.00	2	1.20	1.79	4	1.53	1.79	4	62
C-6 13/26	0.87	0.82	3	1.55	0.40	5	--	--	--	40
C-7 2/35	0.87	0.03	1	1.05	0.03	1	1.07	0.03	1	24
C-8 18/35	0.86	0.11	2	0.96	0.03	2	--	--	--	19
C-9 22/24	0.81	0.25	2	1.02	0.25	2	1.44	0.01	6	60

TABLE D-IV-P: Nine Approximately 5-Yr. Return Period Storms - Philadelphia -
U.S. W.B. Records 1896 to 1935 Inclusive.

D A T E	15-MIN. DURATION			30-MIN. DURATION			60-MIN. DURATION			DURAT. OF EXCESS RATE			
	Ante- Peak		Five Min.	Ante- Peak		Five Min.	Ante- Peak		Five Min.				
	Max. cedent			Max. cedent			Max. cedent						
	Mass	Mass		Mass	Mass		Mass	Mass			Mass	Mass	
P-1 7/17/11	1.24	0.20	2	1.65	0.01	3	--	--	--	32 min.			
P-2 8/16/17	1.09	0.80	3	2.07	0.09	5	--	--	--	31			
P-3 9/14/04	1.04	1.29	3	1.63	0.70	6	2.26	0.30	8	62			
P-4 6/26/30	1.02	0.04	1	1.41	0.04	1	2.01	0.04	1	75			
P-5 8/10/99	0.99	0.40	2	1.48	0.00	4	1.97	0.00	4	55			
P-6 10/4-5/06	0.89	1.42	2	1.44	0.94	1	--	--	--	37			
P-7 9/15-16/00	0.87	2.69	3	1.51	2.29	5	2.23	1.57	11	85			
P-8 9/6/26	0.84	0.01	2	1.16	0.01	2	--	--	--	34			
P-9 6/19/28	0.83	0.27	3	1.20	0.02	5	--	--	--	31			

TABLE D-V: Equivalent Return Period, or Frequency, Storms Given in
Tables D-IV-B,-C, & -P.

DURATION						
15 - minutes		30 - minutes		60 - minutes		
Max.Mass	Frequency	Max.Mass	Frequency	Max.Mass	Frequency	
Baltimore -						
1.43	12.	2.20	20.	- -	- -	
1.18	5.2	1.85	9.	- -	- -	
1.04	3.4	1.30	2.7	- -	- -	
1.03	3.3	1.28	2.6	1.41	2.0	
1.02	3.2	1.24	2.4	- -	- -	
1.01	3.1	1.05	1.7	- -	- -	
0.98	2.8	1.39	3.2	- -	- -	
0.94	2.5	1.25	2.4	- -	- -	
0.91	2.3	1.20	2.3	- -	- -	
Chicago -						
1.17	11.	1.30	3.7	- -	- -	
1.16	11.	1.70	13.	2.30	18.	
1.10	8.	2.03	45.	- -	- -	
0.97	4.1	1.26	3.3	- -	- -	
0.90	3.1	1.20	2.8	1.53	2.8	
0.87	2.7	1.55	8.	- -	- -	
0.87	2.7	1.05	1.9	1.07	1.3	
0.86	2.6	0.96	1.6	- -	- -	
0.81	2.2	1.02	1.8	1.44	2.3	
Philadelphia -						
1.24	18.	1.65	14.	- -	- -	
1.09	9.	2.07	60.	- -	- -	
1.04	7.	1.63	13.	2.26	20.	
1.02	6	1.41	6.	2.01	10.	
0.99	5.0	1.48	8.	1.97	10.	
0.89	3.2	1.44	7.	- -	- -	
0.87	2.9	1.51	9.	2.23	20.	
0.84	2.6	1.16	2.9	- -	- -	
0.83	2.5	1.20	3.2	- -	- -	

CHARACTERISTICS OF FLOW OVER TERMINAL WEIRS AND SILLS^a

Discussion by F. V. A. Engel

F. V. A. ENGEL.¹—Both authors have advanced a very interesting thesis, i.e., that under certain circumstances, a sharp-crested weir will not operate as such, but behaves like a free overfall. For very large area ratios, exceeding say 0.95, the critical depth which is normally a special feature of Venturi or broad-crested weirs, will occur upstream of the sharp-crested weir itself. The observed phenomenon deviates considerably from the usual conception of discharge characteristics over sharp-crested weirs. The authors do not appear to have explained, under what conditions and for what particular reasons this occurs. There may be several reasons. In the following an attempt will be made to put forward an explanation, and the authors are requested to comment on these remarks. This is especially necessary, since the diagrams presented do not permit the arguments advanced to be checked by the writer. It is assumed that the authors have complete sets of tables covering their experimental investigations which would be available to amplify their interesting paper.

Fig. 3 shows that a decrease in the discharge coefficient may occur for area ratios larger than 0.8, which corresponds to a h/w value of 4. Both the Rehbock and von Mises relationship indicate a discharge coefficient characteristic asymptotically approaching infinity. As the rate of flow is finite, the actual discharge coefficient (excluding the velocity of approach factor) should therefore approach zero. Both authorities, however, assume a basic and constant discharge coefficient of 0.605 and 0.611 respectively. The second term in Eq. (8) represents in general the velocity of approach. As previously mentioned, there are reasons why the discharge coefficient of 0.605 should actually decrease rapidly when approaching an area ratio of unity. This may explain the deviation in the discharge coefficient characteristic, as shown in Fig. 3, up to a value of 10 for h/w .

Besides the marked decrease in the discharge coefficient other features may account for the change from the ordinary weir type flow to the "free overfall" characteristic. From the description of the experimental procedure one may conclude that, for the very low weir crests, a considerable boundary or displacement layer may occur. This may affect the geometry of the sharp-crested weir, which projects only slightly over the channel invert so creating artificial nozzle entrance conditions, or again a sharp-crested weir may degenerate into a broad-crested one. However, this feature could only be established by a very careful investigation of the surface of the water level approaching the weir over a considerable length. The profiles given by the

authors in their paper are unfortunately not sufficiently detailed in this respect. Furthermore, boundary layer effects may explain the considerable differences in test results in the two independent investigations by each of the authors, as illustrated in Fig. 3.

The writer² has recently established another criterion of weir flow assuming a constant basic discharge coefficient, as most authorities do, in separating the velocity of approach characteristic as a specific factor. This criterion was developed with analogous arguments comparing the broad-crested or Venturi weir with the sharp-crested weir. In both the former mentioned weir types, critical depth ratios related to the area ratio can be established mathematically. For sharp-crested weirs, the ratio of the depth over the weir crest to the upstream depth over the weir crest, should lie approximately between 0.87 and unity for the complete range of area ratios from zero to unity. This means that the depth over the weir crest is greater than the critical depth.

From the authors' investigations for very large area ratios, and particularly when approaching unity, the depth at the crest will be considerably less than the critical depth. This would appear to contradict the criterion of a sharp-crested weir mentioned above. The question arises, at what area ratio does this change from one condition to the other occur? What is the area ratio for which the sharp-crested weir ceases to act as such and conforms to the performance of a free overfall (or broad-crested weir)?

A diagram presenting the depth ratio as a function of the area ratio $h/(h + w)$ may reveal characteristic features of weir flow dynamics. For instance, some discontinuity may exist. The type of flow may change abruptly from ordinary weir flow where the critical section is situated downstream of the weir crest, to the type of flow with distinct free overfall characteristics. This results in the critical depth being reached by the water surface well upstream of the weir crest. If a boundary layer exists there may be considerable scale effects and the change from one type of flow to the other may not be related to a well defined area ratio. The authors could enhance the value of their important results if they would prepare from the test results of their investigation a diagram based on the outlines mentioned above.

2. Engel, F. V. A. and Stainsby, W., "Velocity-of-approach factors in unified weir equations." Paper No. 6247 to be published in the February 1958 issue "Journ. Inst. Civil Engineers" (London).

100 FREQUENCY CURVES OF NORTH AMERICAN RIVERS^a

Discussion by H. C. Riggs

H. C. RIGGS,¹ A.M. ASCE.—Mr. Kuiper's study of sampling from a log-normal population of 1000 items emphasizes the possible variation of a sample from the population in slope and position as well as in shape. Frequency curves of annual floods on different streams (after adjustment for differences in basin characteristics) would not be expected to vary among themselves by chance alone as greatly as random samples because of a certain amount of dependence associated with their being based on data collected within the last 60 years or so. If chance variation among a group of frequency curves could be removed, the adjusted curves would be more representative of the period of time spanned by the combined records. They would not necessarily be closer to their "true" positions. On the other hand they might represent conditions in the next 60 years as well as the "true" curves.

Many attempts to define a frequency distribution which is generally applicable to annual flood data have been made. The author has demonstrated that the log-normal is an approximation to flood records on 100 American rivers. Most of these rivers are large. Drainage basins of large streams usually comprise sub-basins which differ greatly in flood-producing characteristics. Integration of these effects and attenuation by channel storage tend to result in a certain uniformity between flood characteristics of large streams. Hence the shapes of frequency curves of large streams might be expected to vary less than the shapes of a group of frequency curves of small streams. Many flood-frequency curves of small rivers are curved sharply upward (on paper designed for the theory of extreme values). It has not been determined whether this is a characteristic of small rivers or a function of the relatively short period of record. Few records of 40 years or more are available on small streams.

Certain streams produce floods in response to more than one cause. Some western streams have snow-melt floods in the spring and rain floods at other times of the year. Similarly, floods near the East Coast may be caused by frontal storms or by hurricanes. If the floods resulting from these unlike causes actually belong to different distributions then the distribution of annual floods is unlike either one. Therefore, it would seem desirable to examine the physical and meteorological characteristics of drainage basins and be assured of their reasonable similarity before forcing their frequency curves into statistical agreement.

The writer agrees with the author's statement "--- that frequency curves of maximum annual flood peaks for one particular river station can be drawn

Proc. Paper 1395, October, 1957, by E. Kuiper.
Hydr. Engr., U. S. Geological Survey, Washington 25, D. C.

with greater accuracy when due attention is paid to other frequency curves on the same or comparable streams." If the individual frequency curves are drawn as straight lines then differences in the slopes of those lines are found. These differences result from variation in basin characteristics and from chance variation in weather. If the variation due to basin characteristics were removed, the adjusted slopes could be averaged to remove the chance weather differences. For this approach, selection and measurement of significant basin parameters would be a first requirement.

The author selected 5 parameters and, by a priori reasoning, determined the general effect of each. It has been pointed out in this discussion that non-uniformity in drainage basins is the rule rather than the exception. Such non-uniformity may tend to make the effects of certain parameters compensating and to make others difficult to measure. A parameter describing the integrated effect of soil types in a drainage basin of several thousand square miles would be so difficult to determine that it would be of little practical use.

Nevertheless one must begin with a certain concept, test it with actual data, and accept, reject, or modify it as required. Differences not readily described quantitatively may be allowed for by grouping streams according to certain conditions. For instance, with the exception of regulated ones, the rivers studied by the author might be divided into two groups, (1) those deriving their principal floods from rainfall, and (2) those receiving significant flood volumes from melting snow.

For use in an example of regional analysis, the writer selected 17 of the river-stations according to grouping (1) above. Slopes of the frequency curves for these stations are measured by the author's R factor. However, relating slope of the frequency curve to basin characteristics does not allow slope to vary with discharge. This difficulty is avoided by relating the one per cent flood to the mean flood and to basin characteristics. Preliminary graphical multiple correlation showed a better relation with average discharge of the stream than with drainage area so only the former was used.

The computed regression equation based on data for the 17 stations is

$$1\% \text{ flood} = 2.57 (\text{mean flood})^{1.31} (\text{av. disch.})^{-.40}$$

The standard error is -10% and +12%, about half as large as would be obtained by using a mean value of slope for all stations. Data used in the analysis, and computed values of the "one-per-cent flood" are given in Table 1. The relation is presented only to demonstrate a method of reducing chance variation in slopes of flood-frequency curves. It may not apply to small streams. Use of additional or more appropriate parameters should give better results.

TABLE I
DATA USED AND RESULTS OF REGIONAL FREQUENCY ANALYSIS

Gaging Station	Data used				Results	
	Mean Flood in cfs	Av. Disch. in cfs	1% Flood in cfs	cfs	Comp. 1% Flood	% Diff
Neosho - Iola, Kans.	28,300	1,680	105,000	96,200		- 8.4
Big Blue - Randolph, Kans.	27,600	1,680	96,700	93,100		- 3.7
Miami - Dayton, Ohio	35,900	2,260	108,000	117,000		+ 8.3
Savannah - Augusta, Ga.	112,900	10,540	350,000	286,000		-18.3
W. Br. Susquehanna - Williamsport, Pa.	104,100	8,910	260,000	274,000		+ 5.4
Susquehanna - Towanda, Pa.	107,200	10,370	236,000	269,000		+14.0
Susquehanna - Harrisburg, Pa.	282,600	34,700	594,000	596,000		+ .3
Kanawha - Kanawha Falls, W. Va.	125,600	12,670	276,000	306,000		+10.9
Allegheny - Red House, N. Y.	24,500	2,795	56,400	65,000		+15.3
Iowa - Iowa City, Iowa	13,100	1,560	40,700	35,900		-11.8
Tennessee - Knoxville, Tenn.	94,700	12,820	228,000	209,000		- 8.3
French Broad - Asheville, N. C.	17,500	2,112	45,500	46,700		+ 2.6
Des Moines - Keosauqua, Iowa	41,100	5,351	103,000	99,100		- 3.8
Connecticut - White River Junc., Vt.	53,100	7,190	122,000	123,000		+ .8
Cumberland, Nashville, Tenn.	122,200	20,400	208,000	244,000		+17.3
Hudson - Mechanicville, N. Y.	42,500	7,430	89,300	90,800		+ 1.7
Ohio - Cincinnati	443,700	97,700	800,000	715,000		-10.6

